ABSTRACT

Title of Document: MULTI-MODAL SIGNAL PROGRESSION DESIGN FOR ARTERIALS WITH HEAVY TURNING FLOWS

Yao Cheng, Doctor of Philosophy, 2020

Directed By: Professor Gang-Len Chang

Department of Civil and Environmental Engineering

Most urban commuters have long been plagued by congestion in traffic networks and the resulting impacts on safety as well as travel time uncertainties. Since such undesirable traffic conditions in urban arterials are mainly at intersections, traffic researchers often rely on various signal control strategies to smooth traffic flows and minimize excessive delays. Although the advance in communications and control technologies over the past decades has enabled the traffic community to progress significantly on this regard, much, however, remains to be done to achieve the goal of having an efficient and safe traffic environment. Hence, this study has developed an integrated multi-modal signal progression system that allows the traffic engineers to apply different modules of the developed system to produce the best set of signal

control plans that can effectively work under various constraints associated with arterial traffic patterns and roadway geometric features.

The first primary function of the developed arterial progression system is designed to maximize the progression efficiency of passenger cars on a long arterial comprising heavy left-turn volumes, limited turning bay length, and near-saturated intersections. The developed system with such an embedded function can produce concurrent progression for both the through and left-turn movements with the least likelihood of incurring mutual blockage between them and uneven traffic queues among all critical locations on the arterial. To decompose a long arterial into the optimal number of control segments with well-connected and maximized progression bands, this study has further offered a function of a two-stage optimization process to tackle various critical issues that may prevent vehicles from progressing smoothly over the entire long arterial.

To accommodate heavy passenger car and bus flows over an urban arterial and ensure the progression quality for both modes, this study has advanced the system with an innovative function that can offer concurrent progression to the best selected mode(s) and direction(s), based on traffic volume, bus ratio, and geometric conditions. By weighting the progression bandwidth with the passenger volumes and taking into account all critical issues that may result in their mutual impedance, such

an embedded function of the developed arterial control system can achieve the objective of maximizing the benefit for all roadway users and for all modes.

Most importantly, to ensure the effectiveness of the developed system's key functions under various arterial traffic patterns and control objectives, this study has integrated all key modules developed for, such as, the arterial signal design, allowing users to contend with most challenging scenarios, concurrently decomposing a long arterial into the optimal number of control segments for both modes, maximizing their progression bands within their respective segments, circumventing all geometric constraints, and balancing the progression length and bandwidth between the competing modes. In view of computing efficiency associated with the execution of all interrelated optimizing functions, this study has also designed a customized algorithm to minimize all computation-related tasks.

Rigorous evaluation with extensive numerical studies has verified the effectiveness of the developed arterial system's key functions, and evidenced their contributions with respect to offering best progression and minimizing traffic delays. The developed system's flexibility in circumventing various roadway constraints and traffic queue spillback has also been confirmed from the results of comprehensive simulation experiments with different critical traffic scenarios.

MULTI-MODAL SIGNAL PROGRESSION DESIGN FOR ARTERIALS WITH HEAVY TURNING FLOWS

By

Yao Cheng

Dissertation submitted to the Faculty of the Graduate School of the
University of Maryland, College Park, in partial fulfillment of
the requirements for the degree of
Doctor of Philosophy
2020

Advisory Committee:
Professor Gang-Len Chang, Chair
Professor Ali Haghani
Professor Martin Dresner
Professor Cinzia Cirillo
Associate Professor Shanjiang Zhu at the George Mason University

Dedication

To my mother, Ni Yan, and my father, Sheming Cheng

for their love and support

Acknowledgements

First and foremost, I would like to express my sincere sense of gratitude to my advisor, Dr. Gang-Len Chang, for his patient guidance and constant inspiration throughout my Ph.D. study at the University of Maryland, College Park. Improved by his respected attitude towards academic work was my knowledge and ideas, as well as my view to life and career.

I would also like to express my gratitude to the members of my doctoral examination committee, Dr. Ali Haghani, Dr. Cinzia Cirillo, Dr. Shanjiang Zhu and Dr. Martin Dresner for their enlightening comments and helpful suggestions which enhance my research work from various aspects.

I could not finish my path to the doctoral degree without kind help of Xianfeng Yang, who always instructed, guided, supported and inspired me without any reservation. I would also thank my colleagues in Traffic Safety and Operations Lab, Yaou Zhang, Dr. Hyeonmi Kim, Dr. Yang (Carl) Lu, Dr. Sung Yoon Park, Dr. Liu Xu, Dr. Chien-Lun Lan, Yen-Hsiang Chen, Yukai Huang, Dr. Woon Kim, Dr. Minsu Won, Dr. Yen-Yu Chen, Yi-Chi Lu, Dr. Mark Franz, Anna Petrone and Dawson Do, for their technical and moral support. Furthermore, I would like to thank all dear friends of mine, Dr. Jingxian Wu, Dr. Liang Tang, Dr. Liping Yang, Mengqi Zhang, Weiyi Zhou, Yixuan Pan, Jun Zhao, Tong Zhou, Mibao Xiong, Dr. Zheng Zhu, for their encouragement and company throughout my Ph.D. study.

Finally, I profoundly thank my loving family, especially my mother, Ni Yan and my father, Sheming Cheng, for their lasting dedication and support to my study, my life and my future. They deserve my deepest gratitude, forever.

Table of Contents

List of Tables

List of Figures

Chapter 1: Introduction

1.1 Research Background

Most urban commuters have long been plagued by traffic congestions on urban arterials and their resulting impacts on travel efficiency and travel time uncertainties. Hence, how to improve traffic conditions and enhance the roadway efficiency has long been the top priority that need to be addressed by the responsible traffic agencies and researchers. Since most traffic delays in the urban arterials are mainly at the signalized intersections, development of effective signal control methods to contend with such delays has naturally emerged as the foremost research for the traffic control and engineering communities.

However, despite the emerge of various real-time signal design methodologies and intelligent control devices over the past two decades, much remains to be done with respect to the development of an effective and reliable off-line signal systems, the backbone for any advanced controls, for pretimed operations in congested urban networks. Ideally, such a system should either be operated independently under the scenarios of insufficient sensors, or used as the basis for more advanced adaptive real-time controls (e.g., SCOOT, SCATS, RHODES). Depending on the key features of the target network and the traffic flow patterns, the control objective for such off-line control systems can either be minimizing the total vehicle delay or maximizing the total progression band. The former is adopted in the popular series of TRANSYT family models (Robertson, D. I., 1969), while the latter is championed by the MAXBAND family (Little et al., 1981; Gartner, et al., 1991).

In general, most studies adopting the control objective of delay minimization tend to first analyze the traffic conditions with simulation or macroscopic modelling methods, and then apply some optimization algorithms or heuristics (e.g., Genetic Algorithm) to produce the signal plans. In contrast, the class of methods for the progression band maximization is focused on producing the set of optimized signal offsets that can facilitate the maximal number of vehicles to traverse consecutive intersections without stops. Such studies, extensively evaluated in the recent decades by the traffic community, have been recognized to have the following advantages: 1) their resulting progression bands can be easily visualized and illustrated with time-space diagrams; 2) the progression between intersections is always observable by the drivers and beneficial to the overall traffic conditions regardless of the volume level; and 3) the model can usually be formulated with mixed integer linear programming that can be solved with various existing tools.

However, even though significant research advances have been made by the traffic community on the subject of maximizing the progression bands over the past decades, a robust system that can be applied to various arterial segments with different traffic demand patterns and geometric constraints remains a critical on-going task in the traffic community. For a signal control system with the objective of maximizing progression band to have both sufficient flexibility yet effectiveness to contend with various geometric constraints and flow patterns in urban arterials, there are some vital issues to be addressed. For example, a left-turn bay with insufficient length may easily cause blockage to through or left-turn vehicles, and further impact the progression of traffic flows. In addition, a long arterial segment with a large number of intersections is unlikely to be synchronized effectively in a single progression system. Hence, it is essential in practice to have a rigorous method to determine the boundaries among a set of progression segments.

Moreover, failing to consider the users taking either mode and their mutual interactions in the arterial progression process on an arterial with heavy volumes of both passenger cars and buses may degrade the efficiency of such control operations under the mixed traffic flows.

As such, to have an effective signal control and traffic progression in congested urban networks, it is essential to design a system that is capable of reliably and efficiently tackling the following imperative issues:

- How to minimize the impacts of spillbacks and blockages caused by left-turn bays with limited lengths on the vehicle progression;
- How to reduce the impacts of residual queues consisting of turning vehicle flows from side streets;
- How to divert traffic congestion at near-saturated intersections or short links so as to minimize the bottleneck impacts from individual locations on the entire arterial;
- How to optimize the control boundaries for each progression segment within the target arterial;
- How to select the proper mode(s) and direction(s) to provide vehicle progression when demands of both passenger cars and transit vehicles are significantly high; and
- How to balance the progression level between passenger cars and buses so as to maximize the benefit of all roadway users.

1.2 Research Objectives

To address all aforementioned issues, this study has focused on developing a flexible multi-modal signal progression system that allows users to apply different modules of the developed system to accommodate various traffic demand patterns under geometric constraints on different arterial segments. More specifically, the proposed system has been designed with the following essential functions to

- address the traffic blockage incurred by heavy left-turn volumes from and onto the arterial under the constraint of limited bay length, and also to minimize the left-turn delays by providing concurrent progression for through movements and left-turn movements;
- improve the traffic conditions at near-saturated intersections and short links by distributing the traffic queues to nearby less saturated locations;
- decompose a long arterial into several optimized progression segments for maximizing the progression efficiency along all the intersections;
- offer concurrent progression to both modes (i.e., buses and passenger cars) or to the optimally selected mode(s) and direction(s), based on traffic volume, bus ratio, loading factors and geometric conditions over congested intersections and links; and
- provide essential and flexible modules for design of the optimal arterial signal plan under various traffic and geometric conditions.

To accomplish the above objectives, this dissertation has produced several sets of effective models and formulations to perform the following tasks:

- Estimation of the queue lengths at intersections based on the green splits and offsets between adjacent intersections, and identification of potential blockages at left-turn bays or on near-saturated links;
- Quantifying the trade-offs between the number of subsegments for progression design on a long arterial and the resulting bandwidth for each subsegment, as well as the connection state between two adjacent progression bands;
- Realistically representing the operational features of passenger cars and buses as well as their mutual interruptions on the arterial; and
- Offering a set of effective modules to contend with various traffic conditions and different geometric constraints existing in different segments of a target arterial.

1.3 Organization

Based on the identified research objectives, the research results produced from each task are organized into eight chapters. The key component of these tasks and their relations are illustrated in Figure 1.1.

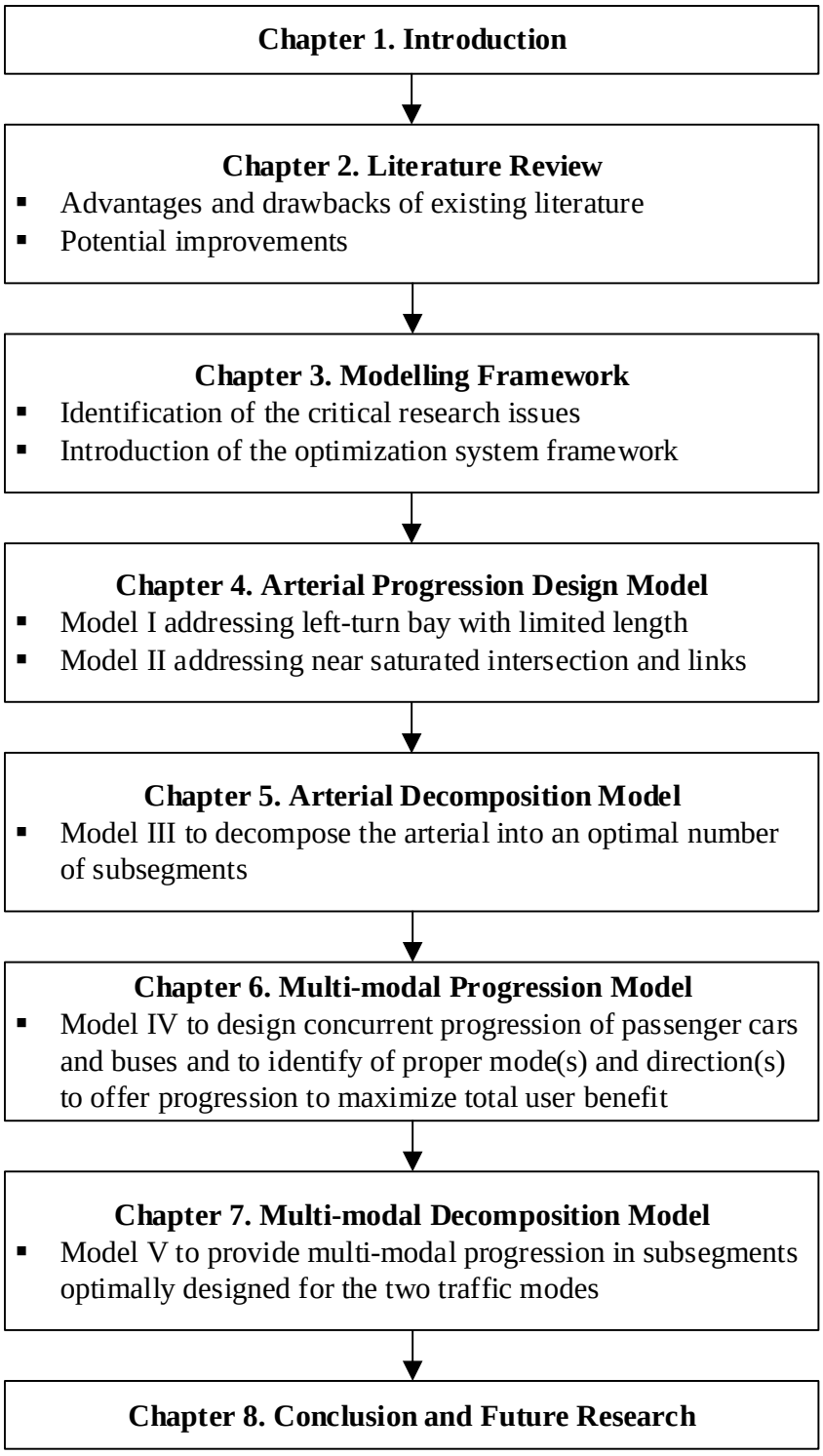

Figure 1.1 Organization or the dissertation

The remaining chapters of this study are organized as follows:

- **Chapter 2** reports the results of a comprehensive review of existing studies on signal optimization for isolated intersections and unban arterials, including arterial decomposition models and transit signal priority strategies. The literature review also summarizes the advantages and deficiencies of these studies, followed by the potential improvements that need to be addressed.
- **Chapter 3** introduces the modelling framework of the proposed signal control system, based on the identified critical issues and research objectives. The framework will illustrate the model inputs, the structure of the system, the proposed models for addressing all identified critical issues, and the interrelations among those optimization modules.
- **Chapter 4** presents the modelling methodology and formulations for signal progression design for an arterial with a bay length constraint. The proposed models will be capable of addressing the following issues: 1) contending with heavy left-turn volumes moving from or onto the arterial under the constraint of insufficient turning bay length; and 2) preventing the formation of excessive queues at near-saturated intersections and on short links along the target arterial.
- **Chapter 5** introduces model formulations for an optimization model to decompose a congested long arterial into the optimal number of subsegments so as to maximize the overall traffic efficiency. Taking advantage of the formulations in Chapter 4, the developed model has the following key features: 1) concurrently decomposing the arterial into short segments, and optimizing their signal offsets as well as phase

sequences; 2) maximizing the sum of progression bandwidths weighted by traffic volume at each intersection; 3) minimizing the expected delay at each decomposition point of the arterial; and 4) accounting for the impacts of queue length or spillback at short links or turning bay in optimizing the progression band; and 5) distributing an arterial's excessive traffic queues to less congested intersections. The effectiveness of the developed decomposition model in maximizing the progression efficiency along the whole arterial has been confirmed with extensive numerical and simulation experiments.

- **Chapter 6** presents a signal optimization model that can offer concurrent progression to both buses and passenger cars or to optimally selected mode(s) and direction(s), based on traffic volume, bus ratio, and geometric conditions. The proposed model has the following key features: 1) maximizing the total benefit of all roadway users by selecting the proper mode(s) and direction(s) to offer progression, subject to the feasible combination of all progression bands; 2) fully accounting for the operational features of passenger cars and buses in design of the progression bands; and 3) considering the mutual interactions between passenger cars and buses and their impacts to the progression efficiency along the roadway. The effectiveness of the model developed for producing concurrent progression bands for both modes has been confirmed with extensive numerical examples and simulation experiments.
- **Chapter 7** integrates all functions in the aforementioned models and designs a comprehensive multi-modal decomposition model to concurrently decompose a long arterial into the optimal number of control segments and to offer the maximized progression for buses and passenger cars within each of their respective segments. The

integrated model can execute all essential tasks to be done by the models discussed in previous chapters, and also with its enhanced capability to address the unique issues in multi-modal progression design on a long arterial, including 1) the competition between two modes on the number of intersections that can experience progression; 2) the competition between two modes on the available progression bandwidths; and 3) the flexibility to allow different decomposition locations for the two modes. The effectiveness of the proposed comprehensive model in producing progression bands for both modes within respectively designated segments has been confirmed with extensive numerical studies and simulation experiments.

- **Chapter 8** summarizes the contributions of this dissertation, and highlights the directions for future research, including development of a network-based progression system to account for crossing major arterials, advancement of the key control models for real-time operations, and enhancement of the current signal design system with advanced information/communication technologies.

Chapter 2: Literature Review

2.1 Introduction

This chapter presents the review of related studies over the past decades on traffic signal optimization and progression design. The remaining critical issues to be addressed in this study will also be summarized in this chapter.

To facilitate the discussion, this chapter will report the review of key related studies along the following three areas:

- **Signal optimization and progression design models**: All models in this area are proposed to optimize fixed-timed signal settings for isolated intersections or arterials and have been extensively evaluated during the past decades. Their primary control objectives are to reduce travel delays, eliminate congestions, and improve the operational efficiency by adjusting cycle length, green splits, phase sequence and offsets.
- **Arterial decomposition models for signal coordination design**: Most models classified in this category for review are developed mainly to facilitate the design of signal progression system for long arterials where traditional two-way band maximization methods may produce very narrow or even zero bandwidth. The focus of the review task will be devoted to the decomposition methodology adopted in various studies for dividing the arterial into a set of subgroups which can then be designed independently for signal progression and coordinated only at their common intersections.

- **Active and passive Transit Signal Priority (TSP) control strategies**: Extensive studies have been conducted by the traffic community to improve bus operations in urban traffic networks, with or without the hardware for bus arrival detection. The primary review efforts on this subject will be given to state-of-the-art models and algorithms developed in the literature to facilitate bus progression with minimal negative impacts on the traffic conditions of the crossing streets.

2.2 Signal Optimization and Progression Design Models

Despite the merge of a rich body of research on network adaptive traffic control, only a few cities have actually deployed such systems in a small network and the project demonstration level due to their complexities and costly implementation. The pre-timed signal control that assigns the right-of-way to traffic movements based on time-of-day traffic volumes with predetermined cycle length, green splits, phase sequences and offsets remains widely used in most states. Those pre-timed signal plans are designed for an isolated intersection or an urban arterial with the control objective to minimize total delay, maximize throughput, optimize a performance index, or maximize progression bands.

2.2.1 Pre-timed signal design for isolated intersections

The objective of all models in this category is to improve the target intersection's efficiency without considering the potential impacts to adjacent intersections. Such studies were initiated since 1950s, when Matson (1955) first presented a method to compute the signal timings, based on the presumed uniform vehicle arrival patterns. Webster (1956) later developed the set of models to determine the optimal and minimum cycle lengths, based on the average intersection delay, estimated with Poisson arrival patterns, as shown in following equations,

$$C_o = \frac{1.5\sum L_i + 5}{1 - \sum x_i} \tag{2.1}$$

$$C_m = \frac{X_c \times \sum L_i}{X_c - \sum x_i} \tag{2.2}$$

Where C_o and C_m denotes optimal and minimum cycle lengths; $\sum L_i$ denotes the total lost time in one cycle; $\sum x_i$ is the ratio of intersection critical lane volume over the saturation flow rate; and X_c refers to the critical V/C ratio for the intersection. These models are still used in many recent studies and applications on intersection control.

Following these two pioneering studies, a large number of researchers have conducted further studies on estimating intersection delays and computing the optimal cycle length as well as signal timings. Among them, Miller (1963) proposed a model to estimate intersection delay for vehicles with different variance-to-mean ratios for the arrival distributions. Cycle lengths and green splits can then be optimized by differentiating the delay equation. Several later studies following this line can be found in the works by Allsop (1971, 1972, 1976) and Burrow (1987).

Note that those models offer practically useful and theoretically elegant methods for field applications if the target intersection is at the under-saturated state. To design signal plans for near- or over-saturated intersections, Gazis (1964) developed a method to minimize the total delay and shorten the queue length by first allocating maximum green time to the major road and minimum green time to minor roads, and then switching these two. Such a method was further enhanced by

Michalopoulos and Stephanopolos (1977a,1977b), who proposed bang-bang control with an optimization model for the switching time point between the two stages.

For the same control objective, Chang and Lin (2000) then developed a discrete version of the Michalopoulos and Stephanopolos model. Using the simulation-based concept, Robertson (1969) also formulated the set of TRANSYT models to produce signal plans for both isolated intersection and arterial by minimizing a pre-defined performance index that could be a combination of total delays and number of stops.

With mathematical programming, another group of researchers focused on proposing various formulations to optimize the cycle length and green splits for isolated intersections. For example, Silcock (1997), Wong and Wong (2003), and Yang et al. (2014) proposed to maximize a common flow multiplier, μ , indicating the maximum amount of increased volume that would not yield over-saturated condition at the intersection. With the maximum value of μ greater than one, the target intersection is expected to operate in an under-saturated condition if with the optimized cycle length and green splits. Taking advantage of linear-programming formulation, this method can yield the global optimal results under the given conditions. Using non-linear programming methods for the same purposes, Lan (2004) formulated two models, respectively, for optimizing cycle lengths and green splits for under-saturated and over-saturation intersections, based on the delay calculated with Highway Capacity Manual (HCM) formula.

2.2.2 Signal optimization for urban arterials

As is well recognized, traffic conditions on most urban arterials' intersections are often mutually dependent due to their close distance. Since the arrival patterns at one intersection would be impacted by the signal settings at the neighboring upstream intersections, the signal optimization methods for isolated intersections may fall short of efficiency. Therefore, a large body of studies have been conducted to design signal plans for arterials to ensure either their progression efficiency or delay minimization. Hence, most of such studies reported in the literature over the past several decades can be classified into two categories: total delay minimization and progression band maximization.

Among those in the first category, TRANSYT (Robertson, 1969) is one of the most widely utilized models which adopt the minimizing delay or other performance index as the control objective for design of signal plans for an arterial, in addition to its models for isolated intersections. Originally developed by Transport Research Laboratory in the United Kingdom, TRANSYT 7 has been updated by Federal Highway Administration (FHWA) and supplemented with localized functions. The updated version, TRANSYT 7-F, offers a macroscopic simulation model to represent the arrival flow patterns, saturation flow patterns and departure flow patterns to each intersection approach. At each time step of the simulation model, the number of vehicles and the queue length to each approach is updated along with the computation of delays experienced by those vehicles. The optimal signal timing is then produced by using the Genetic Algorithm (GA) or Hill Climbing method. Also performing the optimization through simulation, Stevanovic et al. (2007) and Yun and Park (2006) developed mesoscopic models to obtain the optimal signal settings for an arterial. Taking advantage of GA, Hadi and Wallace (1993) and Park et al. (1999)

further developed several models to search for a near-optimal signal timing plan, based on an identified fitness value.

Another group of studies in this category are developed mainly on the concept of Cell Transmission Model (CTM), which was first introduced by Daganzo (1994). With CTM, the target roadway segment is divided into several homogeneous cells so that the traffic conditions in one cell can be considered as uniform, and vehicles may either stay in its cell or travel to the next one over each time step, based on the available space in the adjacent cell. This concept was transformed into various formulations to represent the complex traffic evolution process, including queue formation, queue dissipation, kinematic waves, and congestion patterns (Lo, 1999; Lo et al., 2001; and Lo and Chan 2001). Without utilizing simulation, Liu and Chang (2011) developed a lane-group-based signal optimization model to prevent queue spillback to the upstream intersection and likely mutual blockages between lane groups.

Various related studies but with different solving methods have also been proposed in the literature. Examples of such studies include: the use of a hierarchically intelligent control procedure to manage urban traffic has been proposed by Kashani and Saridis (1983); a robust optimization model to compute the signal timings for an arterial by Yin (2008) and Yang et al. (2013); and some studies following this line by Aboudolas et al. (2010), Li (2012) and Papageorgiou (1995).

All signal optimization studies for arterials classified in the latter category are proposed with the objective to produce the maximum green bands so that vehicles within the bands can travel over several consecutive intersections without stops. One of the pioneer works to maximize

two-way bandwidths was introduced by Morgan and Little (1964), which was later improved by Little (1966) with a model for the concurrent optimization of cycle length, progression speed, and offsets. Taking advantage of the linear programming algorithm, an enhanced version of these studies, called MAXBAND, was proposed by Little et al. (1981) to address the left-turn phase sequence and initial queue issues. Such a model provides a logical method to produce maximum two-way green bands by optimizing offsets and left-turn phase sequences along all intersections on the same arterial. Its core formulations can be summarized as follows, and their key variables are shown in Figure 2.1.

$$Max\ (b + k\bar{b}) \tag{2.3}$$

s.t.

$$(1-\rho)\bar{b} \geq (1-\rho)\rho b \tag{2.4}$$

$$1/C_2 \leq z \leq 1/C_1 \tag{2.5}$$

$$w_i + b \leq 1 - r_i \quad \forall i = 1,...,n \tag{2.6}$$

$$\bar{w}_i + \bar{b} \leq 1 - \bar{r}_i \quad \forall i = 1,...,n \tag{2.7}$$

$$\begin{aligned}(w_i + \bar{w}_i) - (w_{i+1} + \bar{w}_{i+1}) + (t_i + \bar{t}_i) + \delta_i L_i - \bar{\delta}_i \bar{L}_i - m_i \\ = (r_{i+1} - r_i) + (\tau_i + \bar{\tau}_i) + \delta_{i+1} L_{i+1} - \bar{\delta}_{i+1} \bar{L}_{i+1} \quad \forall i = 1,...,n-1\end{aligned} \tag{2.8}$$

$$(d_i / f_i)z \leq t_i \leq (d_i / e_i)z \quad \forall i = 1,...,n-1 \tag{2.9}$$

$$(\bar{d}_i / \bar{f}_i)z \leq \bar{t}_i \leq (\bar{d}_i / \bar{e}_i)z \quad \forall i = 1,...,n-1 \tag{2.10}$$

$$(d_i / h_i)z \leq (d_i / d_{i+1})t_{i+1} - t_i \leq (d_i / g_i)z \quad \forall i = 1,...,n-2 \tag{2.11}$$

$$(\bar{d}_i / \bar{h}_i)z \leq (\bar{d}_i / \bar{d}_{i+1})\bar{t}_{i+1} - \bar{t}_i \leq (\bar{d}_i / \bar{g}_i)z \quad \forall i = 1,...,n-2 \tag{2.12}$$

$$b, \bar{b}, z, w_i, \bar{w}_i, t_i, \bar{t}_i \geq 0 \quad \forall i = 1, ..., n \tag{2.13}$$

$$m_i \text{ integer}; \delta_i, \bar{\delta}_i \text{ binary integers} \quad \forall i = 1, ..., n \tag{2.14}$$

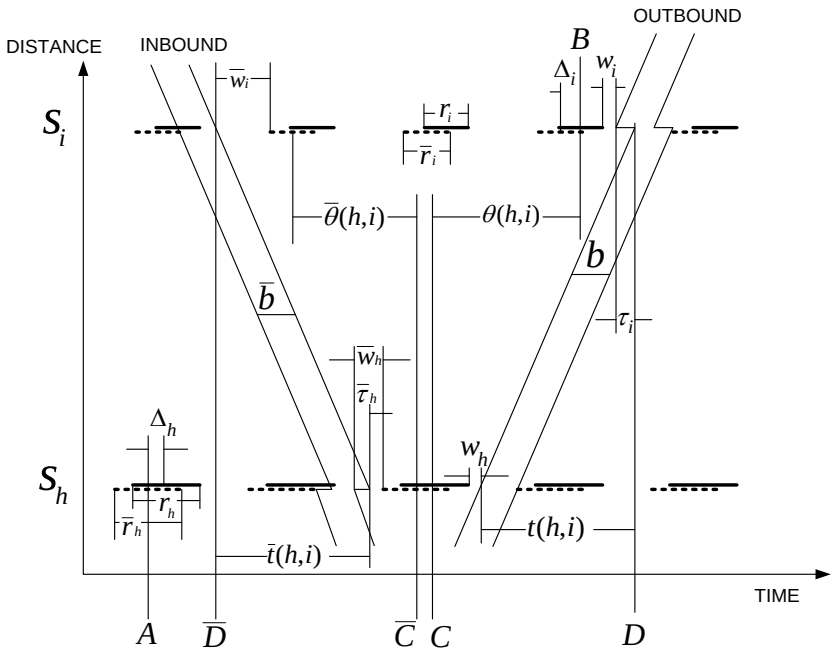

Figure 2.1 Key notations in the MAXBAND model (Little et al., 1981)

Among those parameters shown in the formulations and above figure, r_i denotes the common red time at signal *i*; $L_i(\bar{L}_i)$ is the time allocated to the left-turn movements; C_1 and C_2 and the lower bound and upper bound of the cycle length; e_i, $f_i(\bar{e}_i, \bar{f}_i)$ are the lower and upper limits for the outbound (inbound) speeds; $g_i, h_i(\bar{g}_i, \bar{h}_i)$ represent the lower and upper limits for the outbound (inbound) speed change; ρ is the directional parameter to indicate the preference between the progression in two directions. As for the variables to be determined, $b\left(\bar{b}\right)$ refers to the bandwidths, z denotes the cycle length; $w_i\left(\bar{w}_i\right)$ is the time between the start of a green phase

and the start of its green band; $t_i\left(\overline{t}_i\right)$ represents the travel time between intersections; $\delta_i\left(\overline{\delta}_i\right)$ are binary variables and m_i are integer variables. Particularly, different values of the binary variables, δ_i and $\overline{\delta}_i$, can be used to reflect four possible phase designs to accommodate major arterial flows: outbound left leads and inbound left lags; outbound left lags and inbound left leads; outbound (or inbound) left leads; and outbound (or inbound) left lags.

The objective function, Eq. (2.3) for MAXBAND, is to maximize the weighted sum of the two-way bandwidths. Eq. (2.4) is developed to balance the bandwidth of two directions while one of them is favored. Eq. (2.5) limits the upper and lower bounds of the optimized cycle length. The directional interference constraints in Eqs. (2.6) - (2.7) can ensure the green bandwidth to be within the available green time. The loop integer constraint in Eq. (2.8) is specified to guarantee that vehicles travelling in the designed speed can stay within the band between each pair of intersections. The boundaries and variation of travel times due to the varying travel speeds is constrained by Eqs. (2.9) - (2.12).

The core concept of MAXBAND has also been enhanced by a number of studies in the last decades. One of the key studies along this line was conducted by Gartner et al. (1991), who proposed MULTIBAND to allow the bandwidths to vary among the links so as to accommodate their differences in traffic volumes. Grounded on the core logic of MAXBAND, the study for MULTIBAND adopts an objective function of the sum of link bandwidths weighted by link volumes.

For the similar purpose, Chaudhary et al. (2002) developed the model, PASSER, a progression optimization program using different formulation methods. Zhang et al. (2015) developed an AM-band model that allows asymmetrical green band intervals with respect to the progression line along the arterial. Also taking into account the traffic volumes, Li (2014) proposed a signal optimization model to account for the link travel time uncertainty caused by queues and traffic fluctuations. To accommodate heavy turning movements other than through flows along the arterial, Yang et al. (2015) proposed a multi-path progression model that can concurrently provide the progression for several pre-identified competing vehicle paths with heavy volumes. However, this study requires the knowledge of volume for all paths, which cannot be directly acquired with existing data collection methods. Without the information of the path-flow patterns, Chen et al. (2019) presents a three-staged signal optimization model that can circumvent or minimize the impact of left-turn spillback to the through movements and concurrently minimize the delay of left-turn flows.

Note that some other researchers also extended Little's arterial progression models to various applications, ranging from an unconventional intersection to grid networks. For example, Yang et al. (2014) proposed a signal design model for Diverging Diamond Interchange (DDI) to provide signal progression for both through and ramp movements. For the same unconventional design, Cheng et al. (2018) developed a model to concurrently determine the crossover spacing and the signal timing plans to further enhance the effectiveness of the progression.

Considering the constraints of short bay length and the interrelations between critical movements within the main intersection of a Continuous Flow Intersection (CFI), Yang et al.

(2016) developed a signal design model that can concurrently optimize the cycle length, phasing plan, phase sequence and offsets. Chang et al. (1988) extended MAXBAND to a grid network and proposed MAXBAND-86 to address the issue of left-turn phase sequence in a multi-arterial closed network.

For the similar purposes, MULTIBAND-96 was proposed by Stamatiadis and Gartner (1996). In the later year, Gartner and Stamatiadis (2002) addressed the network progression issue by considering the arterials as network loops. To improve the computational efficiency, Gartner and Stamatiadis (2004) further developed a two-step method to design the signal progression for a traffic network. In their model, the first step is to determine the critical routes carrying large volumes and design offsets for them respectively; the second step then produces offsets or all intersections in the pre-selected route.

2.3 Arterial decomposition models for signal coordination design

Those bandwidth-based models introduced in the last section have been proven to be effective on coordinating traffic signals and providing progression bands for mainly through traffic paths (inbound and outbound direction). However, for a long major arterial that includes a large number of intersections (e.g., 15-20 intersections), existing two-way progression models such as MAXBAND, may not be capable of producing an effective offset plan. This is due to the embedded constraints that the resulting progression bandwidth produced by the MAXBAND model for both through directions will be decreased with the increasing number of intersections, clustered for progression design. Hence, to ensure an effective signal progression plan, it is essential to

decompose the arterial corridor into a set of subgroups and then proceed the progression design for each independently.

In review of the related literature in traffic signal control, only a few studies have highlighted this issue. Among those limited works, Hooks and Albers (1999) suggested some decomposition rules to combine all intersections that are less than half-mile apart (2,500 ft) in one group and then split intersections with more than one mile apart (~5,000 ft) spacing as these decomposition points. For all intersections with spacing between 2,500 and 5,000 ft, one can directly proceed to select the decomposition points with the Coupling Index (CI). Bonneson et al. (2009) suggested to use traffic volumes in both directions of the link and spacing to define a new CI function.

Similar to the aforementioned methods, their proposed models yield an ambiguous range of CI values for the decision by individual users. Tian and Urbanik (2007) presented a grouping technique to increase the efficiency and attainability of the green bandwidth. Their approach is to divide a corridor with ten intersections into three subgroups, based on spacing and traffic demand, and then to optimize each subgroup's green bandwidth. Those steps are followed by adjusting the offset and phase sequences of the boundary intersections in each subgroup so as to ensure the between-group progression.

Wu et al. (2012) developed a group partition method of coordinated arterials for optimal bandwidth, based on comparing traffic volumes (through/turning) at intersections. They compared the bandwidth of every possible subgroup, and proved that their initial partitioning was correct.

Such a method is very time-consuming when the number of intersections in a system increases to a large size.

Zhang and Zhang (2014) present a K-means clustering method to decompose all candidate signals for coordination. In their study, interruptions at intersections due to large through volume and minimum turning traffic should be prevented if the decomposition is to be applied. The main issue with using K-means clustering method is that the value of K should be defined prior to analysis and it requires at least 100 sample sizes to derive a reliable clustering model. In summary, despite a large body of related studies have been reported in the literature, an efficient and reliable optimization tool that can decompose the arterial corridor into an optimal number of progression groups for optimizing their intersection offsets is not yet available.

2.4 Active and passive Transit Signal Priority (TSP) control strategies

Increasing transit system ridership has long been recognized as one of the potentially effective strategies to mitigate urban traffic congestion from the demand side. However, a variety of factors associated with transit operations (e.g., uncertain waiting times at bus stops, variable travel times, and frequent stops at traffic signals) often cause transit systems unfavorable in comparison with the auto mode. In an attempt to enhance transit service reliability, over the past decades a rich body of research has produced various Transit Signal Priority (TSP) strategies, allowing a bus to pass an intersection with less delays. Those studies for improving transit efficiency can be classified into the following two categories: passive or active TSP control.

2.4.1 Active TSP control

Active priority systems need to rely on the sensors located at the upstream of intersections with a specific distance to the stop bar for detection of bus arrival detection. When a transit vehicle reaches the sensors, the signal controller will trigger the activation of a TSP strategy (i.e., green extension, red truncation, or phase insertion) for predetermined or variable durations. Based on how the activation type and duration are determined, one can classify the active TSP strategies into either rule-based or model-based methods.

Unconditional TSP control, as one of the earliest rule-based strategies, is designed to extend green time or truncate the red phase upon the detection of an arriving bus (Ludwick & John, 1974). This method has been evaluated with simulation experiments, and shown to be effective on improving the bus efficiency, without causing significant interruption to the traffic on side streets if the bus demand is not very high. To minimize the potential impact to side street traffic, some rules have been developed to set a limit on the green time extension (Dion & Hesham, 2005). By adopting these rules to keep the cycle length unchanged and to limit the number of priority calls in a single cycle, unconditional TSP strategies can be applicable to arterials in need to accommodate heavy bus flows.

Conditional priority is another kind of rule-based methods, which takes into account the actual bus presence and readiness in order to minimize their impacts on other type of vehicles on this subject. For instance, Ma & Yu (2008) utilized a decision tree to optimize the service sequence of multiple TSP requests under the control objective of minimizing the average person delay. He et al., (2011) developed a heuristic algorithm to achieve near-optimal signal timing when multiple

priority calls need to be responded. Ling & Shalaby (2004) developed an adaptive TSP strategy based on Reinforcement Learning (RL).

To fully take advantage of TSP, Altun & Furth (2009) altered the service design and management policies such that the bus operations can be further improved. Along the same line, Yan et al., (2009) developed a method to determine the optimal location of TSP detectors based on the priority types and durations. Basically, conditional TSP only grants priorities to buses behind the schedule, thus may ignore some requests from some early-arriving buses. On the same subject, some researchers have developed various rules for conditional TSP to constrain the frequency of activating priority control, based on the ridership of the buses or the priority decisions in previous cycles. For example, Evans & Skiles (1970) prevented the activation of red truncation if the previous green period has been extended.

In the studies of Tarnoff (1975) and MacGowan and Fullerton (1979), the signal priority will be activated only when the bus arrival rate reaches a user-specified level. Studies along this line has also been conducted by Allsop (1977) and Cottinet et al. (1980). Gallivan et al. (1980) estimated and validated the feasibility and benefits of green compensation to non-priority movements. However, the studies conducted by El-Reedy & Ashworth (1978) and Cooper et al. (1980) showed extra delay during the compensation cycles. These rule-based methods offer the requested priority controls, based on empirical results, rather than rigorous analytical process. Such models are easy to implement in practice but may not yield the optimal level of performance. (Smith, et al., 2005; Balke et al., 2000; Janos & Furth, 2002; Satiennam et al., 2005)

Model-based methods, generally more complex than rule-based methods, are proposed to grant the priority decisions, based on some performance measures, computed from the detected bus locations, bus operation conditions, and nearby traffic conditions. (Ma et al., 2010; Lin et al., 2013a; Lin et al., 2013b; Lin et al., 2013c) Such methods try to optimize the performance of buses or all kinds of vehicles by quantitatively evaluating the potential cost/benefits resulting from a priority decision. Their objectives can be to minimize the total bus delay and the total person delay. In addition, most model-based methods are more flexible for extension to traffic networks experiencing various levels of congestion.

2.4.2 Passive TSP strategies

Despite the development of the active TSP controls, on the arterials experiencing heavy bus volumes, those strategies may encounter their limitations since: 1) most TSP controls are operated at the isolated intersection level, which is not sufficient to facilitate the progression of buses over consecutive intersections; and 2) the TSP system will yield significant negative impacts to vehicles on non-priority intersection approaches due to the frequent calls by the signal priority control. Though various existing methods reported in the literature intend to reduce the impacts to the non-priority approaches by adding operational rules or balancing the benefits to all types of vehicles, the conventional TSP strategies remains ineffective in minimizing the negative impacts on side-street-traffic flows if the bus volume in the primary arterial frequently calls for activating priority control. This is one of the reasons why most TSP strategies are only demonstrated in simulated systems, or tested under the scenarios of relatively low bus volume. Hence, a passive control strategy may better serve the arterials accommodating heavy bus flows.

Contrast to active TSP control, passive control strategies do not explicitly recognize the presence of buses, but predetermine the signal timings by taking into account the percentage of bus volume in the total traffic flows. (Machemehl, 1996; Zhang et al., 2004; Ji et al., 2005; Feng et al., 2007; Mirchandani et al., 2001) These strategies do not change the signal timings upon the arrival of a bus or penalize vehicles on the cross streets by extending the green time, but to program the signal parameters to favor the bus movements. As such, the passive control strategies do not interrupt traffic in the non-priority approaches. Moreover, since it needs not to detect the arrival of buses, deploying passive control strategies does not incur the costs of installing and operating the bus surveillance systems.

As one of the pioneering researchers on this subject, Urbanik (1977) developed four possible ways to change the signal plan for one or a group of intersections to favor the bus flows. Their proposed strategies include adjustment of cycle length, splitting of phases, area-wide timing plans, and metering of vehicles. Such methods generally require only changes at the control and operational levels, but nearly demand no capital investment. Garrow and Machemehl (1997) utilized TRAF-NETSIM as a simulation tool to test the effectiveness of shortening the cycle length and splitting phase at both isolated intersections and local arterials. Their underlying logic is that a long cycle length is generally designed to maximize vehicle throughput along arterials since it decreases the intersection's lost time and can generally widen the progression bands for through movements, but at the cost of increasing the stop delay. Hence, a short cycle length may serve as a passive transit priority strategy to decrease the stop delay of transit vehicles at intersections.

The concept of splitting phase is to separate the green phase in a cycle for the transit movement into two separate sub phases so that a bus encountering a red phase will only wait for a shorter period before receiving its green indication. By doing so, it is expected that the intersection capacity will be reduced due to the additional lost time. The relationship between the departure frequency of transit vehicles and cycle lengths of the signalized intersections are investigated by Ma and Yang (2007). They concluded that providing priority to buses is much easier if the departure headway is a multiple of half cycle length. They further used simulation to argue that both active and passive strategies can be applied to Bus Rapid Transit (BRT) systems to decrease the delay and headway deviation. In respond to the same concerns, Lin et al. (2013) proposed a passive control strategy for urban arterials by adding a constant dwell time on computation of bus travel time between two intersections.

Aiming to integrate the concept of signal progression into the passive TSP strategies, some researchers have conducted studies on providing progression to buses along the arterial to smooth the bus operations. Lin et al. (2017) integrated the conventional signal progression control with bus progression model to balance the travel delay between the users of passenger cars and buses. Dai et al. (2015) analyzed the relation between the green bands for transit vehicles and passenger cars, and developed a model to minimize the bus dwell time, based on the predetermined maximum and minimum bandwidths for both modes. Their methods can account for the benefits to both modes but need dynamic adjustments of the bus dwell time or travel time with the on-board devices. Dai et al. (2016) further constructed a progression model by categorizing intersections into different groups, based on the location of bus stops and the expected dwell time. To address the impacts of the stochastic bus dwell time, Cheng et al. (2015) proposed a preliminary model to

compute the offset for a bus-based progression for arterials with heavy transit flows using the logic of MAXBAND. Kim et al. (2018) proposed a more comprehensive method to design the progression for buses, considering the impacts of traffic queues to bus operations and the stochastic nature of bus dwell time. By fully considering bus operational features and the interrelations between the two modes, Cheng et al. (2019) presents a bandwidth maximization model that can offer concurrent progression to both modes or to a selected mode(s) in a selected direction(s), based on traffic volume, bus ratio, and geometric conditions.

2.5 Discussion

In summary, this chapter has presented a detailed review of studies on traffic signal optimization for isolated intersections, urban arterials, and transit operations. Despite the abundant studies on the subject of signal progression, to ensure the progression for both through and left-turn flows on arterials of heavy volume, the following two issues which may degrade the progression quality remain to be tackled by the traffic community. First, in optimizing the offsets for the through progression, not adequately accounting for the left-turn volume and the available bay length at some major intersections, may result in rapid queue formation and even the spillback over the turning bay, and consequently block some through lanes. The anticipated level of progression via the provided bands for the entire arterial may thus be degraded or practically unusable due to such spillback from one or more turning bays or the turning volumes from the crossing street.

Secondly, such potential significant negative impacts from the left-turn bay spillback or turning volume from the crossing streets further justify the need to provide progression operations

for not only through movements, but also left-turn flows, especially at those arterial intersections serving two crossing major roads and accommodating heavy turning volumes.

When designing signal progression for long arterials, existing methods do not concurrently design the boundaries for progression segments and determine the signal plans, and may result in a decomposition plan that is likely to yield non-optimal progression bands. Since the obtained bandwidths highly depend on how the arterial is divided, determining the boundaries for progression design and optimizing signal settings should not be addressed independently.

In review of the studies on passive TSP strategies, those models for bus progression are mostly for an arterial with heavy bus flows, and do not provide progression to general traffic. Among very few of such studies considering the benefits of both modes, they failed to fully account for the differences in their operational features and interrelations on the roadway, and thus may not offer the ideal effectiveness of progression.

Therefore, despite the progress of existing studies on signal progression for arterial control, some issues concerning critical traffic scenarios and conditions deserve more investigation. Example of such issues are listed below:

- The heavy left-turn volume on the arterial may result in rapid queue formation and even spillback from the left-turn bay to block the through lanes;
- The heavy tuning-in volumes from the crossing street may form queues at the downstream intersection, thus impeding the progression for the through movements;

- The primary flows on the arterial may not be the through flows, and the progression control needs to be offered to multiple movements;
- The maximum green bandwidth may reduce or diminish with the increasing number of intersections considered in the progression design; and
- Passenger cars and buses may share an arterial where both modes demand the progression services from the signal control.

To contend with these critical issues, this dissertation will develop an integrated system to produce signal progression to the roadway users under various traffic scenarios and geometric constraints.

Chapter 3: System Framework of a Multi-modal Arterial Signal Progression System

3.1 Introduction

This chapter illustrates the framework of the proposed multi-modal arterial signal control strategies. Following the introduction, Section 3.2 will present the interrelations between its two key modules and the mathematical formulations embedded in each module to contend with various critical traffic issues on major arterials.

As discussed in the literature review chapter, although signal progression has long been studied by the traffic community, the complex issue causing by turning vehicles have not been adequately taken into account in most existing studies. The presence of heavy volume of left-turning vehicles turning left from the arterial would result in rapid queue formation and even spillback over the left-turn bay, especially at intersections with a limited length on their turn bays. Such spillbacks often block the through lanes and consequently degrade the anticipated level of progression.

On the other hand, the heavy volumes from the crossing streets onto the main arterial will form a queue line at the downstream intersection if those vehicles are not offered with effective progression. Such residual queues may not only impact the arterial's progression effectiveness, but also block the left-turn vehicles from entering the turning bay due to the queue overflows. Hence, to provide an optimal signal control to arterials with heavy turning volumes, one should consider the potential mutual blockage between through and left-turn movements at intersections with limited bay length so as to ensure the effective progression for those movements with optimized offsets and phase sequences.

Although an arterial link without a left bay or heavy left turns may not suffer from those issues, optimization of offsets and phase sequences is still necessary for providing smooth traffic flows in the presence of short links or near saturated intersections. One shall minimize the likelihood of having excessive vehicles queueing at such locations to prevent queue spillback. Therefore, for an arterial with short links or near saturated intersections, the signal settings should be further optimized so as to yield not only the maximum progression, but also the minimum likelihood of queue formation at those critical locations.

Note that the design for offering one uninterrupted two-way progression system to a long arterial may not be cost-benefit from the system's user perspective, and it is essential to determine the proper design boundaries for decomposing the entire arterial into several subsegments. To do so, one shall have a systematical algorithm to compute the best decomposition location for maximizing the progression efficiency within each segment and between each pair of adjacent segments.

In addition, for an arterial with considerable volumes of passenger cars and buses, one shall ideally provide concurrent progression to both modes, thereby maximizing the total benefit of all roadway users. Furthermore, since the distributions of traffic volumes in both modes and directions may vary over different times of a day, it would thus be desirable that the control model for the arterials can intelligently decide which modes and directions ought to be offered with the progression so as to maximize the benefits of the entire system. To achieve such objectives, the operational feature of these two modes and their interrelations should be fully considered in selection and computation of signal offsets for progression.

In summary, to design dual-modal progression for a long arterial with heavy turning flows, this study intends to address the following vital research issues:

- Design of concurrent progression for through and left-turn flows with bay length constraints and their potential mutual blockage;
- Further adjusting the signal control parameters to prevent excessive queues from occurring at critical locations;
- Identification of the design boundaries for decomposition of a long arterial into a number of segments; and
- Selection of traffic modes and directions to offer progression so as to maximize the total benefit of all roadway users and for design of multi-modal progression.

Furthermore, an integrated model will be developed to include all these functions, and also to serve as a flexible tool for traffic engineers to apply to arterials under different traffic conditions. With the integrated model, the signal control parameters (e.g., offsets and phase sequences) will be optimized to produce the progression bands to the selected modes and directions under the optimized control boundaries for arterial signal operations.

3.2 Modelling framework

In response to those research issues, Figure 3.1 depicts the framework of the proposed signal optimization system and the interrelations between its two key design modules.

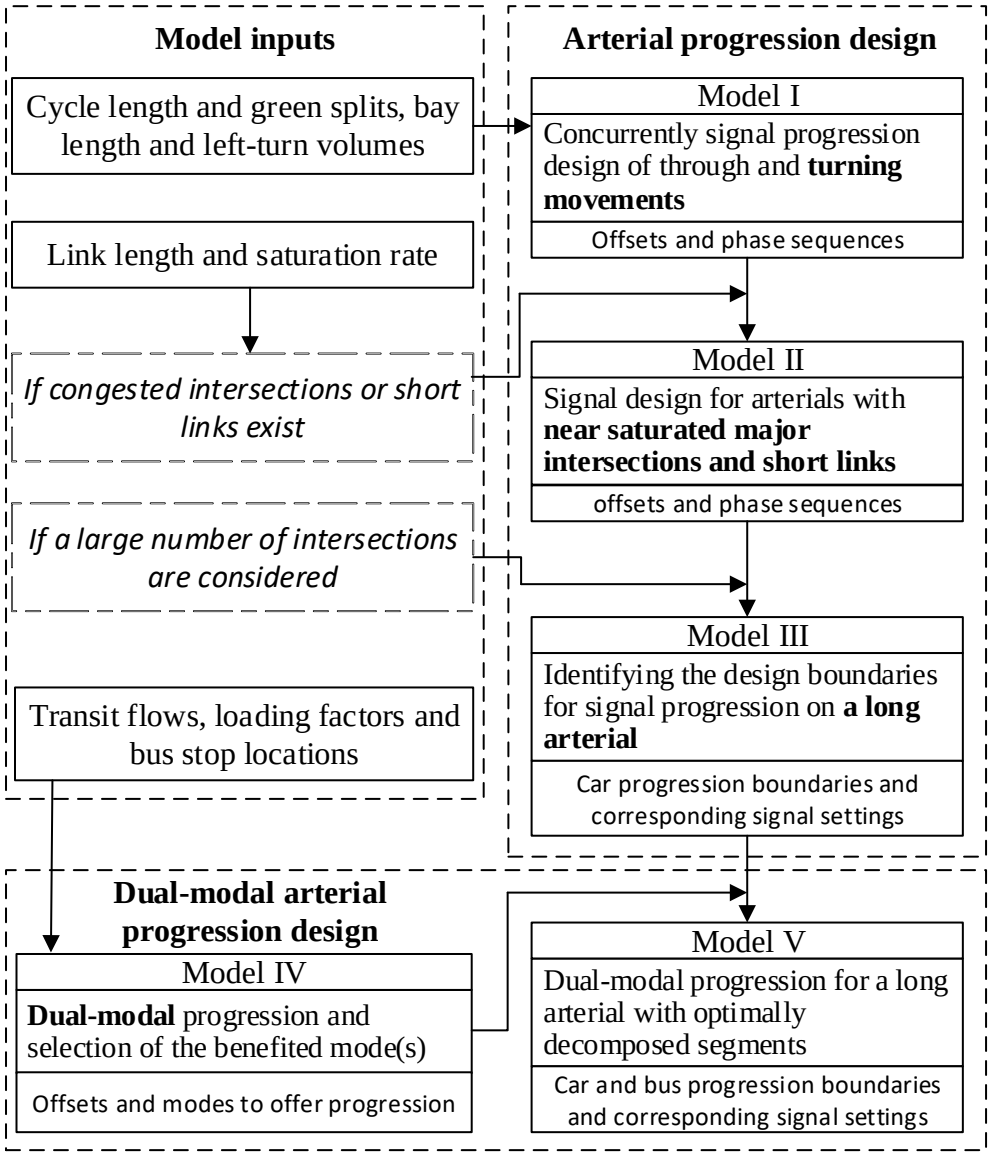

Figure 3.1 Modelling framework of the proposed system

A brief description of each model in the proposed system is presented below:

- **Concurrent signal progression design of through and turning movements:** this model will address the issue incurred by heavy left-turn volumes from and onto the arterial under the constraint of limited bay length. The proposed model on this regard shall have the following key features: 1) minimizing left-turn delays on the arterial and

providing concurrent progression for through and left-turn movements; 2) preventing mutual blockage between through and left-turn movements due to the limited bay length, and 3) accounting for the impacts of residual queues consisting of vehicles turning onto the arterial from the crossing street on the through progression.

- **Signal design for arterials with near saturated major intersections and short links:** To further improve the progression effectiveness when the design with Model I does not yield effective results due to the existence of near saturated intersections or short links, Model II aims to reduce the severe congestions at those critical locations and to minimize the likelihood of causing bottlenecks. In addition to those formulations in Model I, the enhanced features in Model II include: 1) limiting the queue length on each link not to exceed the link length; and 2) distributing the excessive queues to less congested locations.
- **Identifying the design boundaries for signal progression on a long arterial:** This module is used to determine the boundaries that can decompose a long arterial into several optimized progression segments. Aiming to maximize progression efficiency along all such intersections on the arterial, Model III will have the following key features: 1) concurrently decomposing the arterial into short segments, and optimizing their signal offsets as well as phase sequences; 2) maximizing the sum of progression bandwidths weighted by traffic volume at each intersection; 3) minimizing the expected delay at each decomposition point of the arterial; and 4) accounting for the impacts of queue length or spillback at short links or turning bay in optimization of the progression band; and 5) distributing an arterial's excessive traffic queues to less congested intersections.

- **Dual-modal progression and selection of benefited mode(s):** This model is proposed to maximize the total benefit of all roadway users when significant volumes of passenger cars and buses share the same roadway segment. The proposed model is capable of 1) selecting the proper modes to offer progression subject to the feasible combination of the progression bands, 2) fully accounting for the operational features of passenger cars and buses on the mixed arterial traffic flows, and 3) formulating the mutual interactions between passenger cars and buses and their evolution along the arterial.
- **Dual-modal progression for a long arterial with optimally decomposed segments:** This model is proposed to integrate the formulations for all above models and allow the users to execute all embedded functions when needed. By considering the interactions between turning and through movements of both buses and passenger cars, the proposed integrated model can concurrently determine the progression design boundaries, and the progression bandwidths respectively for buses and passenger cars over each segment within the target arterial.

In brief, this study is focused on developing a multi-functional integrated system for design of arterial signal progression. The proposed system with its embedded functions allows users to exercise their preferred progression design, based on actual key system features and various critical traffic related factors, such as geometric constraints, a larger number of intersections, volume distributions for different transportation modes, flow interferences from crossing street at major intersections; and unbalanced directional flows along the arterial.

Chapter 4: Signal Progression Design for an Arterial with Bay Length Constraint

4.1 Introduction

This chapter presents the model formulations for signal progression design for an arterial with the constraints of insufficient bay length and short links. The proposed model will be capable of addressing the following issues: 1) Contending with heavy left-turn volumes moving out from or onto the arterial under the constraint of insufficient turning bay length; 2) Preventing the formation of excessive queues at near-saturated intersections and on short links along the target arterial.

Section 4.2 presents the critical issues and modelling methodology associated with design of such a system. Section 4.3 introduces the formulations of Model I aiming to design of concurrent signal progression for through and turning movements. Section 4.4 presents the formulations of Model II, a signal design model for arterials having near-saturated intersections and short links. Concluding comments along with additional desirable functions will be provided in Section 4.5.

4.2 Critical issues and modelling methodology

--- *Left-turn volumes and limited bay lengths*

As is well recognized, contending with congestion on major urban arterials has long been a priority task for traffic professionals. However, most studies on such issues focus mainly on the efficiency for through movements, but not for the left-turn movements albeit the likely presence of considerable left-turn volumes at some of the arterial's major intersections. In review of the related literature, it is noticeable that there exist only very limited studies on designing signal

progression concurrently for through and turning movements. Among those, Yang et al. (2015) proposed a multi-path progression model that concurrently provides progression bands for several pre-identified vehicle paths to accommodate the heavy turning and through flows along the arterial. However, the proposed model requires the knowledge of volumes for all paths, which is quite challenging in view of existing data collection methods. Moreover, to ensure the progression for both through and left-turn flows on arterials of heavy volume, the following two issues, which may degrade the progression quality, remain to be tackled by the traffic community.

First, in optimizing the offsets for the progression, not adequately accounting for the available bay length at some major intersections may result in turning overflows and rapid queue formation. The queues from a large volume of through vehicles not within the progression band may also cause blockage for left-turn vehicles to enter the bay. Such vehicles may come from the major approach or crossing streets at the upstream intersection. On the other hand, excessive left-turn volumes may also cause queue to spill over the turning bay and consequently block some through lanes. The anticipated level of progression via the provided bands for the entire arterial may thus be degraded or practically unusable due to such spillback or blockage from one or more turning bays.

Secondly, the potentially significant negative impacts from the left-turn bay spillback further justify the need to provide progression operations for not only the through movements but also left-turn flows, especially at those arterial intersections serving two crossing major roads and accommodating heavy turning volumes.

--- *Near-saturated intersections and short links*

Although traffic conditions around near-saturated intersections and on short links are usually complex and may negatively impact the effectiveness of a progression system, some critical issues have not been addressed in the existing signal design models. For an arterial with several pairs of closely located intersections, the queues on a short link should be constrained to be less than the link length so as to prevent the occurrence of gridlocks at its upstream intersection. On the other hand, queues at near-saturated intersections should also be minimized to reduce vehicle delays and to prevent their likely interruption of the progression bands designed for the entire arterial. The core concept of such a design is to redistribute excessive queues at some locations to other less congested intersections or approaches by optimally designing phase sequence and progression offsets.

4.3 Formulation of Model I

To contend with the issues of heavy left-turn volumes and the limited left-turn bay length in design of an arterial progression plan, this section presents a base model to concurrently provide progression to through and left-turn vehicles via the optimized offsets and phase sequences under the bay length constraint. The proposed model features its capability in: 1) designing concurrent progression of through movements and left-turn movements, 2) considering mutual blockage between through and left-turn movements due to the limited bay length, and 3) accounting for the impact of residual queue consisting of turn-in vehicles on the designed through progression.

4.3.1 Progression of through vehicles

To formulate the through progression band, one can directly extend the notion of MAXBAND with the following constraints.

$$w_i \geq \tau_i^t, w_i + b_t \leq g_i^t \tag{4.1}$$

$$\bar{w}_i \geq \bar{\tau}_i^t, \bar{w}_i + \bar{b}_t \leq \bar{g}_i^t \tag{4.2}$$

Eqs. (4.1) and (4.2) are interference constraints; where $g_i^t\left(\bar{g}_i^t\right)$ is the green time for outbound (inbound) through movement; $b_t\left(\bar{b}_t\right)$ represents the through bandwidth for outbound (inbound) direction; $w_i\left(\bar{w}_i\right)$ denotes the time difference between the start of the through phase and the start of the outbound (inbound) band; and $\tau_i^t\left(\bar{\tau}_i^t\right)$ denotes the estimated discharging time of the residual queues for the outbound(inbound) through movement at intersection *i*. This set of constraints is developed to ensure the progression band to be within the green duration. Note that the queue discharging time, varying in nature, has been accounted for in the model.

Eqs. (4.3) - (4.4) are progression constraints, derived to present the progress of the through bands between intersections:

$$\theta_i + \left(1-\xi_i\right)\bar{g}_i^l + w_i + t_i + n_i \geq \theta_{i+1} + \left(1-\xi_{i+1}\right)\bar{g}_{i+1}^l + w_{i+1} \tag{4.3}$$

$$\theta_i + \left(1-\bar{\xi}_i\right)g_i^l + \bar{w}_i + \bar{t}_i + \bar{n}_i \geq \theta_{i+1} + \left(1-\bar{\xi}_{i+1}\right)g_i^l + \bar{w}_{i+1} \tag{4.4}$$

Where θ_i is the offset at intersection *i* for the arterial phases (including through and left-turn phases for the major arterial); $\xi_i\left(\bar{\xi}_i\right)$is a binary variable indicating the phase sequence at intersection *i*, which equals 1 if the outbound (inbound) through phase is ahead of the inbound (outbound) left-turn phase; $g_i^l\left(\bar{g}_i^l\right)$ is the green time for outbound (inbound) through movement;

$t_i(\bar{t}_i)$ represents the travel time from intersection $i(i+1)$ to $i+1(i)$; $n_i(\bar{n}_i)$ is a set of integer variables to indicate the number of cycles.

4.3.2 Local progression for vehicle flows between two adjacent intersections

To account for the impact of vehicle queues on the progression, this study proposes a set of formulations to estimate the number of vehicles forming the left-turn and through queues at an intersection, based on the offsets between two adjacent intersections and signal settings. As shown in Figure 4.1, vehicles not within the local progression band between two adjacent intersections will need to stop at the downstream intersection and form the vehicle queues. Such vehicles contributing to the through queue formation at intersection *i* mainly come from the following three traffic streams (see Figure 4.1):

- m_1 : arterial through movement at two adjacent intersections
- m_2 : left-turn vehicles from the crossing street which take the through movement at the downstream intersection
- m_3 : right-turn vehicles from the crossing street which take the through movement at the upstream intersection

Similarly, the vehicles contributing to the left-turn queue at intersection *i* mainly come from below traffic stream:

- m_4 : through vehicles from the upstream intersection which take the left-turn movement at the downstream intersection

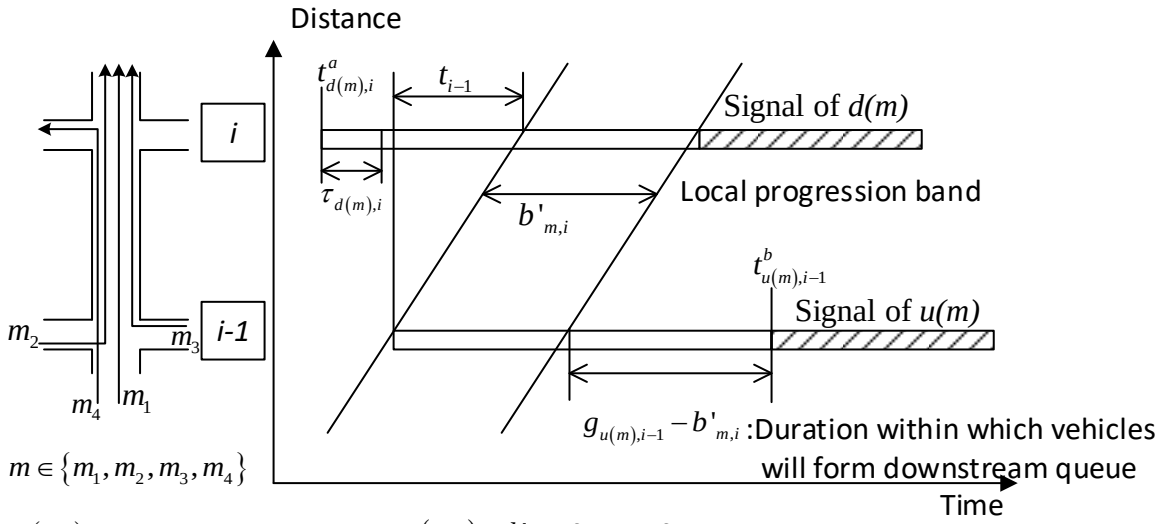

$u(m_1) = t$: through $\quad u(m_2) = l'$: left-turn from crossing street

$d(m_1) = t$: through $\quad d(m_2) = t$: through

$u(m_3) = r'$: right-turn from crossing street $\quad u(m_4) = t$: through

$d(m_3) = t$: through $\quad d(m_4) = l$: left-turn

Figure 4.1 Local progression band between two intersections

To compute the number of vehicles within each of above streams that need to stop at the downstream intersection, e.g. for outbound direction, one can estimate a local bandwidth for each of the four traffic streams with Eq. (4.5):

$$b'_{m,i} = \min\left(t^b_{d(m),i}, t^b_{u(m),i-1} + t_{i-1}\right) - \max\left(t^a_{d(m),i} + \tau_{d(m),i}, t^a_{u(m),i-1} + t_{i-1}\right) \qquad \forall m \in \{m_1, m_2, m_3, m_4\} \tag{4.5}$$

where $b'_{m,i}$ represents the duration within which vehicles from traffic stream m can traverse intersections i-1 and i without stop; $d(m)$ and $u(m)$ refer to the downstream and

upstream movements of traffic stream *m*; $\tau_{d(m),i}$ is the queue clearance time of movement $d(m)$ at intersection *i* (in cycle); t_i refers to the travel time from intersection *i* to *i*+1 (in cycle); $t^a_{d(m),i}$ and $t^b_{d(m),i}$ denote the start and end of the green phase for downstream movement *m* at intersection *i*, respectively; and $t^a_{u(m),i}$ and $t^b_{u(m),i}$ are the start and end of the green phase for upstream movements. Eq. (4.5) calculates the local bandwidth by identifying the starting and ending time. The starting time of the local progression band is expressed with $\max\left(t^a_{d(m),i}+\tau_{d(m),i}, t^a_{u(m),i-1}+t_{i-1}\right)$, which selects the later time between the arrival time of traffic stream *m* at the downstream intersection and the queue clearance time of the movement associated with traffic stream *m*. With the same token, the ending time of the local progression band is denoted by $\min\left(t^b_{d(m),i}, t^b_{u(m),i-1}+t_{i-1}\right)$, which selects the earlier time between the end of the downstream green phase and the last arrival of the vehicle flow to the downstream intersection.

4.3.3 Queue length in the left-turn bay

With the information of local bands for left-turn and through movements, one can calculate the number of vehicles that would join the queue in left-turn and through lanes. In the outbound direction, the queues in the left-turn bay at intersection *i*+1 consist of mainly vehicles from intersection *i* but not experiencing $b_{m4,i+1}$. Therefore, the estimated queue length at the onset of a left-turn phase can be expressed as follows:

$$QL^l_{i+1} = \frac{C}{3600 n^l_{i+1}} V^t_i r^l_{i+1} \times \left(g^t_i - b_{m4,i+1}\right) \tag{4.6}$$

Where QL_i^l denotes the queue length in number of vehicles for the left-turn movement at intersection *i*; *C* represents the cycle length; V_i^t represents the traffic volume of through movement at intersection *i*; n_{i+1}^l refers to the number of left-turn lanes at intersection i+1; and r_i^l refers to the left-turn ratio from arterial at intersection *i*. Eq. (4.6) calculates the number of vehicles passing the upstream intersection within the green phase but not within the local progression band for left-turn at the downstream intersection, based on the intersection's volume counts and turning ratios.

To prevent the impacts of queue spillback from the left-turn bay on the through lanes, one can present the following equation:

$$QL_{i+1}^l \frac{s}{s - V_{i+1}^l / n_{i+1}^l} \times \alpha \le BL_{i+1} \tag{4.7}$$

Where *s* is the saturation flow rate, BL_i is the bay length at intersection *i*, and α is a robustness factor greater than 1 that represents the sensitivity of volume fluctuation to the occurrence of queue spillback. The left-hand-side represents the estimated maximum queue length during a cycle.

The queue discharging time for left-turn queues can then be estimated with the obtained queue length with Eq. (4.11) as follows:

$$\tau_{i+1}^l = QL_{i+1}^l \frac{3600 / C}{s - V_i^l / n_{i+1}^l} \times \alpha \tag{4.8}$$

Following the same logic, one can develop similar constraints as Eqs. (4.6) - (4.8) for the inbound direction.

4.3.4 Queue length in the through lanes

In the outbound direction, the queues in the through lanes at intersection *i*+1 consist of through vehicles from intersection *i* not experiencing the local through progression, turning-in vehicles from intersection *i* not within $b_{m2,i}$, and right-turn vehicles from the side street at intersection *i* not within $b_{m3,i}$. Hence the estimated queue length at the onset of the through phase can be expressed as follows:

$$QL_{i+1}^{t} = \frac{C}{3600 n_{i+1}^{t}} \left(V_i^t r_{i+1}^t \times \left(g_i^t - b_{m1,i+1} \right) + V'^{l}_{i} r_{i+1}^t \times \left(g'^{l}_{i} - b_{m2,i+1} \right) + V'^{r}_{i} r_{i+1}^t \times \left(g'^{r}_{i} - b_{m3,i+1} \right) \right) \qquad (4.9)$$

Where, $V'^{l(r)}_{i}$ is the left-turn (right-turn) volume from side street to the outbound direction of the arterial at intersection *i*; $g'^{l(r)}_{i}$ is the green time assigned to left-turn (right-turn) volume from the side street. In Eq. (4.9), $V_i^t r_{i+1}^t \times \left(g_i^t - b_{m1,i+1} \right)$ denotes upstream through vehicles which contributes to the downstream through queue; $V'^{l}_{i} r_{i+1}^t \times \left(g'^{l}_{i} - b_{m2,i+1} \right)$ and $V'^{r}_{i} r_{i+1}^t \times \left(1 - b_{m3,i+1} \right)$ denote upstream left-turn and right-turn vehicles from side streets that will join the queue on the through lanes at the downstream intersection.

To prevent the blockage to the left-turn bay due to queues on the through lanes, one can introduce Eq. (4.10) as follows,

$$QL_{i+1}^{t} \frac{s}{s - V_{i+1}^t / n_{i+1}^t} \times \alpha \le BL_{i+1} \qquad (4.10)$$

The queue discharging time for the through movement can then be estimated with the obtained queue length with Eq. (4.14) as follows,

$$\tau_{i+1}^{t} = QL_{i+1}^{t} \frac{3600/C}{s - V_{i+1}^{t}/n_{i+1}^{t}} \times \alpha \tag{4.11}$$

Following the same logic, one can develop similar constraints as Eqs. (4.9) - (4.11) for the inbound direction.

4.3.5 Objective function

The objective function of Model I is to maximize the sum of weighted through and local left-turn bands, which can be expressed as below:

$$\max \sum_i V_i^t b_t + \sum_i \bar{V}_i^t \bar{b}_t + \sum_i V_i^l b_{m4,i}^l + \sum_i \bar{V}_i^l \bar{b}_{m4,i}^l + \sum_i V''^l_i b_{m2,i}^l + \sum_i \bar{V}''^l_i \bar{b}_{m2,i}^l \tag{4.12}$$

To ensure the existence of a reasonable bandwidth for passenger cars in the low-volume direction, one shall define the directional balance constraints as follows:

$$(1-K)\bar{b}_t \geq (1-K)Kb_t \tag{4.13}$$

where $K = \bar{V}_c / V_c$ is a directional balance factor.

In brief, Model I can be summarized as follows:

$$\max \sum_i V_i^t b_t + \sum_i \bar{V}_i^t \bar{b}_t + \sum_i V_i^l b_{m4,i}^l + \sum_i \bar{V}_i^l \bar{b}_{m4,i}^l + \sum_i V''^l_i b_{m2,i}^l + \sum_i \bar{V}''^l_i \bar{b}_{m2,i}^l$$

s.t.

$$(1-K)\bar{b}_c \geq (1-K)Kb_c$$

Progression of through vehicles along the arterial:

$$w_i \geq \tau_i^t, w_i + b_t \leq g_i^t$$

$$\bar{w}_i \geq \bar{\tau}_i^t, \bar{w}_i + \bar{b}_t \leq \bar{g}_i^t$$

$$\theta_i + \left(1-\chi_i\right)\bar{g}_i^l + w_i + t_i + n_i \geq \theta_{i+1} + \left(1-\chi_{i+1}\right)\bar{g}_{i+1}^l + w_{i+1}$$

$$\theta_i + \left(1-\bar{\chi}_i\right)g_i^l + \bar{w}_i + \bar{t}_i + \bar{n}_i \geq \theta_{i+1} + \left(1-\bar{\chi}_{i+1}\right)g_i^l + \bar{w}_{i+1}$$

Local progression and queue length calculation:

$$b'_{m,i} = \min\left(t^b_{d(m),i}, t^b_{u(m),i-1} + t_{i-1}\right) - \max\left(t^a_{d(m),i} + \tau_{d(m),i}, t^a_{u(m),i-1} + t_{i-1}\right) \qquad \forall m \in \{m_1, m_2, m_3, m_4\}$$

$$QL^l_{i+1} = \frac{C}{3600 n^l_{i+1}} V^t_i r^l_{i+1} \times \left(g^t_i - b_{m4,i+1}\right)$$

$$QL^l_{i+1} \frac{s}{s - V^l_{i+1}/n^l_{i+1}} \times \alpha \leq BL_{i+1}$$

$$\tau^l_{i+1} = QL^l_{i+1} \frac{3600/C}{s - V^l_i / n^l_{i+1}} \times \alpha$$

$$QL^t_{i+1} = \frac{C}{3600 n^t_{i+1}} \left(V^t_i r^t_{i+1} \times \left(g^t_i - b_{m1,i+1}\right) + V'^l_i r^t_{i+1} \times \left(g'^l_i - b_{m2,i+1}\right) + V'^r_i r^t_{i+1} \times \left(g'^r_i - b_{m3,i+1}\right)\right)$$

$$QL^t_{i+1} \frac{s}{s - V^t_{i+1}/n^t_{i+1}} \times \alpha \leq BL_{i+1}$$

$$\tau^t_{i+1} = QL^t_{i+1} \frac{3600/C}{s - V^t_{i+1}/n^t_{i+1}} \times \alpha$$

$$\bar{b}'_{m,i} = \min\left(\bar{t}^b_{d(m),i}, \bar{t}^b_{u(m),i+1} + \bar{t}_i\right) - \max\left(\bar{t}^a_{d(m),i} + \bar{\tau}_{d(m),i}, \bar{t}^a_{u(m),i+1} + \bar{t}_i\right) \qquad \forall m \in \{\bar{m}_1, \bar{m}_2, \bar{m}_3, \bar{m}_4\}$$

$$\bar{QL}^l_i = \frac{C}{3600 \bar{n}^l_i} \bar{V}^t_{i+1} \bar{r}^l_i \times \left(\bar{g}^t_{i+1} - b_{m4,i}\right)$$

$$\bar{QL}^l_i \frac{s}{s - \bar{V}^l_i / \bar{n}^l_i} \times \alpha \leq \bar{BL}_i$$

$$\bar{\tau}^l_i = \bar{QL}^l_i \frac{3600/C}{s - \bar{V}^l_i / \bar{n}^l_i} \times \alpha$$

$$\bar{QL}_i^t = \frac{C}{3600 n_i^t}\left(\bar{V}_{i+1}^t \bar{r}_i^t \times \left(\bar{g}_{i+1}^t - \bar{b}_{m1,i}\right) + \bar{V}'^{l}_{i+1}\, \bar{r}_i^t \times \left(g'^{l}_{i+1} - b_{m2,i}\right) + \bar{V}'^{r}_{i}\, \bar{r}_{i+1}^t \times \left(g'^{r}_{i+1} - b_{m3,i}\right)\right)$$

$$\bar{QL}_i^t \frac{s}{s - \bar{V}_i^l / \bar{n}_i^l} \times \alpha \le \bar{BL}_i$$

$$\bar{\tau}_i^t = \bar{QL}_i^t \frac{3600 / C}{s - \bar{V}_i^t / \bar{n}_i^t} \times \alpha$$

4.4 Formulation of Model II

Model II is to address the issue of excessive queue lengths on short links and at near saturated intersections when such scenarios exist within the control segment. In addition to formulations in Model I, the enhanced feature in Model II include: 1) limiting the queue length on each link not to exceed the link length; 2) distributing the excessive queue to less congested locations.

4.4.1 Links with short lengths

Note that to minimize the likelihood of having queue spillback on a short link between intersections, one shall set the following constraints:

$$QL_{i+1}^t \frac{s}{s - V_{i+1}^t / n_{i+1}^t} \times \alpha \le LL_i \tag{4.14}$$

$$QL_{i+1}^l \frac{s}{s - V_{i+1}^l / n_{i+1}^l} \times \alpha \le LL_{i+1} \tag{4.15}$$

Where, LL_i is the link length between intersection i and i+1.

4.4.2 Queue distribution among the intersections on the arterial

To reflect the queue distribution between intersections, one can specify the following index, based on the queue length and link length between each pair of intersections.

$$e = \sum_i \frac{1}{\beta - V_i^{total} / s} \times \frac{\max\left(QL_{i+1}^t, QL_{i+1}^l\right)}{LL_i} \tag{4.16}$$

Where V_i^{total} refers to the critical lane volume at intersection i; and β represents a maximum acceptable saturation degree which is less than 1. In Eq. (4.16), a higher queue/link ratio at a more saturated intersection will contribute more significantly to the queue distribution index, which indicates having longer queue lengths at those critical locations. The signal plan, producing a smaller value for this index, will distribute the queues more effectively so that the total delay is less sensitive to traffic volume surge.

Following the same logic, one can develop similar constraints as Eqs. (4.14) - (4.16) for the inbound direction.

4.4.3 Objective function

The objective function of Model II is to maximize the weighted bandwidth for through and left-turn movements but minimize the queue distribution index, which can be expressed as follows:

$$\max \sum_i V_i^t b_t + \sum_i \bar{V}_i^t \bar{b}_t + \sum_i V_i^l b_{m4,i}^l + \sum_i \bar{V}_i^l \bar{b}_{m4,i}^l + \sum_i V'^l_i b_{m2,i}^l + \sum_i \bar{V}'^l_i \bar{b}_{m2,i}^l - \gamma_e e \tag{4.17}$$

Where γ_e is a small weighting factor to make sure that the band maximization has a higher priority than optimizing queue distribution.

In brief, Model II can be summarized as follows:

$$\max \sum_i V_i^t b_t + \sum_i \bar{V}_i^t \bar{b}_t + \sum_i V_i^l b_{m4,i}^l + \sum_i \bar{V}_i^l \bar{b}_{m4,i}^l + \sum_i V'^l_i b_{m2,i}^l + \sum_i \bar{V}'^l_i \bar{b}_{m2,i}^l - \gamma_e e$$

s.t.

$$(1-K)\bar{b}_c \geq (1-K) K b_c$$

Progression of through vehicles along the arterial:

$$w_i \geq \tau_i^t, w_i + b_t \leq g_i^t$$

$$\bar{w}_i \geq \bar{\tau}_i^t, \bar{w}_i + \bar{b}_t \leq \bar{g}_i^t$$

$$\theta_i + (1-\chi_i)\bar{g}_i^l + w_i + t_i + n_i \geq \theta_{i+1} + (1-\chi_{i+1})\bar{g}_{i+1}^l + w_{i+1}$$

$$\theta_i + (1-\bar{\chi}_i) g_i^l + \bar{w}_i + \bar{t}_i + \bar{n}_i \geq \theta_{i+1} + (1-\bar{\chi}_{i+1}) g_i^l + \bar{w}_{i+1}$$

Local progression and queue length calculation:

$$b'_{m,i} = \min\left(t_{d(m),i}^b, t_{u(m),i-1}^b + t_{i-1}\right) - \max\left(t_{d(m),i}^a + \tau_{d(m),i}, t_{u(m),i-1}^a + t_{i-1}\right) \qquad \forall m \in \{m_1, m_2, m_3, m_4\}$$

$$QL_{i+1}^l = \frac{C}{3600 n_{i+1}^l} V_i^t r_{i+1}^l \times \left(g_i^t - b_{m4,i+1}\right)$$

$$QL_{i+1}^l \frac{s}{s - V_{i+1}^l / n_{i+1}^l} \times \alpha \leq BL_{i+1}$$

$$\tau_{i+1}^l = QL_{i+1}^l \frac{3600/C}{s - V_i^l / n_{i+1}^l} \times \alpha$$

$$QL_{i+1}^t = \frac{C}{3600 n_{i+1}^t}\left(V_i^t r_{i+1}^t \times \left(g_i^t - b_{m1,i+1}\right) + V'^l_i r_{i+1}^t \times \left(g'^l_i - b_{m2,i+1}\right) + V'^r_i r_{i+1}^t \times \left(g'^r_i - b_{m3,i+1}\right)\right)$$

$$QL_{i+1}^t \frac{s}{s - V_{i+1}^t / n_{i+1}^t} \times \alpha \leq BL_{i+1}$$

$$\tau_{i+1}^{t} = QL_{i+1}^{t} \frac{3600 / C}{s - V_{i+1}^{t} / n_{i+1}^{t}} \times \alpha$$

$$\bar{b}'_{m,i} = \min\left(\bar{t}_{d(m),i}^{b}, \bar{t}_{u(m),i+1}^{b} + \bar{t}_{i}\right) - \max\left(\bar{t}_{d(m),i}^{a} + \bar{\tau}_{d(m),i}, \bar{t}_{u(m),i+1}^{a} + \bar{t}_{i}\right) \qquad \forall m \in \left\{\bar{m}_1, \bar{m}_2, \bar{m}_3, \bar{m}_4\right\}$$

$$\bar{QL}_{i}^{l} = \frac{C}{3600 \bar{n}_{i}^{l}} \bar{V}_{i+1}^{t} \bar{r}_{i}^{l} \times \left(\bar{g}_{i+1}^{t} - b_{m4,i}\right)$$

$$\bar{QL}_{i}^{l} \frac{s}{s - \bar{V}_{i}^{l} / \bar{n}_{i}^{l}} \times \alpha \le \bar{BL}_{i}$$

$$\bar{\tau}_{i}^{l} = \bar{QL}_{i}^{l} \frac{3600 / C}{s - \bar{V}_{i}^{l} / \bar{n}_{i}^{l}} \times \alpha$$

$$\bar{QL}_{i}^{t} = \frac{C}{3600 n_{i}^{t}} \left(\bar{V}_{i+1}^{t} \bar{r}_{i}^{t} \times \left(\bar{g}_{i+1}^{t} - \bar{b}_{m1,i}\right) + \bar{V}'^{l}_{i+1} \bar{r}_{i}^{t} \times \left(g'^{l}_{i+1} - b_{m2,i}\right) + \bar{V}'^{r}_{i} \bar{r}_{i+1}^{t} \times \left(g'^{r}_{i+1} - b_{m3,i}\right)\right)$$

$$\bar{QL}_{i}^{t} \frac{s}{s - \bar{V}_{i}^{l} / \bar{n}_{i}^{l}} \times \alpha \le \bar{BL}_{i}$$

$$\bar{\tau}_{i}^{t} = \bar{QL}_{i}^{t} \frac{3600 / C}{s - \bar{V}_{i}^{t} / \bar{n}_{i}^{t}} \times \alpha$$

$$QL_{i+1}^{t} \frac{s}{s - V_{i+1}^{t} / n_{i+1}^{t}} \times \alpha \le LL_{i}$$

$$QL_{i+1}^{l} \frac{s}{s - V_{i+1}^{l} / n_{i+1}^{l}} \times \alpha \le LL_{i}$$

$$e = \sum_{i} \frac{1}{\beta - V_{i}^{total} / s} \times \frac{\max\left(QL_{i+1}^{t}, QL_{i+1}^{l}\right)}{LL_{i}}$$

$$\bar{QL}_{i}^{t} \frac{s}{s - \bar{V}_{i}^{t} / \bar{n}_{i}^{t}} \times \alpha \le \bar{LL}_{i}$$

$$\bar{QL}_{i}^{l} \frac{s}{s - \bar{V}_{i}^{l} / \bar{n}_{i}^{l}} \times \alpha \le \bar{LL}_{i}$$

Distributing queues to less congested locations:

$$\bar{e} = \sum_i \frac{1}{\beta - \bar{V}_i^{total} / s} \times \frac{\max\left(\bar{Q}\bar{L}_i^t, \bar{Q}\bar{L}_i^l\right)}{\bar{L}\bar{L}_i}$$

4.5 Closure

This chapter has presented the model formulations for signal progression design for an arterial under the constraint of insufficient bay length. Model I focuses on contending with heavy left-turn volumes, moving out from or onto the arterial under the constraint of insufficient turning bay length. With the proposed constraints, the queue length on the left-turn bay of each intersection is expected to be within the bay length and the through queues are not expected to cause blockages to left-turn bays. The sum of through and local left-turn bands, weighted by the corresponding traffic volumes, is maximized in the objective function of Model I.

Model II has been developed to yield balanced queues among all critical locations and restrain the queue length at the short links. With the specified objective function, Model II will minimize a queue distribution index to distribute the queues more effectively so that the total delay is less sensitive to traffic volume surge.

Chapter 5: Decomposing a long arterial into subsegments for maximizing progression efficiency.

5.1 Introduction

The formulations for Model I and Model II developed in Chapter 4 aim to address various issues that are associated with the turning volumes, left-turn bays, near-saturated intersections, and short links. However, those optimization models for two-way progression may yield undesirably narrow bandwidth for traffic flows if a large number of congested intersections need to be included in the arterial's control system. Over the past decades, despite the significant progress made by traffic researchers on the subject of the arterial signal optimization, an efficient and reliable tool that can optimally decompose a congested arterial corridor into the optimal number of progression groups so as to maximize its overall traffic efficiency is not yet available in the literature.

Hence, this chapter presents the formulations for an optimization model that is designed to decompose a congested long arterial into an optimal number of subsegments so as to maximize overall traffic efficiency. Taking advantage of the formulations in Chapter 4, the proposed model will have the following key features: 1) concurrently decomposing the arterial into short segments, and optimizing their signal offsets as well as phase sequences; 2) maximizing the sum of progression bandwidths weighted by traffic volume at each intersection; 3) minimizing the expected delay at each decomposition point over the arterial; and 4) accounting for the impacts of queues or spillback at short links or turning bay in optimizing the progression band; and 5) distributing an arterial's excessive traffic queues to less congested intersections.

5.2 Critical issues and modelling methodology

To maximize the effectiveness of traffic progression over a long arterial with the optimized decomposition and signal plan, the proposed model should be capable of addressing the following issues.

--- *Trade-off between the length of a progression segment and its bandwidth*

Most existing methods for signal coordination can generate an acceptable bandwidth for traffic progression if the target arterial segment includes a small number of intersections. Figure 5.1 (a) illustrates the bandwidth for the two-way progression bands for an arterial segment of three intersections. Such a bandwidth is noticeably getting narrower, or even does not exist if the number of intersections covered in the control boundaries is increased to a critical level, as shown in Figure 5.1 (b)-(c).

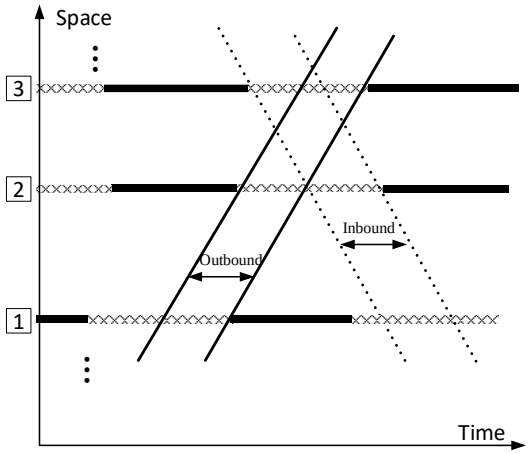

(a)

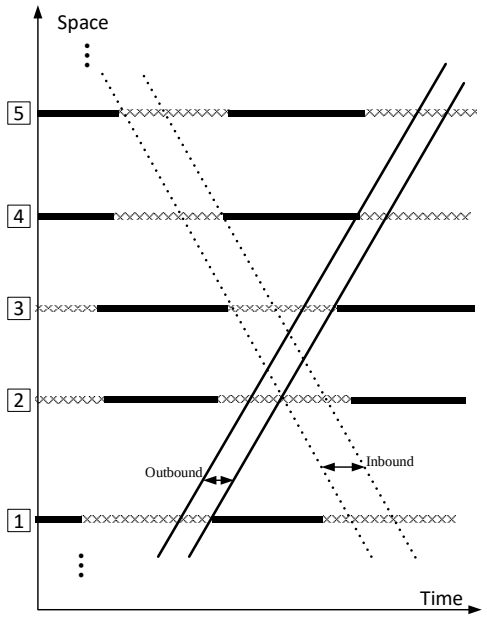

(b)

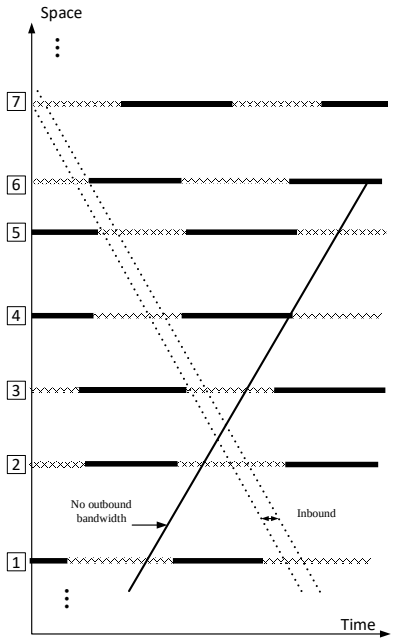

(c)

Figure 5.1 Maximized two-way progression bandwidth with various numbers of intersections within the control segment: a) 3 intersections; b) 5 intersections; c) 7 intersections.

Therefore, an arterial with a large number of intersections needs to be optimally decomposed into multiple shorter segments to ensure that each can be so designed to have a practically effective band.

--- *Connection between two consecutive progression segments*

The progression efficiency along the entire arterial would be impacted not only by the progression bandwidth for each segment, but also by how those consecutive progression bands between the neighboring decomposed segments are connected. Hence, the method for optimal decomposition of the target arterial shall also account for the task of optimizing the connection pattern between neighboring segments.

--- *Impacts of queue formation on signal progression*

Note that vehicles, not experiencing signal progression, may form queues at some intersections within each control segment. The size of such queues may vary with not only the bandwidth of the traffic progression, but also the offset between two adjacent intersections. One can thus derive such queue length with formulations introduced in Section 4.3.

--- *Left-turn bay spillback and blockage*

At intersections with short left-turn bays, it may incur mutual blockage between the through queues and spillback flows from the left-turn bay. Hence, to identify the optimal offsets for traffic progression, it is imperative to account for such mutual blockages at critical arterial intersections.

--- *Excessive queue lengths at potentially oversaturated intersections*

Those short links or highly congested intersections on an arterial are most likely to experience the state of queue spillback or oversaturation due to the fluctuation of daily time-varying volumes. Hence, the signal plan and arterial decomposition shall be so designed to redistribute the queues at those critical locations to ensure the effectiveness of traffic progression. The formulations for such estimation can take advantage of the model developed in section 4.4.

5.3 Formulations of Model III

In response to the aforementioned critical issues, this study presents a two-stage signal optimization model which can concurrently decompose a long arterial into the optimal number of segments, and connect them with the set of optimized offsets and phase plans to maximize the

progression efficiency, based on the geometric conditions and pre-defined critical intersections. The framework for the entire model and its key components is shown in Figure 5.2.

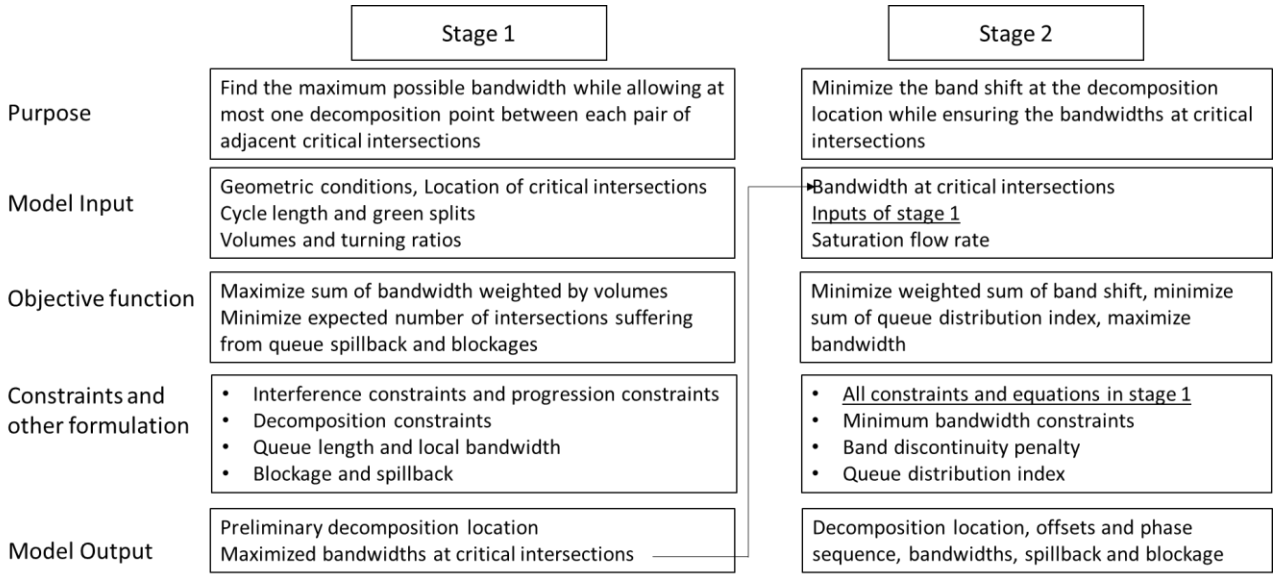

Figure 5.2 Structure of the proposed two-stage model for design of optimal arterial decomposition and traffic progression

Stage 1 is to determine the maximum possible bandwidth at critical intersections and yield an initial solution for the decomposition plan under a pre-specified constraint, i.e., only one decomposition location between two adjacent critical intersections. Note that to have the identical set of maximized bandwidths for all critical intersections, Stage 1 model may yield multiple solutions for the decomposition locations, the intersection offsets, and band connection states between two progression segments. Thus, the maximized bandwidth at each critical intersection obtained in Stage 1 will serve as an input for Stage 2 model to select the optimal decomposition location so that the band discontinuity can be minimized with the optimized phase sequence and signal offsets. In brief, the entire two-stage model is designed to execute the following tasks:

- Decomposing the arterial into several segments and generating a maximized progression band for each segment based on the pre-specified critical intersections;
- Estimating traffic queues on both the left-turn bays and through lanes on the arterial, consisting of vehicles coming from the major road and the crossing street;
- Identifying those left-turn bays that are likely to incur queue spillback or blocked by the through vehicles under the existing signal settings;
- Analyzing the temporal relationship between two neighboring progression bands; and
- Computing the temporal and spatial distribution of queue patterns at each arterial intersection under the optimized decomposition and signal plans.

These sets of formulations developed for performing the above tasks are presented hereafter with the key notations shown in Figure 5.3.

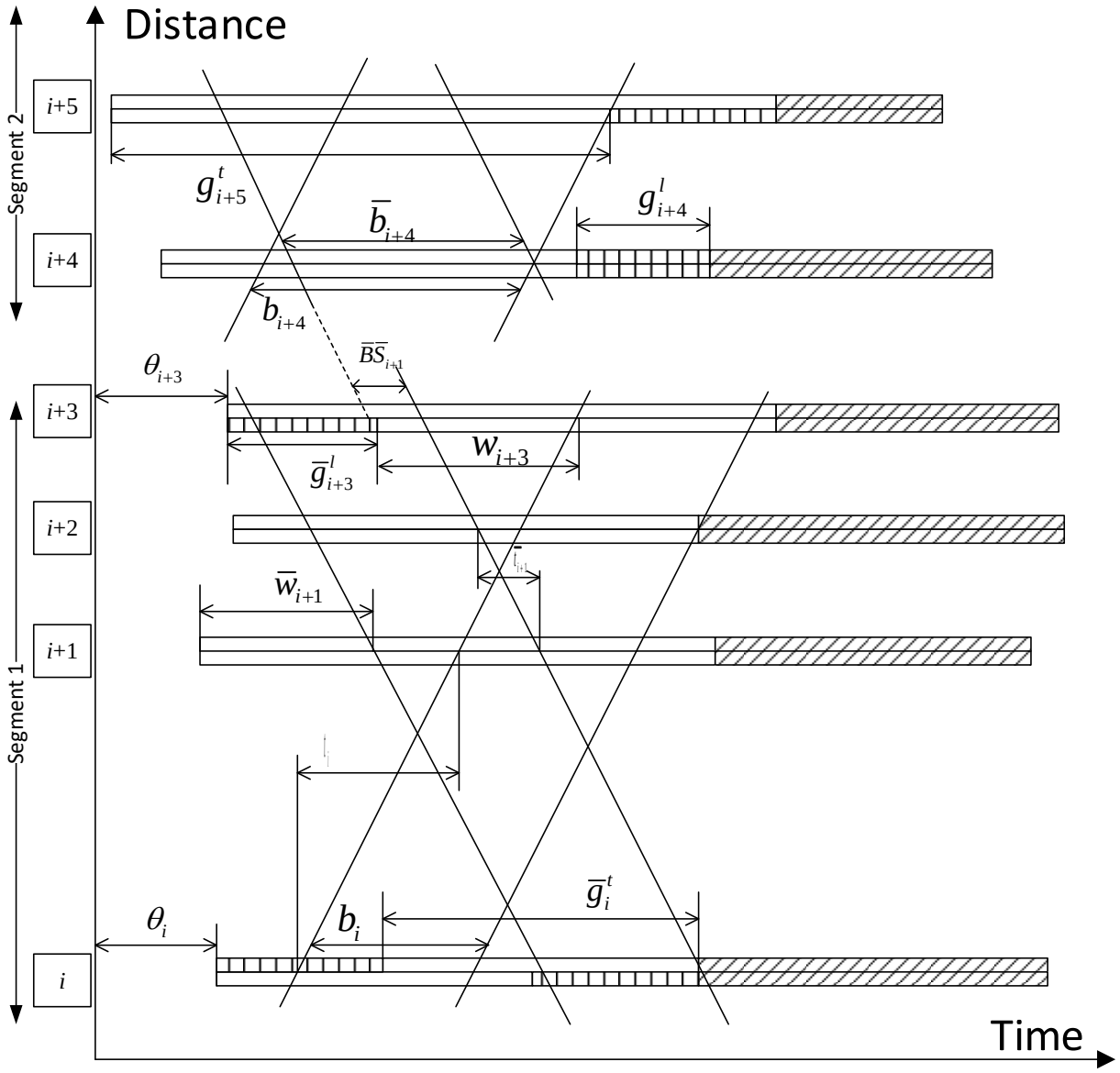

Figure 5.3 Key notations adopted in the proposed model

5.3.1 Formulations for Decomposition of the Long Arterial

First, one can employ a set of integer variables, x_i, to indicate the progression segment that intersection *i* belongs to. For example, as shown in Figure 3, if intersections *i* through *i*+3 are

assigned to Segment 1 and intersections *i*+4 and *i*+5 belong to segment 2, $x_i = x_{i+1} = x_{i+2} = x_{i+3} = 1$ and $x_{i+4} = x_{i+5} = 2$. Then, the following constraints are derived to regulate the decomposition along the arterial:

$$x_i - x_{i+1} \le b_{i+1} - b_i \le x_{i+1} - x_i \tag{5.1}$$

$$0 \le x_{i+1} - x_i \le 1 \tag{5.2}$$

$$0 \le x_{cr_k} - x_{cr_{k+1}} \le 1 \tag{5.3}$$

$$x_{i+3} - x_i \le 1 \tag{5.4}$$

where $b_i\left(\bar{b}_i\right)$ denotes the through bandwidth at intersection *i* and cr_k denotes the *k*th critical intersection. Eq. (5.1) functions to ensure that the bandwidths at two adjacent intersections must be identical if they are clustered to the same progression segment. Eq. (5.2) is to ensure that the segment numbering used to classify each intersection can only be the identical or one more unit than that of its upstream one. Eq. (5.3) is developed to limit the difference of the segment numbers between two adjacent critical intersections so that only one decomposition point may exist between two neighboring critical intersections. Eq. (5.4) is derived to set the minimum segment length in terms of the number of intersections (i.e., 3 intersections in this study).

5.3.2 Formulating the relation between traffic flow patterns and left-turn bay spillback and blockage

It is noticeable that left-turn bay spillback or blockage may inevitably exist on a long arterial segment. However, the occurrence of such scenarios should be minimized by optimizing the signal offsets and phase sequences. With the information the available queue length estimated with the formulations in section 4.3, one can estimate whether a left-turn bay spillback or blockage may occur in the outbound direction with Eqs. (9)-(10):

$$QL_i^l h \frac{s}{s - V_{m,i}} \le L_i + M \times \gamma_i^s \tag{5.5}$$

$$QL_i^t h \frac{s}{s - V_{m,i}} \le L_i + M \times \gamma_i^b \tag{5.6}$$

where γ_i^s is a binary variable which equals 1 if a left-turn bay spillback would occur at intersection *i*; γ_i^b is a binary variable which equals 1 if the through queue would be excessive long and block the left-turn bay at intersection *i*; *h* denotes the average vehicle headway in the queue (in feet); L_i represents the left-turn bay length at intersection *i*; and *M* is a large number. The left-hand sides of Eqs. (5.5) and (5.6) indicate the furthest queue distance from the stop bar of the left-turn and the through lanes during the corresponding green phase. The formulations for the inbound direction can be derived with the same logic and similar constraints.

5.3.3 Formulating the connection state between two progression segments

Figure 5.4 shows the least and most desirable connection states between two neighboring sets of progression bands. Figure 5.4(a) shows a scenario having no overlapped time duration between two neighboring progression bands. Specifically, the upstream band arrives at the

downstream intersection when its band ends, causing the vehicles within the upstream band less likely to catch the downstream band. On contrast, depending on the bandwidth of the upstream and downstream segment, Figures 5(b) and 5(c) show the two most desirable connection states between two neighboring progression bands. In Figure 5(b) where the upstream bandwidth is wider than the downstream one, it is desirable that the two bands end at the same time so that vehicles in the upstream band can move into the downstream band with minimal delay. On the other hand, if its downstream bandwidth is wider (See Figure 5(c)), the desirable connection state is to have both two bands start concurrently.

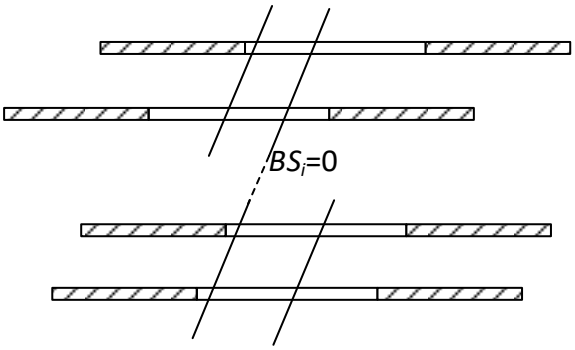

(a)

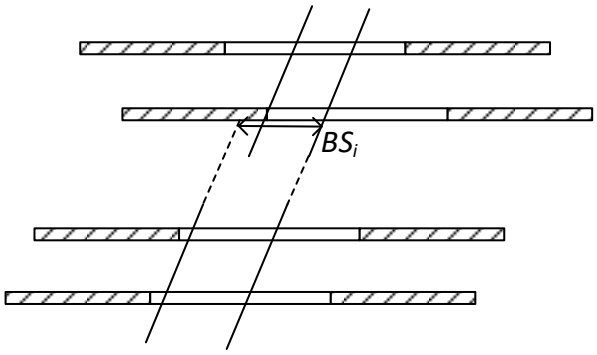

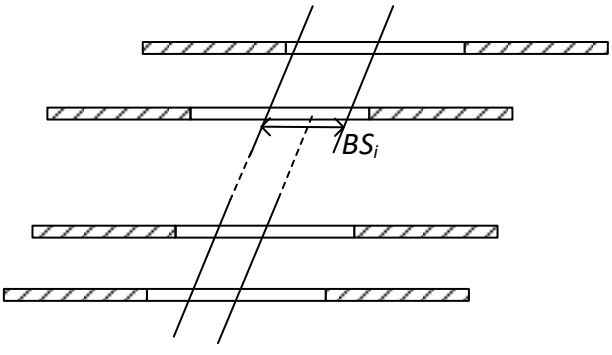

(b) (c)

Figure 5.4 Three cases for band connection state between two adjacent progression segments: (a) the least desirable case; (b) the most desirable case, when the downstream band is smaller; (c) the most desirable case, when the upstream band is smaller.

To account for various band connection states in optimizing the arterial decomposition, this study has introduced a band discontinuity penalty index that will show the least desirable connection relationship with the largest value. To compute such an index, this study employs the band shift, BS_i, to denote the time difference between the end of a downstream band and the arrival time of its upstream band at connection points (See Figure 5.4). For example, when the upstream bandwidth is wider than the downstream one, the band discontinuity index equal 1 under the scenario shown in Figure 5.4(a) (BS_i=0), and equal 0 under the scenarios shown in Figure 5.4(b) (BS_i = upstream bandwidths). Such band connection state, represented with the penalty index, can be expressed with Eqs. (5.7)-(5.8):

$$BS_i = t_{t,i}^a + w_i + b_i - \left(t_{t,i-1}^a + t_{i-1}\right) \tag{5.7}$$

$$P_i = \begin{cases} \dfrac{\max\left(b_{d,i} - BS_i, 0\right)}{b_d} + \dfrac{\max\left(BS_i - b_{d,i}, 0\right)}{1 - b_d} & \text{if } b_u < b_d \\ \dfrac{\max\left(b_{u,i} - BS_i, 0\right)}{b_u} + \dfrac{\max\left(BS_i - b_{u,i}, 0\right)}{1 - b_u} & \text{if } b_u > b_d \end{cases} \tag{5.8}$$

where, BS_i denotes the band shift; P_i indicates the penalty due to the band discontinuity at the intersection serving as the decomposition point; and $b_{d,i}\left(b_{u,i}\right)$ represents the

downstream(upstream) bandwidth. Since only one decomposition point is allowed between each pair of adjacent critical intersections, $b_{d,i}\left(b_{u,i}\right)$ will be equal to the bandwidth at the closest downstream (upstream) critical intersection, which can be obtained from the optimization results of Stage 1. The formulations for the inbound direction can be derived with the same logic and similar constraints.

5.3.4 Enhanced progression constraints for Model III

Note that the progression constraints should be applied between two adjacent intersections within a progression segment, but not at the decomposition location. Therefore, the progression constraints, shown in Eq. (4.3)-(4.4)s should be enhanced to accommodate such flexibility, as expressed below:

$$\theta_i + \left(1-\xi_i\right)\bar{g}_i^l + w_i + t_i + n_i \geq \theta_{i+1} + \left(1-\xi_{i+1}\right)\bar{g}_{i+1}^l + w_{i+1} - M \times \left(x_{i+1} - x_i\right) \tag{5.9}$$

$$\theta_i + \left(1-\xi_i\right)\bar{g}_i^l + w_i + t_i + n_i \leq \theta_{i+1} + \left(1-\xi_{i+1}\right)\bar{g}_{i+1}^l + w_{i+1} + M \times \left(x_{i+1} - x_i\right) \tag{5.10}$$

$$\theta_{i+1} + \left(1-\bar{\xi}_{i+1}\right)g_{i+1}^l + \bar{w}_{i+1} + \bar{t}_{i+1} + \bar{n}_{i+1} \geq \theta_i + \left(1-\bar{\xi}_i\right)g_i^l + \bar{w}_i - M \times \left(\bar{x}_{i+1} - \bar{x}_i\right) \tag{5.11}$$

$$\theta_{i+1} + \left(1-\bar{\xi}_{i+1}\right)g_{i+1}^l + \bar{w}_{i+1} + \bar{t}_{i+1} + \bar{n}_{i+1} \leq \theta_i + \left(1-\bar{\xi}_i\right)g_i^l + \bar{w}_i + M \times \left(\bar{x}_{i+1} - \bar{x}_i\right) \tag{5.12}$$

Eqs. (5.9)-(5.12) will be relaxed when $x_{i+1} - x_i = 1$, i.e., when intersections *i* and *i*+1 are assigned to different segments. Otherwise, the last term in these constraints equals zero and the

equality between left and right-hand sides will be forced to meet the constraint, identical to Eq. (4.3)-(4.4), to ensure that intersection *i* and *i*+1 are in one progression segment.

5.3.5 Objective function and summary of Stage 1

The objective function in Stage 1, as expressed in Eq. (5.13), aims to first maximize the sum of bandwidth weighted by the through volume and then to minimize the expected number of intersections suffering from queue blockage or spillover:

$$\text{Maximize } \sum_i \left(V_i^t b_i + \bar{V}_i^t \bar{b}_i\right) - k_1 \left(V_i^t \gamma_i^s + \bar{V}_i^t \bar{\gamma}_i^s + V_i^l \gamma_i^b + \bar{V}_i^l \bar{\gamma}_i^b\right) \tag{5.13}$$

Where, $V_i^t \left(\bar{V}_i^t\right)$ denotes the outbound (inbound) through volume; $V_i^l \left(\bar{V}_i^l\right)$ denotes the outbound (inbound) left-turn volume at intersection *i*; and k_1 is weighting factor significantly smaller than 1.

In brief, the stage 1 of Model III can be summarized as follows:

$$\text{Maximize } \sum_i \left(V_i^t b_i + \bar{V}_i^t \bar{b}_i\right) - k_1 \left(V_i^t \gamma_i^s + \bar{V}_i^t \bar{\gamma}_i^s + V_i^l \gamma_i^b + \bar{V}_i^l \bar{\gamma}_i^b\right)$$

s.t.

Progression of through vehicles along the arterial:

$$w_i \geq \tau_i^t, w_i + b_t \leq g_i^t$$

$$\bar{w}_i \geq \bar{\tau}_i^t, \bar{w}_i + \bar{b}_t \leq \bar{g}_i^t$$

$$\theta_i + \left(1-\xi_i\right)\bar{g}_i^l + w_i + t_i + n_i \geq \theta_{i+1} + \left(1-\xi_{i+1}\right)\bar{g}_{i+1}^l + w_{i+1} - M \times \left(x_{i+1} - x_i\right)$$

$$\theta_i + \left(1-\xi_i\right)\bar{g}_i^l + w_i + t_i + n_i \leq \theta_{i+1} + \left(1-\xi_{i+1}\right)\bar{g}_{i+1}^l + w_{i+1} + M \times \left(x_{i+1} - x_i\right)$$

$$\theta_{i+1} + \left(1-\bar{\xi}_{i+1}\right)g_{i+1}^l + \bar{w}_{i+1} + \bar{t}_{i+1} + \bar{n}_{i+1} \geq \theta_i + \left(1-\bar{\xi}_i\right)g_i^l + \bar{w}_i - M \times \left(\bar{x}_{i+1} - \bar{x}_i\right)$$

$$\theta_{i+1} + \left(1-\bar{\xi}_{i+1}\right)g_{i+1}^l + \bar{w}_{i+1} + \bar{t}_{i+1} + \bar{n}_{i+1} \leq \theta_i + \left(1-\bar{\xi}_i\right)g_i^l + \bar{w}_i + M \times \left(\bar{x}_{i+1} - \bar{x}_i\right)$$

Local progression and queue length calculation:

$$b'_{m,i} = \min\left(t^b_{d(m),i}, t^b_{u(m),i-1} + t_{i-1}\right) - \max\left(t^a_{d(m),i} + \tau_{d(m),i}, t^a_{u(m),i-1} + t_{i-1}\right) \qquad \forall m \in \left\{m_1, m_2, m_3, m_4\right\}$$

$$QL_{i+1}^l = \frac{C}{3600 n_{i+1}^l} V_i^t r_{i+1}^l \times \left(g_i^t - b_{m4,i+1}\right)$$

$$\tau_{i+1}^l = QL_{i+1}^l \frac{3600/C}{s - V_i^l / n_{i+1}^l} \times \alpha$$

$$QL_{i+1}^t = \frac{C}{3600 n_{i+1}^t}\left(V_i^t r_{i+1}^t \times \left(g_i^t - b_{m1,i+1}\right) + V'^l_i r_{i+1}^t \times \left(g'^l_i - b_{m2,i+1}\right) + V'^r_i r_{i+1}^t \times \left(g'^r_i - b_{m3,i+1}\right)\right)$$

$$\tau_{i+1}^t = QL_{i+1}^t \frac{3600/C}{s - V_{i+1}^t / n_{i+1}^t} \times \alpha$$

$$QL_i^l h \frac{s}{s - V_{l,i}} \leq L_i + M \times \gamma_i^s$$

$$QL_i^t h \frac{s}{s - V_{t,i}} \leq L_i + M \times \gamma_i^b$$

$$\bar{b}'_{m,i} = \min\left(\bar{t}^b_{d(m),i}, \bar{t}^b_{u(m),i+1} + \bar{t}_i\right) - \max\left(\bar{t}^a_{d(m),i} + \bar{\tau}_{d(m),i}, \bar{t}^a_{u(m),i+1} + \bar{t}_i\right) \qquad \forall m \in \left\{\bar{m}_1, \bar{m}_2, \bar{m}_3, \bar{m}_4\right\}$$

$$\bar{Q}\bar{L}_i^l = \frac{C}{3600\bar{n}_i^l}\bar{V}_{i+1}^t \bar{r}_i^l \times \left(\bar{g}_{i+1}^t - b_{m4,i}\right)$$

$$\bar{\tau}_i^l = \bar{Q}\bar{L}_i^l \frac{3600/C}{s - \bar{V}_i^l / \bar{n}_i^l} \times \alpha$$

$$\bar{Q}\bar{L}_i^t = \frac{C}{3600 n_i^t}\left(\bar{V}_{i+1}^t \bar{r}_i^t \times \left(\bar{g}_{i+1}^t - \bar{b}_{m1,i}\right) + \bar{V}'^l_{i+1}\, \bar{r}_i^t \times \left(g'^l_{i+1} - b_{m2,i}\right) + \bar{V}'^r_i\, \bar{r}_{i+1}^t \times \left(g'^r_{i+1} - b_{m3,i}\right)\right)$$

$$\bar{\tau}_i^t = \bar{Q}\bar{L}_i^t \frac{3600/C}{s - \bar{V}_i^t / \bar{n}_i^t} \times \alpha$$

$$\bar{Q}\bar{L}_i^l h \frac{s}{s - \bar{V}_{l,i}} \le \bar{L}_i + M \times \bar{\gamma}_i^s$$

$$\bar{Q}\bar{L}_i^t h \frac{s}{s - \bar{V}_{t,i}} \le \bar{L}_i + M \times \bar{\gamma}_i^b$$

Decomposition of the arterial

$$x_i - x_{i+1} \le b_{i+1} - b_i \le x_{i+1} - x_i$$

$$x_i - x_{i+1} \le \bar{b}_{i+1} - \bar{b}_i \le x_{i+1} - x_i$$

$$0 \le x_{i+1} - x_i \le 1$$

$$0 \le x_{cr_k} - x_{cr_{k+1}} \le 1$$

$$x_{i+3} - x_i \le 1$$

5.3.6 Objective function and a summary of Stage 2 formulations

The objective function in Stage 2 is to minimize the band discontinuity penalty index and the queue distribution index, and then to maximize the bandwidth at non-critical intersections, as expressed in Eq. (26):

$$\text{Minimize } \sum_i \left(V_i^t P_i + \bar{V}_i^t \bar{P}_i\right) + e + \bar{e} - k_2 \sum_i \left(V_i^t b_i + \bar{V}_i^t \bar{b}_i\right) \tag{5.14}$$

where, k_2 is weighting factor significantly smaller than 1

The obtained maximized bandwidths at critical intersections from Stage 1 will serve as an input of Stage 2 to ensure the same maximized bandwidth at each critical intersection. The optimization of Stage 2 should also ensure that the number of intersections, suffering from left-turn spillbacks and blockages, is less than or equal to the results from Stage 1, which can be expressed with the following constraints:

$$b_i \geq B_i, \bar{b}_i \geq \bar{B}_i \quad \forall i = \text{critical intersection} \tag{5.15}$$

$$\sum_i \gamma_i^s \leq \sum_i \Gamma_i^s, \sum_i \bar{\gamma}_i^s \leq \sum_i \bar{\Gamma}_i^s \tag{5.16}$$

$$\sum_i \gamma_i^b \leq \sum_i \Gamma_i^b, \sum_i \bar{\gamma}_i^b \leq \sum_i \bar{\Gamma}_i^b \tag{5.17}$$

Where, $B_i\left(\overline{B}_i\right)$ denotes the outbound(inbound) bandwidth at intersection *i* obtained from Stage 1; $\sum_i \Gamma_i^s \left(\sum_i \overline{\Gamma}_i^s \right)$ refers to the number of intersections suffering from left-turn bay spillbacks from Stage 1; and $\sum_i \Gamma_i^b \left(\sum_i \overline{\Gamma}_i^b \right)$ is for blockages to the left-turn bay.

In brief, the stage 2 of Model III can be summarized as follows:

Maximize $\sum_i \left(V_i^t P_i + \overline{V}_i^t \overline{P}_i \right) + e + \overline{e} - k_2 \sum_i \left(V_i^t b_i + \overline{V}_i^t \overline{b}_i \right)$

s.t.

Progression of through vehicles along the arterial:

$$w_i \geq \tau_i^t, w_i + b_t \leq g_i^t$$

$$\overline{w}_i \geq \overline{\tau}_i^t, \overline{w}_i + \overline{b}_t \leq \overline{g}_i^t$$

$$\theta_i + \left(1 - \xi_i\right) \overline{g}_i^l + w_i + t_i + n_i \geq \theta_{i+1} + \left(1 - \xi_{i+1}\right) \overline{g}_{i+1}^l + w_{i+1} - M \times \left(x_{i+1} - x_i \right)$$

$$\theta_i + \left(1 - \xi_i\right) \overline{g}_i^l + w_i + t_i + n_i \leq \theta_{i+1} + \left(1 - \xi_{i+1}\right) \overline{g}_{i+1}^l + w_{i+1} + M \times \left(x_{i+1} - x_i \right)$$

$$\theta_{i+1} + \left(1 - \overline{\xi}_{i+1}\right) g_{i+1}^l + \overline{w}_{i+1} + \overline{t}_{i+1} + \overline{n}_{i+1} \geq \theta_i + \left(1 - \overline{\xi}_i\right) g_i^l + \overline{w}_i - M \times \left(\overline{x}_{i+1} - \overline{x}_i \right)$$

$$\theta_{i+1} + \left(1 - \overline{\xi}_{i+1}\right) g_{i+1}^l + \overline{w}_{i+1} + \overline{t}_{i+1} + \overline{n}_{i+1} \leq \theta_i + \left(1 - \overline{\xi}_i\right) g_i^l + \overline{w}_i + M \times \left(\overline{x}_{i+1} - \overline{x}_i \right)$$

Local progression and queue length calculation:

$$b'_{m,i} = \min\left(t^b_{d(m),i}, t^b_{u(m),i-1} + t_{i-1}\right) - \max\left(t^a_{d(m),i} + \tau_{d(m),i}, t^a_{u(m),i-1} + t_{i-1}\right) \qquad \forall m \in \{m_1, m_2, m_3, m_4\}$$

$$QL^l_{i+1} = \frac{C}{3600 n^l_{i+1}} V^t_i r^l_{i+1} \times \left(g^t_i - b_{m4,i+1}\right)$$

$$\tau^l_{i+1} = QL^l_{i+1} \frac{3600/C}{s - V^l_i / n^l_{i+1}} \times \alpha$$

$$QL^t_{i+1} = \frac{C}{3600 n^t_{i+1}} \left(V^t_i r^t_{i+1} \times \left(g^t_i - b_{m1,i+1}\right) + V'^l_i r^t_{i+1} \times \left(g'^l_i - b_{m2,i+1}\right) + V'^r_i r^t_{i+1} \times \left(g'^r_i - b_{m3,i+1}\right)\right)$$

$$\tau^t_{i+1} = QL^t_{i+1} \frac{3600/C}{s - V^t_{i+1} / n^t_{i+1}} \times \alpha$$

$$QL^l_i h \frac{s}{s - V_{l,i}} \le L_i + M \times \gamma^s_i$$

$$QL^t_i h \frac{s}{s - V_{t,i}} \le L_i + M \times \gamma^b_i$$

$$\bar{b}'_{m,i} = \min\left(\bar{t}^b_{d(m),i}, \bar{t}^b_{u(m),i+1} + \bar{t}_i\right) - \max\left(\bar{t}^a_{d(m),i} + \bar{\tau}_{d(m),i}, \bar{t}^a_{u(m),i+1} + \bar{t}_i\right) \qquad \forall m \in \{\bar{m}_1, \bar{m}_2, \bar{m}_3, \bar{m}_4\}$$

$$\bar{QL}^l_i = \frac{C}{3600 \bar{n}^l_i} \bar{V}^t_{i+1} \bar{r}^l_i \times \left(\bar{g}^t_{i+1} - b_{m4,i}\right)$$

$$\bar{\tau}^l_i = \bar{QL}^l_i \frac{3600/C}{s - \bar{V}^l_i / \bar{n}^l_i} \times \alpha$$

$$\bar{QL}^t_i = \frac{C}{3600 n^t_i} \left(\bar{V}^t_{i+1} \bar{r}^t_i \times \left(\bar{g}^t_{i+1} - \bar{b}_{m1,i}\right) + \bar{V}'^l_{i+1} \bar{r}^t_i \times \left(g'^l_{i+1} - b_{m2,i}\right) + \bar{V}'^r_i \bar{r}^t_{i+1} \times \left(g'^r_{i+1} - b_{m3,i}\right)\right)$$

$$\bar{\tau}^t_i = \bar{QL}^t_i \frac{3600/C}{s - \bar{V}^t_i / \bar{n}^t_i} \times \alpha$$

Occurrence of left-turn bay spillback and blockage:

$$\bar{Q}\bar{L}_i^l h \frac{s}{s-\bar{V}_{l,i}} \le \bar{L}_i + M \times \bar{\gamma}_i^s$$

$$\bar{Q}\bar{L}_i^l h \frac{s}{s-\bar{V}_{t,i}} \le \bar{L}_i + M \times \bar{\gamma}_i^b$$

Decomposition of the arterial:

$$x_i - x_{i+1} \le b_{i+1} - b_i \le x_{i+1} - x_i$$

$$x_i - x_{i+1} \le \bar{b}_{i+1} - \bar{b}_i \le x_{i+1} - x_i$$

$$0 \le x_{i+1} - x_i \le 1$$

$$0 \le x_{cr_k} - x_{cr_{k+1}} \le 1$$

$$x_{i+3} - x_i \le 1$$

Band connection states:

$$BS_i = t_{t,i}^a + w_i + b_i - \left(t_{t,i-1}^a + t_{i-1}\right)$$

$$P_i = \begin{cases} \dfrac{\max\left(b_{d,i} - BS_i, 0\right)}{b_d} + \dfrac{\max\left(BS_i - b_{d,i}, 0\right)}{1-b_d} & \text{if } b_u < b_d \\ \dfrac{\max\left(b_{u,i} - BS_i, 0\right)}{b_u} + \dfrac{\max\left(BS_i - b_{u,i}, 0\right)}{1-b_u} & \text{if } b_u > b_d \end{cases}$$

Distributing queues to less congested locations:

$$e = \sum_i \frac{1}{\beta - V_i^{total} / s} \times \frac{\max\left(QL_{i+1}^t, QL_{i+1}^l\right)}{LL_i}$$

$$\bar{e} = \sum_i \frac{1}{\beta - \bar{V}_i^{total} / s} \times \frac{\max\left(\bar{Q}\bar{L}_i^t, \bar{Q}\bar{L}_i^l\right)}{\bar{L}\bar{L}_i}$$

Ensuring the bandwidths at critical intersections and upper bound of number of intersections suffering from left-turn bay spillback and blockage:

$$b_i \geq B_i, \bar{b}_i \geq \bar{B}_i \quad \forall i = \text{critical intersection}$$

$$\sum_i \gamma_i^s \leq \sum_i \Gamma_i^s, \sum_i \bar{\gamma}_i^s \leq \sum_i \bar{\Gamma}_i^s$$

$$\sum_i \gamma_i^b \leq \sum_i \Gamma_i^b, \sum_i \bar{\gamma}_i^b \leq \sum_i \bar{\Gamma}_i^b$$

5.4 Case study

The case study is designed to first analyze the optimization results, and then to focus on: (1) demonstrating the proposed model's function in concurrently optimizing the decomposition location and maximizing progression effectiveness along the entire arterial; and (2) assessing the queue impacts on design of the optimized signal progression.

The second part of the case study aims to verify the need of Stage 2 functions in the proposed model, that is, to optimize the progression band connection state between two sets of subsegments. The third part of the case study is to perform simulation comparison of the proposed model with other well-established models for arterial signal design. The proposed model's function to reduce the queue lengths along the arterial will also be verified in the simulation experiments.

The simulation platform is designed with VISSIM 9, and the MOEs are collected from the extensive experiments of 2-hour simulation.

5.4.1 Site Description

Figure 5.5 shows the key geometric features and signal timing information for the arterial of 16 intersections on North Ave. in Baltimore, MD, from N Smallwood St. to Charles St., for the case study. Four critical intersections on the arterial are denoted by the names of the crossing roads. Note that Mt. Royal Ave. serves as a connection to a freeway ramp.

Cycle length: 150 seconds

	Intersection Number															
	1	2	3	4	5	6	7	8	9	10	11	12	13	14	15	16
OB Green Time (s)	87	69	78	66	57	93	84	72	75	120	72	63	99	66	69	96
IB Green Time (s)	87	69	78	66	57	93	84	99	75	90	72	63	69	66	93	75
OB LT bay length (ft)	-	-	-	-	121	-	-	-	159	134	208	180	70	-	-	100
IB LT bay length (ft)	-	-	-	-	139	-	-	160	112	-	226	188	-	130	110	-
OB Thru volume (vph)	780	920	878	990	700	880	1050	950	760	890	790	950	960	1150	990	820
IB Thru volume (vph)	780	900	850	860	680	810	920	720	740	760	780	890	900	950	860	690

*OB: Outbound; IB: Inbound; LT: Left-turn

Figure 5.5 Key information associated with the study site

5.4.2 Optimization Results

To ensure that an arterial under the optimal decomposition can yield the best overall benefits, this case study has conducted comparison between the proposed model and a heuristic approach, developed by Tian and Urbanik's (2007), which sequentially divides the arterial system into subsegments with three to five intersections, optimizes offsets in each subsegment and then optimally connects subsegments under the rule of favoring the peak direction (i.e., outbound direction in this study). The comparisons between the following models are evaluated with the sum of through bandwidths weighted by the through volume at each intersection with:

- Model 1: the proposed model;
- Model 2a: the heuristic approach by Tian and Urbanik's (2007); and
- Model 2b: the heuristic approach by Tian and Urbanik's (2007) but only including the effective green bands that are not impeded by residual queues.

Figure 5.6(a) shows the bandwidths obtained with those models for comparison. To demonstrate the model's capability in optimizing the decomposition location, the bandwidths obtained by those models under various predetermined decomposition plans are also shown in Figure 5.6(a). Four predetermined decomposition plans, together with the optimized plan from the proposed model, are shown in Figure 5.6(b).

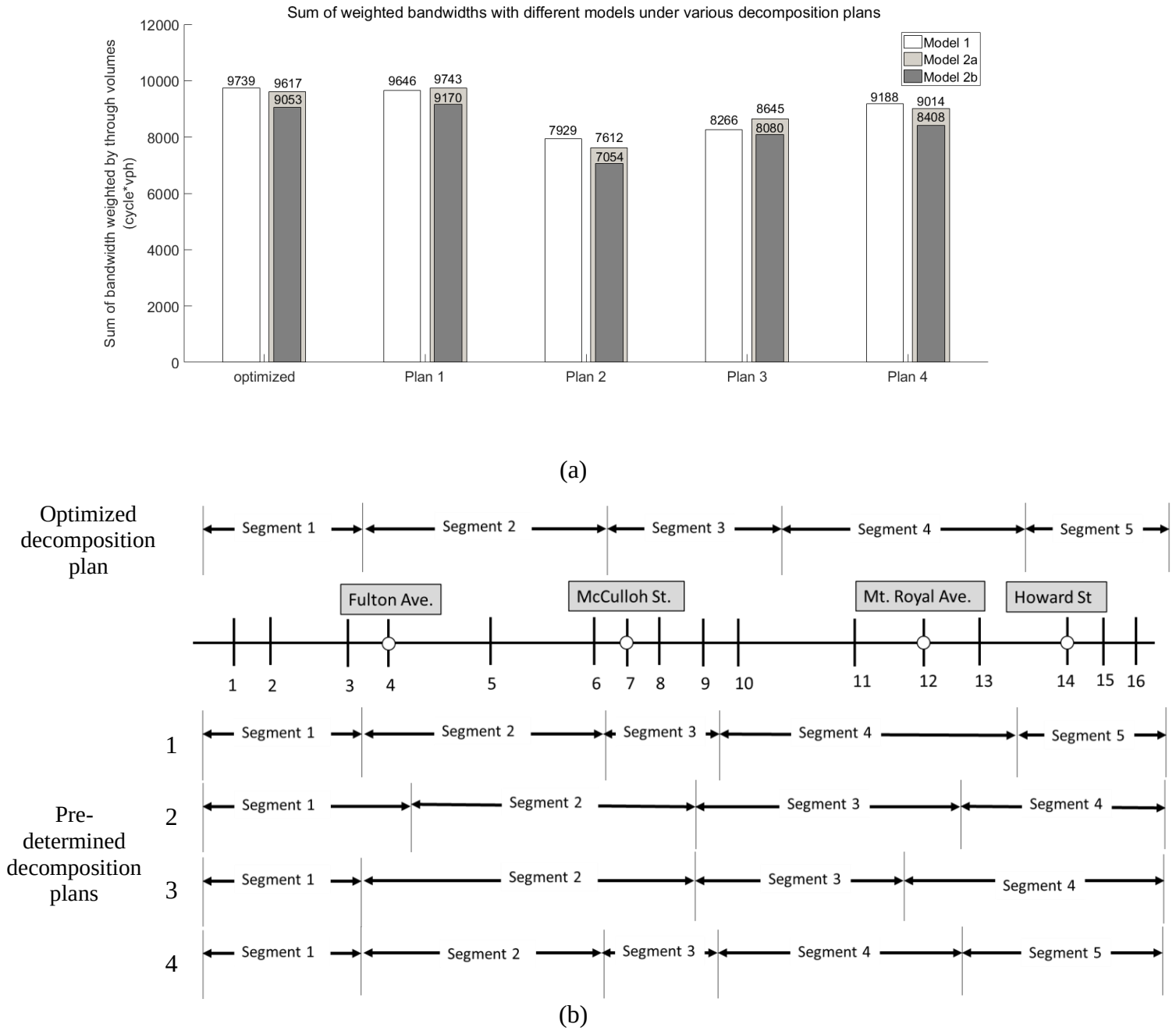

Figure 5.6 Optimization results (a) sum of bandwidths weighted by through volumes (b) optimal and predetermined decomposition plans

As shown in Figure 5.6, among the bandwidths obtained with the proposed model under different decomposition plans, the one under the optimized plan (9739/cycle*vph) is wider than

that under any pre-determined decomposition plan shown in Figure 5.6(b), ranging from 7929 to 9646 (cycle*vph). Such results should be attributed to the function of the proposed model that can automatically select the optimal decomposition intersections within the arterial, based on traffic volumes, geometric information, and predetermined critical intersections. The results in Figure 5.6(a) also shows that the bandwidth along a long arterial, if not optimized concurrently with the decomposition plan, may easily deviate from the optimal value. Further observations to the bandwidths under each decomposition plan with different models show that the proposed model, accounting for traffic queues in the design of the signal progression, generates greater effective bands not impeded by the residual queues at intersections. For example, although Model 2, under the predetermined plan 1, can generate larger bandwidth of 9743 (cycle*vph), compared to 9646 (cycle*vph) under the proposed model, a portion of such bands would be practically unusable due to the vehicle queues, resulting in an effective bandwidth of 9170 (cycle*vph).

5.4.3 Simulation Evaluation 1

The first simulation evaluation aims to demonstrate the capability of the model with respect to optimizing the connection state of the progression bands between two adjacent subsegments. The signal plans, obtained in Stage 1 and Stage 2, both applied to the study site, and Table 5.1 shows their average vehicle delays along the arterial and at the selected decomposition locations.

Table 5.1 Average delay and number of stops for through movements along the arterial and at selected decomposition locations under the signal plan of Stage 1 and Stage 2

	Average delay (s/veh)		Number of stops	
	Stage 1	Stage 2	Stage 1	Stage 2
Arterial				
Outbound	441.7	116.8	10.49	3.76
Inbound	268.3	201.8	7.11	5.01
Total	359.3	157.2	8.88	4.35
Link between intersections 6-7				
Outbound	46.0	13.3	0.76	0.41
Inbound	39.1	3.1	0.77	0.07
Total	42.6	8.4	0.76	0.24
Link between intersections 10-11				
Outbound	4.06	6.4	0.10	0.16
Inbound	17.6	7.4	0.96	0.25
Total	11.3	6.9	0.56	0.21

The results in Table 5.2 show a significant improvement of progression efficiency along the arterial of Stage 2 model over Stage 1, evidenced by a 56.3% (from 359.35s to 157.21s) reduction of average delay and a 51.0% (from 8.88 to 4.35) reduction of number of stops for through vehicles along the arterial. The improvement at the decomposition locations is also considerable. For example, the Stage 2 model, with the capability to optimize the band connection states, can reduce the average delay from 42.6s to 8.4s, and number of stops from 0.76 to 0.24 on the link between Intersection 6 and Intersection 7. Such improvements also show the necessity to optimize the connection state between two sets of progression bands in decomposing a long arterial into the optimal number of subsegments.

5.4.4 Simulation Evaluation 2

To ensure that the objective of maximizing progression bands would not compromise other measures of effectiveness (MOEs), this study has further conducted the simulation experiments with respect to the progression effectiveness along a long arterial, in terms of average vehicle delay,

number of stops, and queue lengths. Since two-way progression bands cannot be found for the study site of 16 intersections with existing methods, a signal plan providing only progression for the direction with higher through volume has also been adopted to justify the need of proper decomposition. Hence, the simulation experiments for performance comparison include:

- Model 2a with the predetermined plan 1
- Model 3: a signal plan only providing progression for outbound traffic

Figure 5.7 shows the average delay and number of stops for through movements along the arterial and at the critical intersections under these three models. Figure 5.8 shows the time dependent queue lengths at four selected intersections.

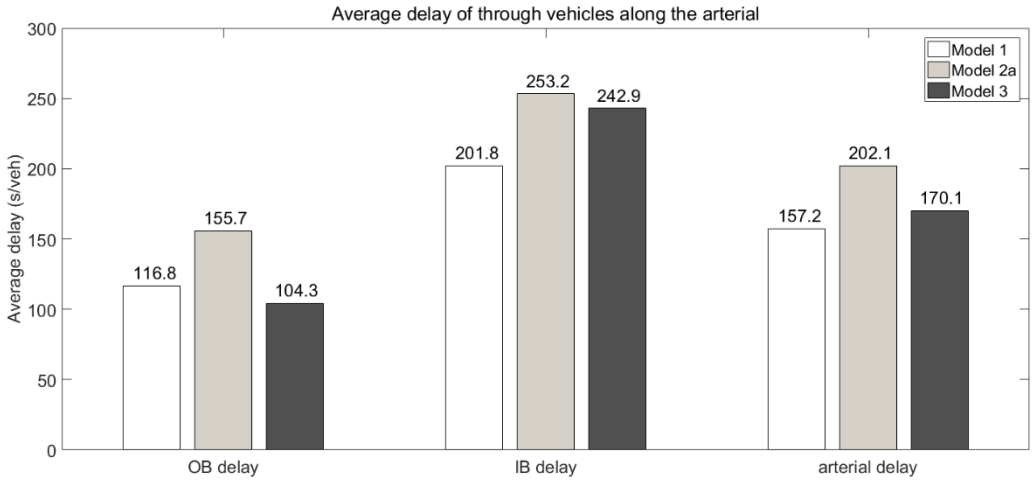

(a)

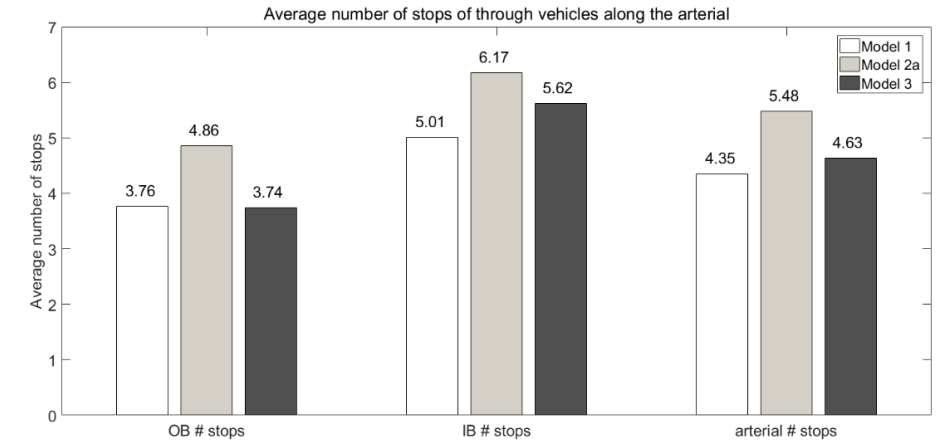

(b)

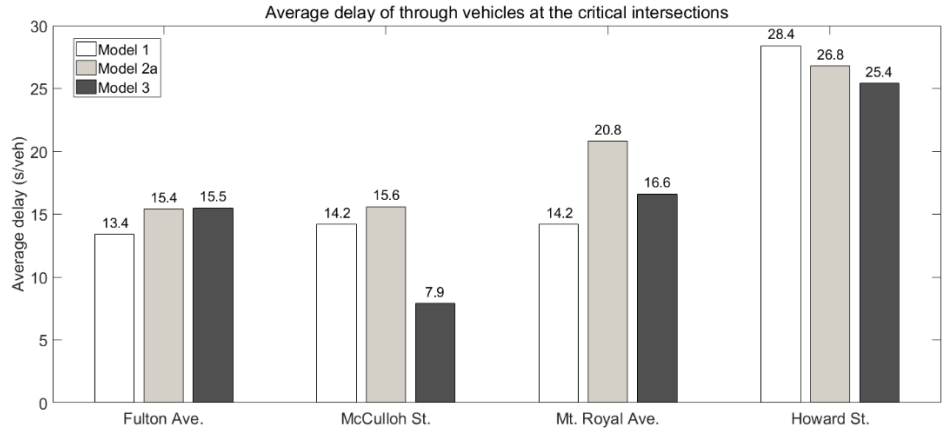

(c)

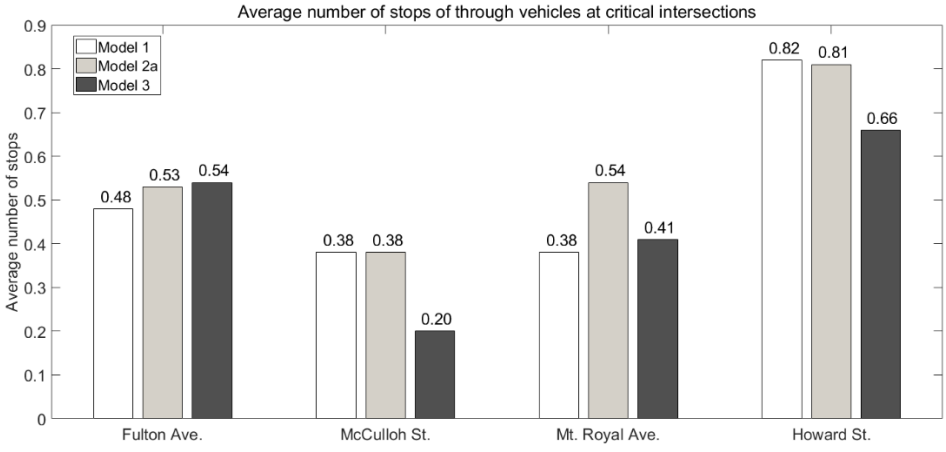

(d)

Figure 5.7 Average delay and number of stops for through movements along the arterial and at those critical intersections

As shown in Figure 5.7, the proposed model, as expected, can reduce the average through vehicle delay both for the entire arterial and at most critical intersections by optimally decomposing the arterial into several segments and fully incorporating the impacts of traffic queues in the signal design. For example, compared Model 3 which is focused on the benefit of the outbound direction, the proposed model yields a 16.8% reduction (from 242.9s to 201.8s) on inbound through delay. Such improvement contributes to a reduction in average delay for two-way through traffic by 22.2% (from 202.1s to 157.2s) and 7.6% (from 170.1s to 157.2s) , respectively, compared to the results from Model 2 and Model 3. The improvements with the propose model should attribute to its capability of decomposing the arterial into the optimal sets of subgroups, based on the two-way through volumes at each intersection. Moreover, the proposed model can yield lower average delay and number of stops at critical intersections than with Model 2 and Model 3. For example, at Mt. Royal Ave. which connects to freeway ramps, the proposed model can reduce the average delay by 31.7% (from 20.8s to 14.2s), as well as the number of stops by 29.6% (from 0.54 to 0.38), compared to Model 2.

The comparison in Figures 5.8(a) shows that the signal plan generated by the proposed model can yield a queue length shorter than or close to the left-turn bay length (188 ft) for inbound left-turn vehicles in most cycles at Mt. Royal Ave, one of the critical intersections, on contrast, the other two models may produce queues constantly longer than the bay length on the same approach, causing left-turn bay spillback and thus interrupting the through traffic. For a less congested movement, for example, the outbound left-turn at intersection 11, the signal plans under all three models may not suffer from queue spillback, while the proposed model still yields shorter queue lengths than any other model in most cycles. Such a function offered by the

proposed model on reducing the queue length and preventing the spillback would in turn minimize the impact of traffic queues on the progression, as evidenced by the lower average through delays produced by the propose model.

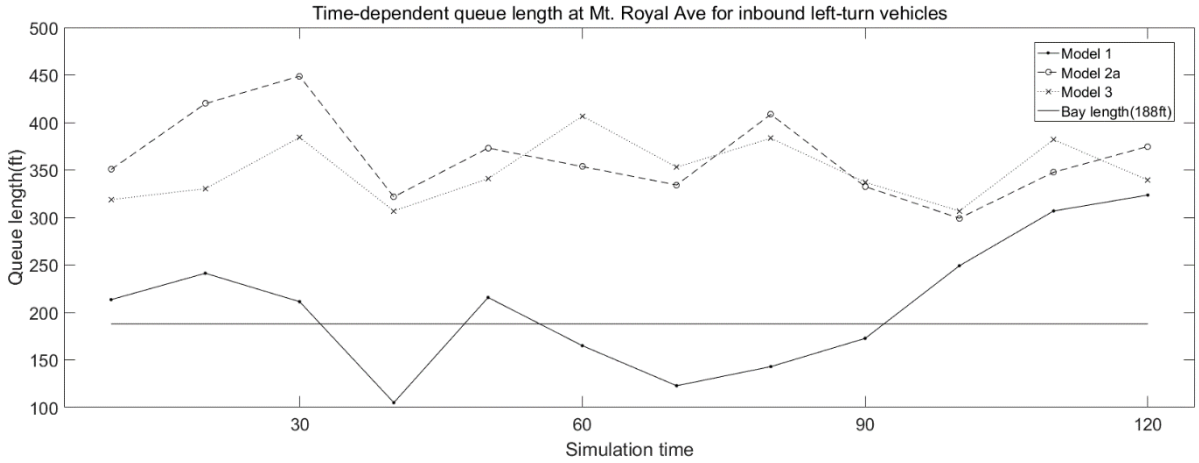

(a)

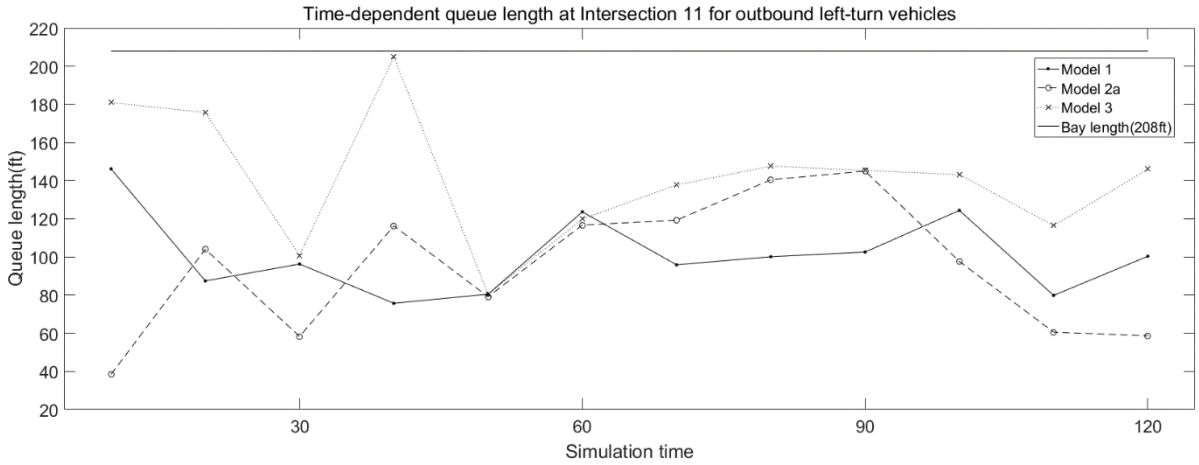

(b)

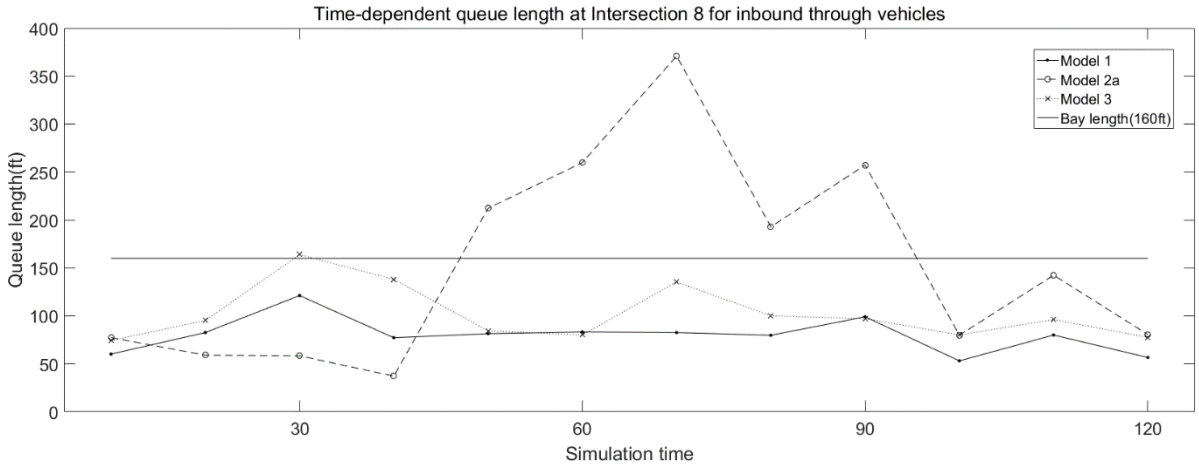

(c)

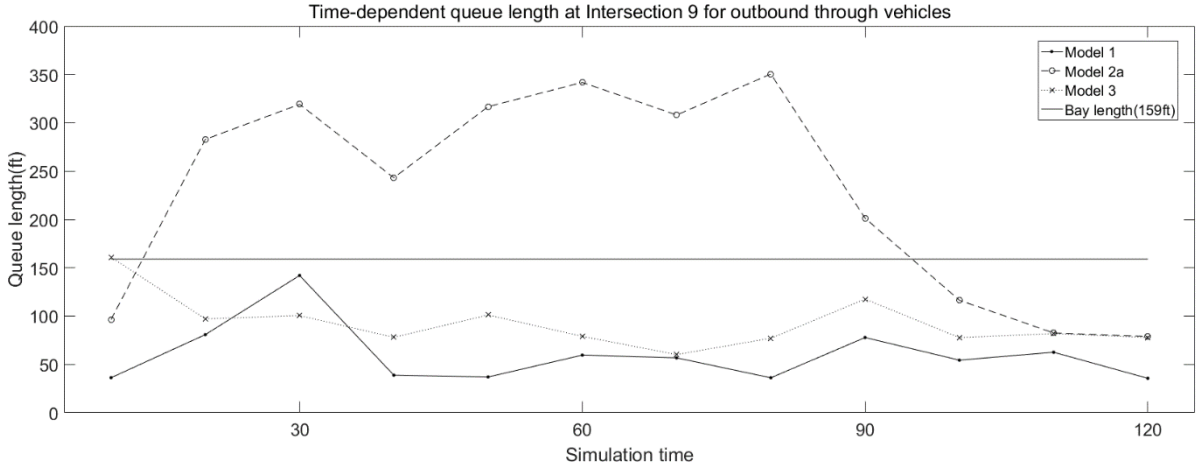

(d)

Figure 5.8 Time-dependent queue length: (a) at critical intersection at Mt. Royal Ave; (b) at intersection 11, (c)-(d) at intersection 8 and intersection 9 with short link lengths

As demonstrated in Figure 5.8(c)-(d), the proposed signal plan can yield a shorter through queue size, compared to that under the other two models on the short link of 501ft between Intersections 8 and 9, indicating the model's capability to avert long queues on these short links. The comparison results between the queue length and the bay length in Figure 5.8(c)-(d) show

that the proposed model can also prevent the queue from exceeding the bay length at those two intersections, which cannot be ensured in every cycle if under other models.

In summary, the proposed model can outperform the existing method and the signal plan solely designed for outbound through vehicles in terms of average delay and number of stops experienced by through vehicles along the entire arterial and at the critical locations. This is due to all embedded functions that allow the model to concurrently decompose the arterial into the optimal set of subsegments, and each is designed with the optimal progression that can account for the impact of vehicle queues on the traffic flows. With the objective of minimizing the number of intersections suffering from left-turn bay blockages or spillbacks and distributing the queues to less critical locations, the proposed model can also yield shorter queue lengths than other methods along the arterial and minimize the likelihood of having queue spillbacks.

5.5 Closure

To ensure traffic efficiency over a long arterial, this study has developed a signal optimization model to concurrently decompose the arterial into the optimal number of control segments and offer each with the maximized progression band.

To identify the optimized decomposition locations and the signal plans under the given geometric constraints, the study has proposed a two-stage model to formulate various issues that may prevent vehicles from progressing smoothly over the entire arterial. Such critical issues include the relation between the decomposition intersections and the maximized bandwidth in each segment, progression discontinuity between segments, queue formation on travel lanes and its

impact on signal progression, left-turn bay spillback and blockage, and excessive queue lengths at specific critical locations.

Performance evaluation with a real-world arterial system and extensive simulation experiments have demonstrated that the proposed model can outperform other arterial signal design models with the resulting lower average delay and smaller number of stops both along the arterial and at the critical intersections. The results from the simulation evaluation also show that queue lengths at the critical locations can also be reduced with the proposed model, thus causing less left-turn bay spillbacks or blockages.

Chapter 6: Dual-modal progression for an arterial having heavy transit flows

6.1 Introduction

Increasing transit system's ridership has long been recognized as one of the potentially effective strategies to mitigate urban traffic congestion from the demand side. However, a variety of factors associated with transit operations (e.g., uncertain waiting times at bus stops, variable travel times, and frequent stops at traffic signals) often cause transit system unfavorable in comparison with the auto mode. In an attempt to enhance transit service reliability, a rich body of research over the past decades has proposed various Transit Signal Priority (TSP) strategies for a bus to pass an intersection without excessive delays. Those studies can be classified into two classes: passive or active control, and the later one contains unconditional or conditional priority.

Passive TSP control, typically operated without detectors and based mainly on the off-line information of transit routes and ridership patterns, is generally viewed as effective under the scenarios of high transit frequencies, predictable transit travel times, and light or moderate traffic volumes. In contrast, active TSP control demands the placement of bus detectors at the target intersection to exercise a green extension or red truncation based on the detected bus information. Despite the effectiveness of the unconditional active TSP on improving bus efficiency, some concerns have also been raised about its potential negative impacts on the side street traffic and the signal coordination if TSP are frequently requested or when excessive activations occur for buses ahead of schedule.

In response to such challenges, some researchers have proposed the conditional active TSP, which sets constraints on granting signal priority, including the maximum number of priority calls

over a preset period, consistent cycle lengths, and only for buses behind the schedule. However, the effectiveness of such strategies diminishes when the bus volume increases, because some percentage of the behind-schedule buses will not experience the signal priority and the negative impacts on side street and general traffic may also negate the total benefits under such control. These real-time strategies may be further constrained by their demands of data quality and the long-lasting maintenance issues. Hence, design of bus-based signal coordination systems, considering the bus flow patterns in design of off-line signal control, emerges as one viable cost-benefit option.

However, those transit-friendly signal plans, considering only bus flows, often fail to provide the expected performance due to various interruptions from the passenger-car flows which are not included in the progression design. Additionally, designing signal progression for buses without concurrently accounting for the benefit of general traffic may result in excessive high delay for passenger cars since the travel times between intersections of these two modes are quite different. Hence, for an arterial with considerable flows of passenger cars and buses, one shall ideally provide concurrent progression to both modes, thereby maximizing the total benefit of all roadway users. Furthermore, since the distributions of traffic volumes in both modes and directions may vary over different times of a day, it would thus be desirable that the signal control model adopted for the arterials can intelligently decide which mode(s) and direction(s) ought to be offered with the progression so as to maximize the benefits of the entire system.

This chapter will present a signal optimization model that can offer concurrent progression to both modes or to selected mode(s) and direction(s), based on traffic volume, bus ratio, and

geometric conditions. The proposed model has the following key features: 1) maximizing the total benefit of all roadway users by selecting the proper mode(s) and direction(s) to offer progression, subject to the feasible combination of all passible bands; 2) fully accounting for the operational features of passenger cars and buses; and 3) considering the mutual interference between passenger cars and buses on the arterial.

6.2 Modelling methodology

To successfully progress vehicles of both modes (i.e., passenger cars and buses) over an arterial segment, one shall take into account the differences of their operational features and their interactions in their spatial evolution over a link. Some of those key features captured in the model formulations are listed below:

--- *Discrete nature for design of the bus band*

Due to the larger physical size and longer discharging headway of transit vehicles, compared to passenger cars, the width of an effective bus band should be adjusted at the increment of bus cruising headway, since additional bandwidth will not be usable if less than a bus's required cruising headway. For example, assuming a bus headway of 6 seconds, an 8-second band will yield no significant difference from a 6-second band in terms of the number of accommodated buses.

--- *Maximum bus bands per cycle*

To ensure that the provided bus band can be effectively used by the transit vehicles, its length should not exceed the number of buses per cycle or the bus stop capacity so that the green times for passenger car bands will not be unjustifiably reduced to produce excessive bus bands.

--- *Preventing intersection queues from blocking the bus stop*

Since passenger cars, forming queues at an intersection, may block the bus stop, those vehicles should be discharged prior to the arrival of buses to their stops to ensure their progression quality.

--- *Preventing the bus queues from blocking the progression band for passenger cars*

If the starting period of a green phase is used by queuing buses to discharge, passenger cars on the rightmost lane will not have the progression band. Hence, at an intersection where many buses are expected to encounter the red phase, the efficiency of a passenger car band needs to be adjusted, based on its temporal relation with respect of the start of a green phase.

--- *Preventing passenger car flows from the blockage by buses at their roadside stops*

Regardless of how the signals are designed, buses would dwell at the bus stops and temporarily block the traffic flows if without a bus bay. Figure 6.1 shows two examples of such interruptions to the passenger car bands, as indicated in the shaded area. In Figure 5.1(a), buses are expected to dwell at the bus stop before the end of each passenger car band while in Figure 5.1(b), the first several vehicles on the rightmost lane within the band are likely to encounter a stopping bus.

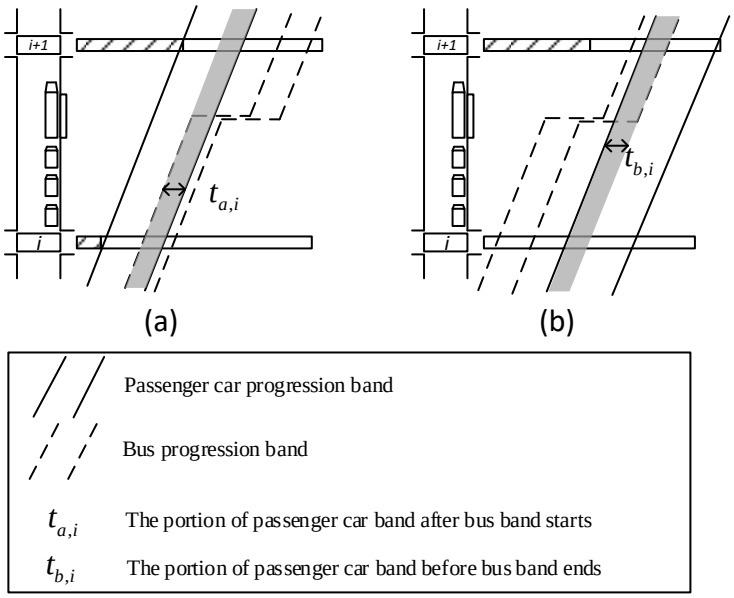

Figure 6.1 Interruption to passenger cars due to buses at bus stops.

--- *Selecting the proper modes and directions for progression design*

Based on the bus dwell time, link travel time and green ratios, providing concurrent progression to buses and passenger cars for both directions may not be either feasible or yielding the best benefits to the entire arterial's users. In view of the competing nature between the progression bands for these two modes, an effective progression optimization model should be capable of selecting the proper mode(s) and direction(s) to offer the optimal progression bands, based on the volumes and loading factors of passenger cars and buses.

6.3 Model formulations

This section presents formulations of the proposed model which can provide dual-modal progression to both passenger cars and buses based on the key operational characteristics and interrelations along an arterial. The key notations used in the formulations are shown in Figure 6.2.

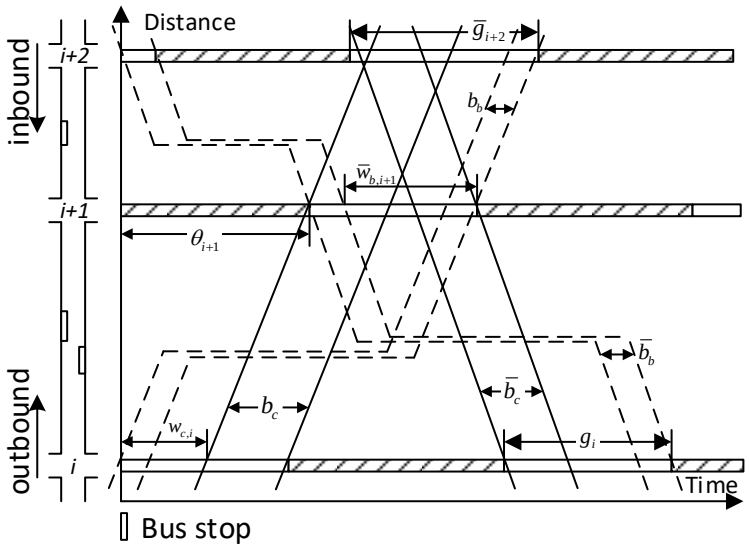

Figure 6.2 Key notations used in the proposed model.

6.3.1 Generating the progression band for passenger cars

To formulate the passenger car progression band, one can directly extend the notion of MAXBAND with the following constraints.

$$w_{c,i} \geq 0, w_{c,i} + b_c \leq g_i \tag{6.1}$$

$$\bar{w}_{c,i} \geq 0, \bar{w}_{c,i} + \bar{b}_c \leq \bar{g}_i \tag{6.2}$$

Eqs. (6.1) and (6.2) are interference constraints; where $g_i\left(\bar{g}_i\right)$ is the green time for outbound (inbound) through movement; $b_c\left(\bar{b}_c\right)$ represents the passenger car bandwidth for outbound (inbound) direction; $w_{c,i}\left(\bar{w}_{c,i}\right)$ denotes the time difference between the start (end) of the

green phase and the start (end) of the outbound (inbound) band. This set of constraints is developed to ensure the band to be within the green time.

Eqs. (6.3) - (6.6) are progression constraints derived to present the progress of the passenger car bands between intersections:

$$\theta_i + w_{c,i} + t_i + n_{c,i} \geq \theta_{i+1} + w_{c,i+1} + n_{c,i+1} - M\left(1 - x_c\right) \tag{6.3}$$

$$\theta_i + w_{c,i} + t_i + n_{c,i} \leq \theta_{i+1} + w_{c,i+1} + n_{c,i+1} + M\left(1 - x_c\right) \tag{6.4}$$

$$-\theta_i - r_i + \overline{w}_{c,i} + \overline{t}_i + \overline{n}_{c,i} \geq -\theta_{i+1} - r_{i+1} + \overline{w}_{c,i+1} + \overline{n}_{c,i+1} - M\left(1 - \overline{x}_c\right) \tag{6.5}$$

$$-\theta_i - r_i + \overline{w}_{c,i} + \overline{t}_i + \overline{n}_{c,i} \leq -\theta_{i+1} - r_{i+1} + \overline{w}_{c,i+1} + \overline{n}_{c,i+1} + M\left(1 - \overline{x}_c\right) \tag{6.6}$$

Where θ_i is the offset at intersection *i*; r_i is the time difference between the start of the outbound green phase and the end of the inbound green phase; $t_i\left(\overline{t}_i\right)$ represents the travel time from intersection *i*(*i*+1) to *i*+1(*i*); $n_{c,i}\left(\overline{n}_{c,i}\right)$ is a set of integer variables to indicate the number of cycles; M is a large positive number; and $x_c\left(\overline{x}_c\right)$ is a binary variable denoting the existence of the outbound (inbound) passenger car band, which equals 1 if cars are provided with a progression band. In this study, $x_c\left(\overline{x}_c\right)$ is introduced to allow the model to select proper modes to provide progression. When x_c equals 1, the last terms in Eqs. (6.3) and (6.4) become 0, forcing

$\theta_i + w_{c,i} + t_i + n_{c,i}$ to be equal to $\theta_{i+1} + w_{c,i+1} + n_{c,i+1}$ to satisfy both equations, which ensures that the vehicles in the band would traverse the arterial segment without stops, as shown by the solid line between two adjacent intersections in Figure 6.2; otherwise, x_c equals 0, indicating Eqs. (6.3) and (6.4) are relaxed and no longer effective.

Then, one can introduce the following constraints formulated to capture the relations between the bandwidth and the variable x_c:

$$b_c \le x_c \tag{6.7}$$

$$\bar{b}_c \le \bar{x}_c \tag{6.8}$$

$$b_c \ge \beta - M\left(1 - x_c\right) \tag{6.9}$$

$$\bar{b}_c \le \beta - M\left(1 - \bar{x}_c\right) \tag{6.10}$$

Eqs. (6.7) and (6.8) force the bandwidth to be zero when the band is removed from the optimization (i.e., $x_c = 0$), while Eqs. (6.9) and (6.10) function to guarantee the minimum effective bandwidth β.

6.3.2 Defining the progression band for buses

By following the same logic as those for passenger cars, the interference constraints and progression constraints for the bus band can be expressed as follows:

$$w_{b,i} \geq 0, w_{b,i} + b_b \leq g_i \tag{6.11}$$

$$\bar{w}_{b,i} \geq 0, \bar{w}_{b,i} + \bar{b}_b \leq \bar{g}_i \tag{6.12}$$

$$\theta_i + w_{b,i} + t_i + n_{b,i} \geq \theta_{i+1} + w_{b,i+1} + n_{b,i+1} - M\left(1 - x_b\right) \tag{6.13}$$

$$\theta_i + w_{b,i} + t_i + n_{b,i} \leq \theta_{i+1} + w_{b,i+1} + n_{b,i+1} + M\left(1 - x_b\right) \tag{6.14}$$

$$-\theta_i - r_i + \bar{w}_{c,i} + \bar{t}_i + \bar{t}_{d,i} + \bar{n}_{b,i} \geq -\theta_{i+1} - r_{i+1} + \bar{w}_{b,i+1} + \bar{n}_{b,i+1} - M\left(1 - \bar{x}_b\right) \tag{6.15}$$

$$-\theta_i - r_i + \bar{w}_{b,i} + \bar{t}_i + \bar{t}_{d,i} + \bar{n}_{b,i} \leq -\theta_{i+1} - r_{i+1} + \bar{w}_{b,i+1} + \bar{n}_{b,i+1} + M\left(1 - \bar{x}_b\right) \tag{6.16}$$

$$b_b \leq x_b \tag{6.17}$$

$$\bar{b}_b \leq \bar{x}_b \tag{6.18}$$

where *b* refers to bus as the subscript in variables $w_{b,i}\left(\bar{w}_{b,i}\right), b_b\left(\bar{b}_b\right), n_{b,i}\left(\bar{n}_{b,i}\right)$ and $x_b\left(\bar{x}_b\right)$; $t_{d,i}\left(\bar{t}_{d,i}\right)$ refers to the average dwell time at the outbound (inbound) bus stop between intersections *i* and *i*+1.

This study has further considered various operational features of buses that are different from passenger cars. The first one is the discretization of the bus band due to the large size and long headway of buses, and the following constraints can be derived to address this issue:

$$m_b u_b \xi \le b_b \tag{6.19}$$

$$\bar{m}_b u_b \xi \le \bar{b}_b \tag{6.20}$$

where $m_b\left(\bar{m}_b\right)$ is the number of buses accommodated in the outbound (inbound) bus band; u_b is the bandwidth for one bus, which is defined as bus cruising headway in this study; and ξ refers to the reciprocal of the cycle length. With Eqs. (6.19) and (6.20), one can obtain the maximum number of accommodated buses in the band.

Note that the bus band should be constrained by the number of the buses per cycle and the bus stop capacity to ensure that the model will not yield the excess width of bus band at the cost of passenger car bands. The constraints for such needs are shown below:

$$m_b \le \frac{V_b}{3600\xi} \tag{6.21}$$

$$\bar{m}_b \le \frac{\bar{V}_b}{3600\xi} \tag{6.22}$$

$$m_b \le q_i \tag{6.23}$$

$$\bar{m}_b \le \bar{q}_i \tag{6.24}$$

where $V_b\left(\bar{V}_b\right)$ indicates the outbound (inbound) bus volume (in vehicle/hour); and q_i denotes the maximum number of buses in a bus stop. The aforementioned constraints are to formulate the operational features of passenger cars and buses.

6.3.3 Passenger Car Queue Blocking Bus Stop

Passenger cars not experiencing progression between two intersections may form queues and thus block the bus stop. Hence, their offsets should be so designed that the passenger car queues will be fully discharged by the arrival of bus flows. To determine whether the maximum vehicle queues may block the bus stop or not, one shall first estimate the queue length at the end of red phase. Such queues typically consist of through vehicle flows from the upstream intersection that cannot experience progression and those turning from side streets heading to intersection *i*+1. The length of those queues at the end of the red phase can be expressed as below:

$$l_{i+1} = \left(f_i^t \left(g_i - \min\left(\theta_i + g_i + t_i - \theta_{i+1}, \theta_{i+1} + g_{i+1} - \theta_i - t_i\right)\right) + f_i^c \right) \frac{h}{3600\xi} \tag{6.25}$$

where l_i denotes the vehicle queue length at the end of the red phase; f_i^t denotes the through volume from intersection *i* to *i*+1 (in veh/lane/hr); f_i^c represents the turning volume from the side streets at intersection *i* to *i*+1 (in veh/lane/hr); and *h* denotes the vehicle's space headway (in feet). The term of $\min\left(\theta_i + g_i + t_i - \theta_{i+1}, \theta_{i+1} + g_{i+1} - \theta_i - t_i\right)$ is to calculate the progression duration between two consecutive intersections.

To indicate whether the traffic queue will block the bus stop or not, a set of binary variables are introduced as below,

$$y_i = \begin{cases} 1, & l_i s/(s-f_i) \geq d_i^s \\ 0, & \text{otherwise} \end{cases} \tag{6.26}$$

where y_i is a binary variable, indicating whether the bus stop between intersection *i*-1 and *i* would be blocked by the vehicle queues; d_i^s denotes the distance between intersection *i* and the bus stop at its upstream (in feet); *s* denotes the saturation flow rate; and f_i represents the arriving through volume at intersection *i* (in veh/lane/hr). The term of $l_i s/(s-f_i)$ is to calculate the furthest point of the queue length from the stop line.

If the vehicle queues block the bus stop, then the bus band should be designed to be free from the interruption by the queue. To do so, one can develop the following set of constraints,

$$w_{b,i+1} - t_i \frac{l_{i+1} s/(s-f_{i+1})}{d_i} - t_{d,i} \geq \frac{l_{i+1}}{s-f_{i+1}} \xi - (1-y_i) \times M \tag{6.27}$$

where d_i represents the distance between intersections *i* and *i*+1 (in feet).

In Eq. (6.27), the left-hand-side represents the time of the first bus within the bus band to reach the furthest point of the vehicle queues, and the right-hand-side denotes the time when the queue is fully discharged. Eq. (6.27) will be relaxed when y_i equals 0, indicating that the traffic

queue does not block the bus stop. One can develop similar constraints for inbound direction, following the logic of Eq. (6.25) - (6.27).

6.3.4 Intersection Bus Queues Blocking the Passenger Car Progression

To quantify the interruption to passenger-car progression due to bus queues at the intersection, one shall first estimate the expected number of those buses, following the concept in Eq. (6.25), as below,

$$\gamma_i = \frac{V_b}{3600\xi}\left(g_i - \min\left(\theta_i + g_i + t_i + t_{d,i} - \theta_{i+1}, \theta_{i+1} + g_{i+1} - \theta_i - t_i - t_{d,i}\right)\right) / g_i \tag{6.28}$$

where γ_i denotes the expected number of buses waiting at the stop line of intersection *i+1* during each cycle. The term $\min\left(\theta_i + g_i + t_i + t_{d,i} - \theta_{i+1}, \theta_{i+1} + g_{i+1} - \theta_i - t_i - t_{d,i}\right)$ refers to the available progression duration for buses between two adjacent intersections. It takes $\gamma_i \mu_b$ duration for these buses to discharge. If the time between the start of a green phase and the start of the passenger car band is smaller than $\gamma_i \mu_b$, then the interrupted portion of the band can be expressed as $\gamma_i \mu_b \xi - w_i$. During the interrupted period, passenger cars on the rightmost lane cannot have the progression. Hence, one needs to adjust the offsets and the bandwidth at intersection *i*, considering the interruption to passenger cars, as follows:

$$b'_{c,i} = b_c - \max\left(\gamma_i u_b \xi - w_i, 0\right) / z_i \tag{6.29}$$

where $b'_{c,i}$ represents the effective passenger car bandwidth under the interruption of intersection bus queues; and z_i denotes the number of lanes on the upstream link of intersection i.

6.3.5 Buses at Bus Stops Blocking Passenger Cars

To estimate the interruption to passenger car progression due to buses waiting at bus stops, one can apply Eqs. (6.30)-(6.31) to find the portion of passenger car band after the start of the bus band, and that before the end of the bus band, denoted by $t_{a,i}$ and $t_{b,i}$, respectively, as shown in Figure 1.

$$t_{a,i} = \max\left(0, \min\left(1, w_{c,i} + b_c - w_{b,i}\right)\right) \tag{6.30}$$

$$t_{b,i} = \max\left(0, \min\left(1, w_{b,i} + b_b - w_{c,i}\right)\right) \tag{6.31}$$

If the sum of $t_{a,i}$ and $t_{b,i}$ is smaller than the bandwidth, the interrupted portion of the passenger car band can be expressed by $t_{a,i} + t_{b,i}$; otherwise, the interrupted portion equals $t_{a,i} + t_{b,i} - b_c$. In general, the effective bandwidth $b''_{c,i}$, considering the interruption to passenger car bands due to buses waiting at bus stops and intersection stop lines, can be expressed as follows:

$$b''_{c,i} = b'_{c,i} - \left(t_{a,i} + t_{b,i} - b_c \times p_i\right) \tag{6.32}$$

where p_i is a binary variable which equals 1 if $t_{a,i} + t_{b,i}$ is greater than the passenger car bandwidth.

Following the same logic, one can develop similar constraints as Eqs. (6.28) - (6.32) for the inbound direction.

6.3.6 Objective Function

The objective function of this study is to maximize the sum of all bandwidths weighted by the number of passengers with each mode and in each direction, which can be expressed as follows:

$$\max \sum_{i}^{N-1} b''_{c,i} V_c k_c + \sum_{i}^{N-1} \bar{b}''_{c,i} \bar{V}_c \bar{k}_c + (N-1) m_b u_b \xi V_b k_b + (N-1) \bar{m}_b u_b \xi \bar{V}_b \bar{k}_b \quad (6.33)$$

where $k_c(\bar{k}_c)$ and $k_b(\bar{k}_b)$ denote the loading factors of passenger cars and buses, respectively; and N is the number of intersections for the study segment. Note that the effective bus band is measured with the number of accommodated buses, while the effective passenger car band has accounted for the interruptions due to buses dwelling at bus stops or at the intersection. With the specified objective function, the proposed model can concurrently yield the progression bands for both buses and passenger cars if both of their demand levels justify to do so. However, the priority will be first assigned to the mode carrying more passengers, and then the model will accommodate the other with the remaining green duration. Depending on the distribution of volumes for bus and passenger car flows and all related factors (e.g., green time, bus stop capacity, and distance between intersections), the best benefit for the arterial flows may not be offering concurrent progression. Then, the proposed model with its embedded formulations is capable of selecting both the proper modes and directions to exercise the progression and yield the best

benefits for the perspective of entire arterial. To ensure the reasonable bandwidth for passenger cars on the direction with a low volume, the directional balance constraint is defined as follows:

$$(1-K)\bar{b}_c \geq (1-K)Kb_c - M - (2 - x_c - \bar{x}_c) \tag{6.34}$$

where $K = \bar{V}_c / V_c$ is a directional balance factor. Note that this constraint will be relaxed when the passenger car band for either direction does not exist.

In brief, the dual-modal progression design model for an arterial segment with transit flows can be summarized as follows:

$$\max \sum_{i}^{N-1} b''_{c,i} V_c k_c + \sum_{i}^{N-1} \bar{b}''_{c,i} \bar{V}_c \bar{k}_c + (N-1) m_b u_b \xi V_b k_b + (N-1) \bar{m}_b u_b \xi \bar{V}_b \bar{k}_b$$

s.t.

Progression of through vehicles along the arterial:

$$(1-K)\bar{b}_c \geq (1-K)Kb_c - M - (2 - x_c - \bar{x}_c)$$

$$w_{c,i} \geq 0, w_{c,i} + b_c \leq g_i$$

$$\bar{w}_{c,i} \geq 0, \bar{w}_{c,i} + \bar{b}_c \leq \bar{g}_i$$

$$\theta_i + w_{c,i} + t_i + n_{c,i} \geq \theta_{i+1} + w_{c,i+1} + n_{c,i+1} - M(1 - x_c)$$

$$\theta_i + w_{c,i} + t_i + n_{c,i} \le \theta_{i+1} + w_{c,i+1} + n_{c,i+1} + M\left(1 - x_c\right)$$

$$-\theta_i - r_i + \bar{w}_{c,i} + \bar{t}_i + \bar{n}_{c,i} \ge -\theta_{i+1} - r_{i+1} + \bar{w}_{c,i+1} + \bar{n}_{c,i+1} - M\left(1 - \bar{x}_c\right)$$

$$-\theta_i - r_i + \bar{w}_{c,i} + \bar{t}_i + \bar{n}_{c,i} \le -\theta_{i+1} - r_{i+1} + \bar{w}_{c,i+1} + \bar{n}_{c,i+1} + M\left(1 - \bar{x}_c\right)$$

$$b_c \le x_c$$

$$\bar{b}_c \le \bar{x}_c$$

$$b_c \ge \beta - M\left(1 - x_c\right)$$

$$\bar{b}_c \le \beta - M\left(1 - \bar{x}_c\right)$$

Progression of buses along the arterial:

$$w_{b,i} \ge 0, w_{b,i} + b_b \le g_i$$

$$\bar{w}_{b,i} \ge 0, \bar{w}_{b,i} + \bar{b}_b \le \bar{g}_i$$

$$\theta_i + w_{b,i} + t_i + n_{b,i} \ge \theta_{i+1} + w_{b,i+1} + n_{b,i+1} - M\left(1 - x_b\right)$$

$$\theta_i + w_{b,i} + t_i + n_{b,i} \le \theta_{i+1} + w_{b,i+1} + n_{b,i+1} + M\left(1 - x_b\right)$$

$$-\theta_i - r_i + \bar{w}_{c,i} + \bar{t}_i + \bar{t}_{d,i} + \bar{n}_{b,i} \geq -\theta_{i+1} - r_{i+1} + \bar{w}_{b,i+1} + \bar{n}_{b,i+1} - M\left(1 - \bar{x}_b\right)$$

$$-\theta_i - r_i + \bar{w}_{b,i} + \bar{t}_i + \bar{t}_{d,i} + \bar{n}_{b,i} \leq -\theta_{i+1} - r_{i+1} + \bar{w}_{b,i+1} + \bar{n}_{b,i+1} + M\left(1 - \bar{x}_b\right)$$

$$b_b \leq x_b$$

$$\bar{b}_b \leq \bar{x}_b$$

Bus operational features:

$$m_b u_b \xi \leq b_b$$

$$\bar{m}_b u_b \xi \leq \bar{b}_b$$

$$m_b \leq \frac{V_b}{3600\xi}$$

$$\bar{m}_b \leq \frac{\bar{V}_b}{3600\xi}$$

$$m_b \leq q_i$$

$$\bar{m}_b \leq \bar{q}_i$$

Local progression and queue length calculation:

$$l_{i+1} = \left(f_i^t \left(g_i - \min\left(\theta_i + g_i + t_i - \theta_{i+1}, \theta_{i+1} + g_{i+1} - \theta_i - t_i\right)\right) + f_i^c \right) \frac{h}{3600\xi}$$

$$\bar{l}_i = \left(\bar{f}_{i+1}^t \left(\bar{g}_{i+1} - \min\left(\theta_{i+1} + \bar{g}_{i+1} + \bar{t}_i - \theta_i, \theta_i + \bar{g}_i - \theta_{i+1} - \bar{t}_i\right)\right) + \bar{f}_i^c \right) \frac{h}{3600\xi}$$

Mutual interruptions between passenger cars and buses:

$$w_{b,i+1} - t_i \frac{l_{i+1} s / \left(s - f_{i+1}\right)}{d_i} - t_{d,i} \geq \frac{l_{i+1}}{s - f_{i+1}} \xi - \left(1 - y_i\right) \times M$$

$$\bar{w}_{b,i} - t_i \frac{\bar{l}_i s / \left(s - \bar{f}_i\right)}{\bar{d}_i} - \bar{t}_{d,i} \geq \frac{\bar{l}_i}{s - \bar{f}_i} \xi - \left(1 - \bar{y}_i\right) \times M$$

$$\gamma_i = \frac{V_b}{3600\xi} \left(g_i - \min\left(\theta_i + g_i + t_i + t_{d,i} - \theta_{i+1}, \theta_{i+1} + g_{i+1} - \theta_i - t_i - t_{d,i}\right)\right) / g_i$$

$$\bar{\gamma}_i = \frac{\bar{V}_b}{3600\xi} \left(\bar{g}_{i+1} - \min\left(\theta_{i+1} + \bar{g}_{i+1} + \bar{t}_i + \bar{t}_{d,i} - \theta_i, \theta_i + \bar{g}_i - \theta_{i+1} - \bar{t}_i - \bar{t}_{d,i}\right)\right) / \bar{g}_{i+1}$$

$$b'_{c,i} = b_c - \max\left(\gamma_i u_b \xi - w_i, 0\right) / z_i$$

$$\bar{b}'_{c,i+1} = b_c - \max\left(\bar{\gamma}_i u_b \xi - \left(\bar{g}_{i+1} - \bar{w}_{i+1} - \bar{b}_c\right), 0\right) / z_i$$

$$t_{a,i} = \max\left(0, \min\left(1, w_{c,i} + b_c - w_{b,i}\right)\right)$$

$$t_{b,i} = \max\left(0, \min\left(1, w_{b,i} + b_b - w_{c,i}\right)\right)$$

$$b''_{c,i} = b'_{c,i} - \left(t_{a,i} + t_{b,i} - b_c \times p_i\right)$$

$$\bar{t}_{a,i} = \max\left(0, \min\left(1, \bar{w}_{b,i+1} + \bar{b}_b - \bar{w}_{c,i}\right)\right)$$

$$\bar{t}_{b,i} = \max\left(0, \min\left(1, \bar{w}_{c,i} + \bar{b}_c - \bar{w}_{b,i}\right)\right)$$

$$\bar{b}''_{c,i} = \bar{b}'_{c,i} - \left(\bar{t}_{a,i} + \bar{t}_{b,i} - \bar{b}_c \times \bar{p}_i\right)$$

In summary, the proposed model considers the operational features of passenger car and buses, as well as the interrelation between those two modes in the evaluation of arterial traffic flows. The proposed model is formulated as mixed-integer-linear-programming and can be solved with existing solvers.

6.4 Numerical examples

To evaluate the performance and effectiveness of the proposed model, this section has shown the results from both numerical analyses and simulation experiments. The first part of the analyses is designed to evaluate the model's unique functions for assessing the need of offering the progression bands for buses or passenger cars only, or for both under the detected traffic volumes, the percentage of buses and their loading factors, and geometric conditions. Second part of the analysis is focused on the effectiveness of the model formulations, especially on:

- The impacts of bus stop capacity on the effective bus band width;
- Formulations of bus stops blocked by passenger car queues;
- The potential interruption of bus queues at the intersection's stop line on the progression band designed for passenger cars; and
- The potential interruption of buses dwelling at bus stops on the progression band designed for passenger cars

Performance comparison with state-of-the-art models have also been conducted to ensure the proposed model's potential for field applications.

6.4.1 Design of Experiments

Figure 6.3 shows the key geometric, bus operational, and signal timing information for the arterial of six intersections on Luomashi St. in Beijing, China, for experimental analysis; seven traffic volume scenarios with different bus ratios for performance evaluation are shown in Table 6.1.

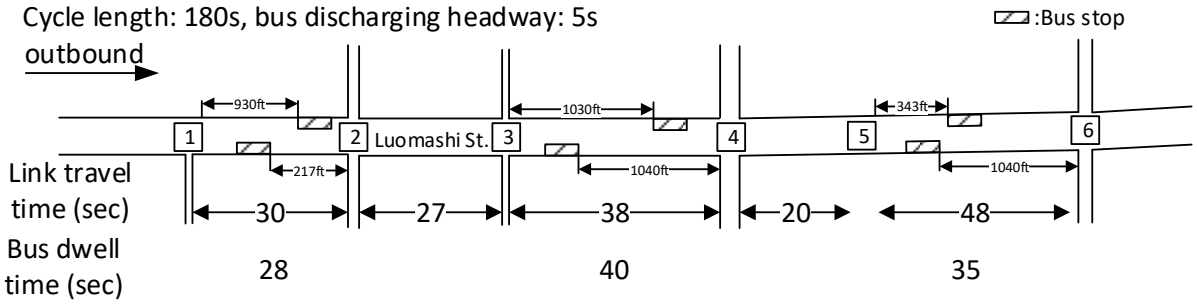

Scenario	Bus stop capacity	Green split (in cycle) for the through movements at each intersection					
		1	2	3	4	5	6
1-4	2	0.63	0.50	0.57	0.50	0.84	0.56
5	2	0.63	0.50	0.57	0.45	0.84	0.69
6	3	0.63	0.50	0.57	0.45	0.84	0.69
7	3	0.63	0.35	0.57	0.35	0.84	0.46

Figure 6.3 The key information associated with the study site

Table 6.1 Traffic Volumes and Loading Factors Adopted in the Numerical Experiments

Scenario	Car volume (vehicle per hour)		Bus volume (vehicle per hour)		Bus loading factors (person per vehicle)	
	Outbound	Inbound	Outbound	Inbound	Outbound	Inbound
1	2000	1800	48	48	50	50
2	2000	1800	3	3	20	20
3	2000	1800	30	30	30	30
4	2000	2200	30	60	30	40
5	2000	2200	60	60	50	50
6	2000	2200	60	30	20	20
7	2000	1800	100	100	80	80

- Car loading factor: 1.2 (person per vehicle)

6.4.2 Numerical Analysis

The resulting bandwidths obtained from the proposed model are shown in Table 2. All experimental results have been obtained with the computing time of less than 20 seconds. Based on the selected modes and directions, one can categorize the results of maximizing progression into three types as follows:

Type-1: concurrent progression for both buses and passenger cars

Scenarios 1, 5 and 6 fit to this type of design. Such progression plan may be essential if both of their demand levels justify to do so. Taking Scenario 1 as an example, demands for both passenger cars and buses in the outbound direction are the same at the level of 2,400 persons and

both would benefit from the progression design. Certainly, the feasibility of offering such a design also depends on other factors such as green ratios and geometric conditions.

Type-2: two-way progression for a single mode (i.e., passenger cars or buses)

Scenarios 2 and 7 are justified to have such design, because the demand from one mode far exceeds the other. For example, under Scenario 2 with low bus volumes and small bus loading factors, the proposed model provides progression only for cars.

Type-3: one-way progression for both modes (i.e., passenger cars and buses)

For the maximum benefits of the entire arterial users, one shall have Type-3 progression design for Scenarios 3 and 4. Such results may occur if traffic demand for one direction is significantly higher than the other.

Table 6.2 Summary of the Produced Progression Strategies and the Resulting Bands

Scenario	Bus bands (seconds)[a]		PC bands (seconds)[b]		Produced bands
	Outbound	Inbound	Outbound	Inbound	
1	10 (2)	5 (1)	90	0	Two-way bus bands+one-way car band
2	0 (0)	0 (0)	35	31	Two-way car bands
3	0 (0)	5 (1)	90	0	One-way car band+one-way bus band
4	0 (0)	10 (2)	0	90	One-way car band+bus band
5	10(2)	10 (2)	37	41	Two-way car bands+bus bands
6	15(3)	0	37	41	Two-way car bands+one-way bus band
7	15(3)	15 (3)	0	0	Two-way bus bands

[a] Numbers in parenthesis represent the number of accommodated buses in the bus band
[b] PC: passenger cars

Table 6.3 and Figure 6.4 further show the progression bands generated by the proposed model under different inputs and formulation conditions for Scenarios 6 and 7. First, by comparing the allocated bandwidth to buses and passenger cars in Scenarios 7 and 7(a), the proposed model with its constraints for bus stop capacity will reduce the inbound bus band from 15 seconds in Scenario 7 to 0 seconds in Scenario 7(a) with the reduced capacity (2 buses) of bus stops in the inbound direction, because some portion of the initially allocated bus band under the reduced bus stop capacity will be unusable, and thus the system shall reallocate those green time to the passenger car band, followed by redesign of the signal offsets to support such changes in geometric conditions.

Table 6.3 Numerical Experiment Results to Evaluate the Performance of Developed Constraints

Scenario	Bus bands (seconds)[a]		PC bands (seconds)		Conditions
	OB[b]	IB	OB	IB	
6	15(3)	0	37	41	
6(a)	15(3)	10(2)	37	41	A model without constraints reflecting interruptions of buses at bus stops
6(b)	15(3)	0	37	41	A model without constraints reflecting interruptions of buses at stop bars

7	15(3)	15(3)	0	0	
7(a)	15(3)	0	0	57	Reduced capacity of bus stops in IB of 2 buses
7(b)	15(3)	0	0	50	Higher turn-in volumes from side streets

[a] Numbers in parenthesis represent the number of accommodated buses in the band
[b] OB: outbound; IB: inbound

Secondly, the results shown in Scenarios 7 and 7(b) are used to justify the need for modeling the impacts of high turn-in volumes from side streets that often form the queues and block the links having the bus stops. In Scenario 7(b), inbound buses, for the perspective of the entire arterial users' benefits, should not be given the desirable progression due to the inevitable presence of passenger car queues and their blockage to bus stops caused by the higher passenger car volumes. Hence, for the benefits of the entire system, the proposed model will offer progression to only passenger cars instead of providing an inefficient band to buses for the inbound direction, to best use the available green time.

The comparison results between Scenarios 6 and 6(a) are designed to evaluate the constraints formulated to reflect the impacts of buses dwelling at bus stops on the progression bands for passenger cars while maximizing the bands for two modes. Without such constraints (in Scenario 6(a)), the produced signal settings and offsets generate a 10-second bus band for the inbound direction which will cause the passenger car band to be blocked by bus platoon dwelling at the stops. Therefore, the proposed model would not compromise car band to generate the bus band.

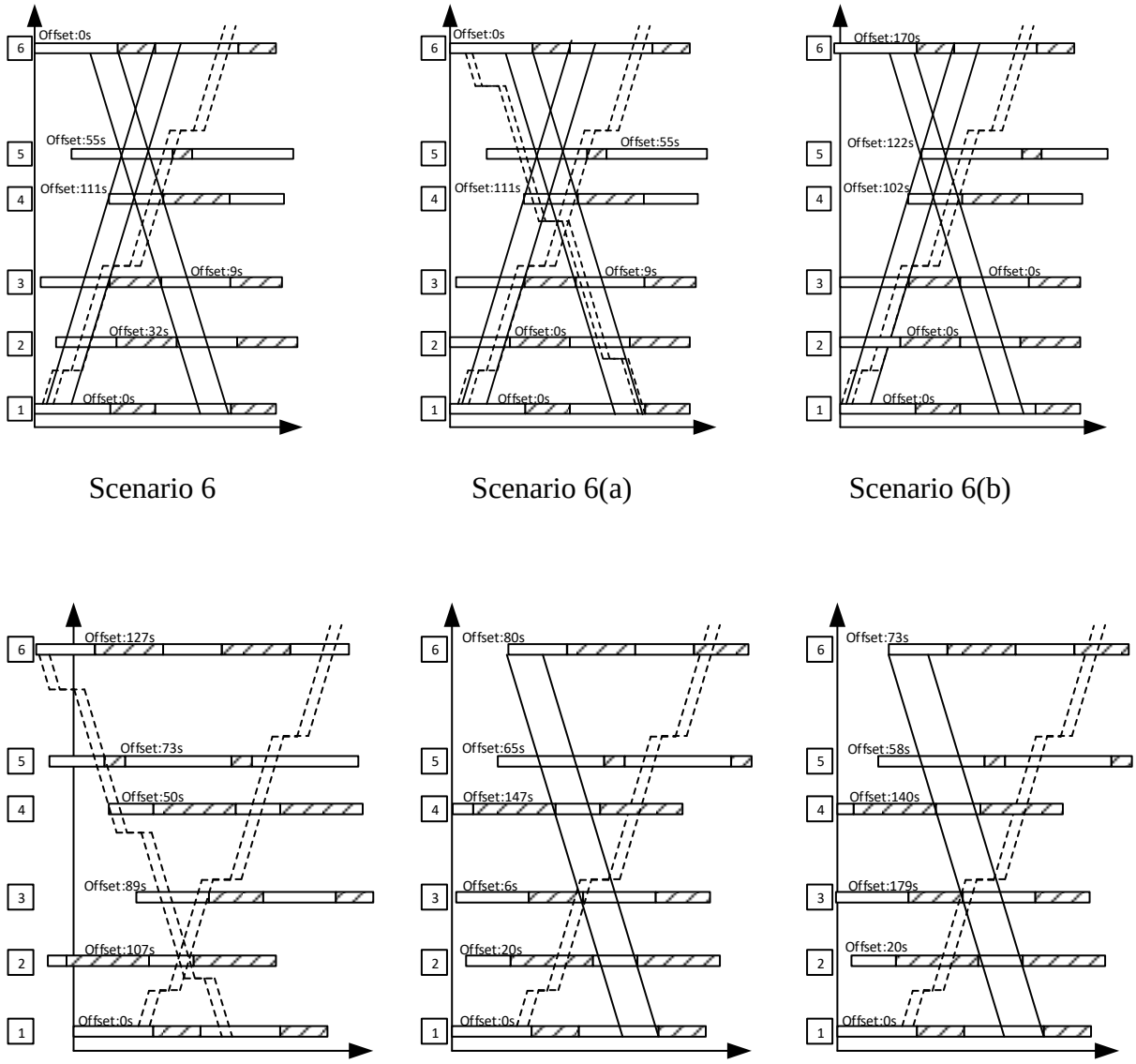

Scenario 6 Scenario 6(a) Scenario 6(b)

Scenario 7 Scenario 7(a) Scenario 7(b)

Figure 6.4 progression bands and offsets generated by the proposed model

The comparison results between Scenarios 6 and 6(a) are designed to evaluate the constraints formulated to reflect the impacts of buses dwelling at bus stops on the progression bands for passenger cars while maximizing the bands for two modes. Without such constraints (in Scenario 6(a)), the produced signal settings and offsets generate a 10-second bus band for the

inbound direction which will cause the passenger car band to be blocked by bus platoon dwelling at the stops. Therefore, the proposed model would not compromise car band to generate the bus band.

Lastly, Scenario 6(b) without the constraints of reflecting interruptions by the buses at an intersection's stop line generates the same bandwidth as for Scenario 6 but with different offsets. Without a bus band in the inbound direction, buses are more likely to be stopped by the signal at Intersection 5. Scenario 6(b) fails to take this situation into account and produces an ineffective passenger band at the start of green time at this intersection. With such constraints, the proposed model would adjust offsets between each pair of intersections to ensure that buses out of the band would not block the passenger car progression band.

Table 6.2 shows that the proposed model is capable of best selecting both the directions and modes to offer the progression from the perspective of maximizing the benefits of the entire system, based on the constraints such as volumes of buses and cars, cycle length, and spacing between intersections. The numerical experiments in Table 6.3 and Figure 6.4 have further shown the necessity and effectiveness of each set of constraints developed for the proposed model. To further evaluate the operational performance of the signal plan obtained from the proposed model, this study has implemented VISSIM to conduct simulation evaluation using the study site under various traffic volumes. This is to ensure that implementing the operational progression strategy can also yield the benefits for the system even evaluated with measures of effectiveness (MOEs) other than bandwidths.

6.4.3 Simulation Evaluation

The purpose of simulation experiments is to evaluate the proposed model's performance, designed to maximize the weighted total bandwidth, with other MOEs. The following two models have also been simulated for performance comparison.

- MULTIBAND: a state-of-the-art model to design two-way progression for passenger cars
- MULTIBAND-B: a revised MULTIBAND model for bus progression where the average dwell time at bus stops is added to the link travel time

Scenarios 1 to 3 are adopted in the simulation evaluation, and the results with respect to the car and bus delays are shown in Table 6.4. The number of stops for passenger cars and buses are also shown in Table 6.5.

As shown in Table 6.4, for Scenarios 1 and 3 with a considerable number of bus passengers, the proposed model, as expected, can yield lower bus delays than with MULTIBAND, and lower car delay than with MULTIBAND-B, since it concurrently considers the benefits of both modes. The same improvements by the proposed model also exist when evaluated with the MOE of number of stops, as shown in Table 6.5. The results in Scenario 2 show that the proposed model produces a similar car delay with MULTIBAND and even a smaller number of stops than MULTIBAND since the proposed model does not provide bands for buses due to the very low bus volume, indicating the proposed model's flexibility to function as a conventional model for passenger car progression under the low bus volume scenario. Under Scenario 3, buses are presumed to take a considerable number of passengers, although they are fewer than those by cars.

The proposed model is able to produce a lower delay and the number of stops for passenger cars since it can yield passenger car bands without the interruption of buses to passenger cars.

Table 6.4 Average Delay of Two Modes along the Arterial (seconds)

Scenario	Model	Passenger cars			Buses		
		OB	IB	Total	OB	IB	Total
1	Proposed model	85	193	135	157	213	184
	MULTIBAND	168	169	168	228	221	224
	MULTIBAND-B	150	164	156	144	208	175
2	Proposed model	137	164	149	212	172	190
	MULTIBAND	140	148	144	198	202	199
	MULTIBAND-B	148	165	156	95	184	137
3	Proposed model	90	190	137	139	201	169
	MULTIBAND	157	154	156	218	201	209
	MULTIBAND-B	150	167	158	120	199	158

*OB: outbound, IB: inbound

Table 6.5 Number of Stops of Two Modes along the Arterial

Scenario	Model	Passenger cars			Buses		
		OB	IB	Total	OB	IB	Total
1	Proposed model	2.58	4.53	3.49	3.22	4.59	3.87
	MULTIBAND	3.55	4.57	4.04	4.76	4.73	4.74
	MULTIBAND-B	4.52	4.08	4.32	3.07	4.15	3.59
2	Proposed model	3.16	3.60	3.37	3.73	2.95	3.31
	MULTIBAND	2.86	4.16	3.48	2.95	3.50	3.23
	MULTIBAND-B	4.45	3.87	4.18	1.50	2.98	2.19
3	Proposed model	2.68	4.35	3.47	2.18	4.05	3.08
	MULTIBAND	3.26	4.08	3.65	3.93	3.73	3.82
	MULTIBAND-B	4.48	4.16	4.33	2.14	3.58	2.83

*OB: outbound, IB: inbound

Figure 6.5 shows the average arterial delay produced from the progression plan by each model, including person delay under different traffic demand scenarios. The error bars show the 90% confidence interval of the delays obtained from the simulation runs. The proposed model, as expected, can reduce person delays along the arterial by considering traffic volumes of both modes and their loading factors, and be more efficient than either MULTIBAND or MULTIBAND-B. Under Scenario 1 where two modes have balanced numbers of passengers, the advantage of the

proposed model becomes more pronounced as it can provide concurrent progression for both modes. Under Scenario 2, although the proposed model yields higher bus delays than with MULTIBAND-B, designed mainly for bus progression, its average person delay is smaller than with MULTIBAND-B due to the low bus volume, which does not degrade the effectiveness of the proposed model. Moreover, it would not yield significantly lower average delay than MULTIBAND, suggesting the capability of the proposed model in selecting a proper mode to provide progression. Under Scenario 3, the proposed model can also balance the benefit of two modes and minimize their interruptions, evidenced by the lower average person delay than both MULTIBAND and MULTIBAND-B.

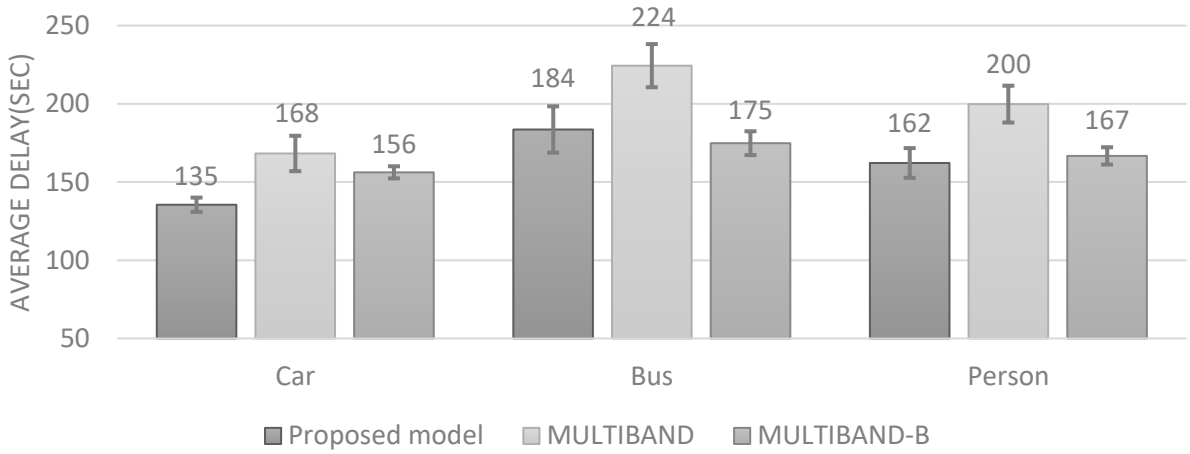

(a) Scenario 1

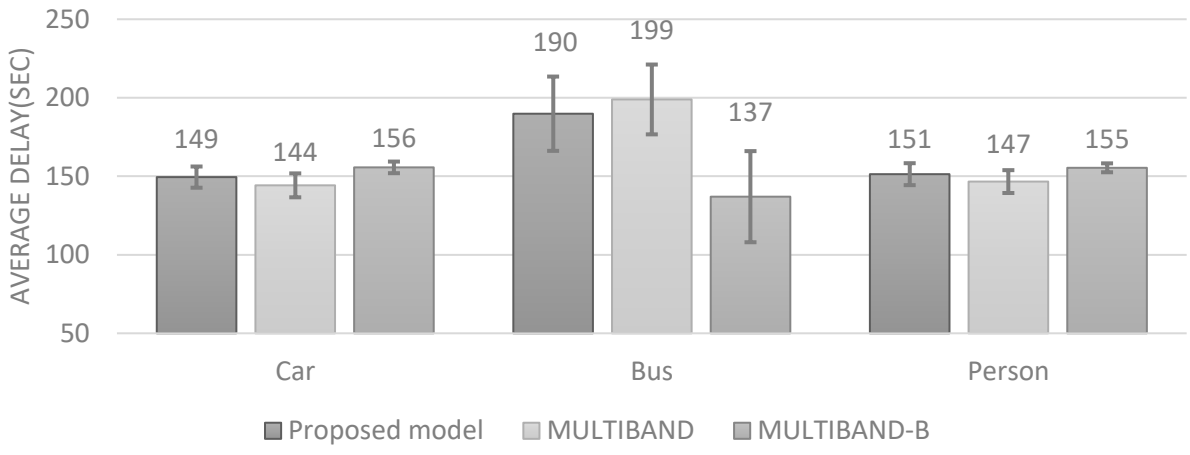

(b) Scenario 2

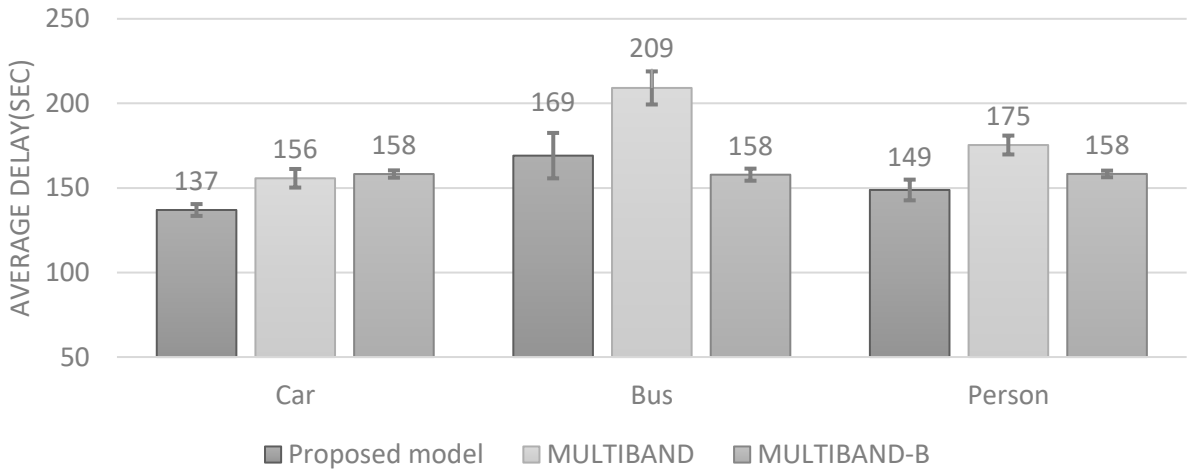

(c) Scenario 3

Figure 6.5 Average delay under different volume scenarios.

To sum up, the proposed model can outperform MULTIBAND and MULTIBAND-B in terms of person delay since it can produce progression bands for both buses and passenger cars, and account for both the number of users and volume in each mode, as well as their interrelations

in the arterial traffic evaluation progress. Moreover, under different passenger ratios between bus and car modes, geometric and signal conditions, the proposed model is capable of selecting the proper modes and directions to yield the progression design that can maximize the total benefits to the entire system users. Such a vital and effective feature will allow the traffic control center to dynamically adjust the signal progression plan so as to best the traffic condition in commuting arterials experiencing significant volumes of both modes.

6.5 Closure

Due to the unique operational characteristics of transit vehicles and their needs to stop at the roadside stations, most urban arterials, accommodating heavy passenger and transit flows, are often congested by the mutual blockage of these two modes, even though their signal plans have been designed with state-of-the-art progression maximization methods. Hence, both for ensuring an arterial's traffic efficiency and improving the transit service quality, the study has developed a dual-modal progression model to offer concurrent progression bands for both passenger and transit flows. The produced signal plan can serve as a base plan for other real-time control systems, including adaptive signal control and transit signal priority since those strategies can take advantage of the progression information in their dynamic response and adjustment process. For example, if TSP is implemented with the proposed signal plan, the estimated benefit of green extension will depend on whether or not the added green time may widen the bus band and/or the passenger car band. Moreover, the proposed model can be used to determine the initial offsets for adaptive control methods since the optimized offsets are sensitive to traffic volumes.

To identify the available progression bands for both modes under the given cycle length and signal settings, the proposed model has tackled various issues that may prevent both types of flows from progressing smoothly over consecutive intersections and link segments. Examples of such critical issues include the potential blockage of passenger car queues to the roadside bus stops, the excessive start-up delays caused by transit vehicles queueing at the intersections stop line, and the impedance to the travel lanes due to the buses dwelling at their roadside stations of limited storage capacity. In addition, weighted with the passenger volumes by mode and by direction in the objective function, the proposed model is capable of offering the progression only to the mode(s) and the direction(s) that are justified to do so from the perspective of maximizing the benefits for the entire arterial users.

Our numerical analysis results have confirmed the effectiveness of the proposed model in producing concurrent progression bands for both modes under various realistic constraints and volume levels. Further evaluation with a real-world arterial system and extensive simulation experiments have also demonstrated that the proposed model yielded about 11 to 23 percent lower bus delays than with MULTIBAND, and about 6 to 23 percent lower car delay than with MULTIBAND-B under different traffic conditions; and the benefits offered by the proposed dual-modal signal progression model will not be at the cost of other MOEs such as average person delay and number of stops.

CHAPTER 7： Arterial decomposition model for dual-modal progression for an arterial with heavy transit flows

7.1 Introduction

Note that Model III and Model IV, presented in Chapter 5 and Chapter 6, are respectively formulated to address two major arterial progression issues: decomposition of a long arterial and multi-modal progression. These two issues, however, may exist concurrently on urban arterials and ought to be addressed concurrently to best the benefits of all arterial users. An effective model, designed to tackle these two vital issues, shall be capable of providing the following functions:

- Design of concurrent progression for passenger cars and buses with minimal mutual interruptions between them;
- Minimizing the occurrence of left-turn bay spillover or blockage due to short bay lengths and high volumes;
- Selecting the modes, directions, and the optimized segments to offer the progression so as to maximize the total benefit of all roadway users;
- Identification of the design boundaries for optimal decomposition of a long arterial with multiple intersections; and
- Optimization of the offsets and phase sequence to prevent excessive queues at critical locations.

This chapter presents the formulations and evaluation of a two-stage optimization model to concurrently decompose a congested long arterial into an optimal number of subsegments for both modes so as to maximize the overall traffic efficiency for all roadway users. Such a model can not only execute those functions in Model III and Model IV, but also tackle additional issues

associated with the design of multi-modal progression on a long arterial, including 1) the competition between two modes on the number of intersections for progression; 2) the competition between two modes on the progression bandwidths; and 3) the flexibility for each mode to have its own decomposition locations.

7.2 Critical issues

--- *Competition between two modes on their progression bandwidths*

As stated in Chapter 6, passenger cars and transit vehicles by nature may compete for their own progression bandwidth within the limited green time at each intersection because the dwell time at bus stops will deviate the bus bands from the passenger car bands. Hence, regardless of the property of an arterial's decomposition design, an effective progression optimization model should be capable of selecting the proper mode(s) and direction(s) to offer the maximized progression bands, based on the volumes and loading factors of passenger cars and buses.

--- *Competition between two modes with respect to the number of intersections in each progression segment*

Since offering concurrent two-way progression to both modes may not be either feasible or yield the best benefits to the entire arterial's users, the optimal design may generate the output that one of those two modes shall not be provided with progression at some intersections in either direction.

--- *Flexibility in selecting the decomposition locations for each mode*

Note that the optimal decomposition locations for progression of passenger car and bus flows may differ with their travel times between each pair of adjacent intersections. Hence, to maximize the benefits to all arterial users, a decomposition model for multi-modal progression should allow both modes to decompose their progression bands at different locations.

7.3 Formulations of Model V

Grounded on the same logic for the two-stage signal optimization model (see Chapter 5) and the focus of the above critical issues, the formulations presented hereafter are developed to concurrently decompose a long arterial into the optimal number of segments and each with the optimized offsets and phase sequences. The logic framework for the entire model is shown in Figure 7.1.

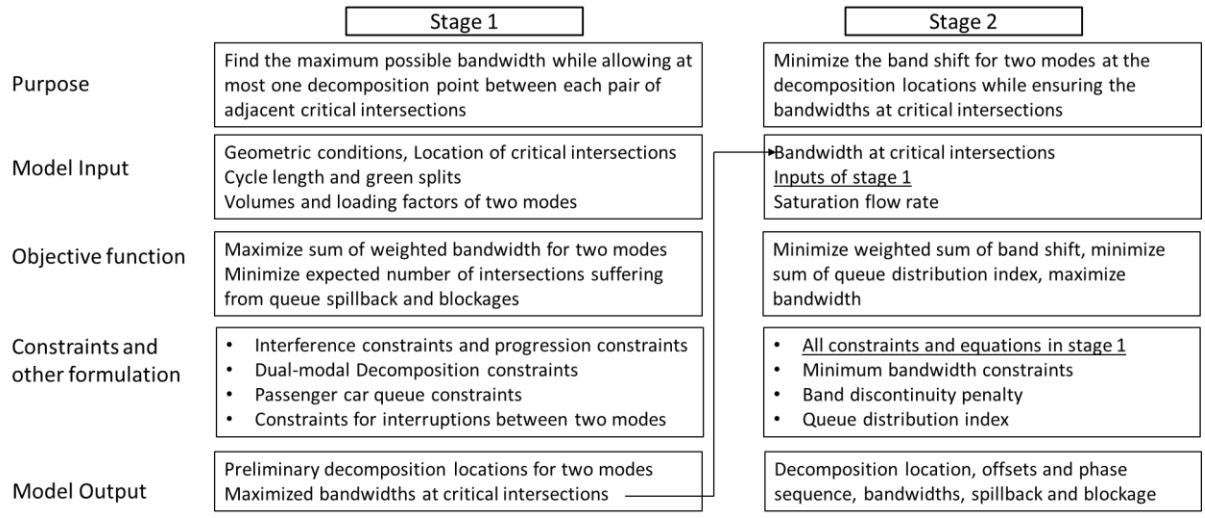

Figure 7.1 Structure of the proposed two-stage model for design of optimal arterial decomposition and progression for both passenger cars and buses

Based on each mode's volume and loading factors in each direction, the focus of Stage 1 is to compute the maximum bandwidth for passenger cars and buses at each critical intersection and yield an solution for the initial decomposition under a pre-specified constraint (i.e., only one decomposition location between two adjacent critical intersections). Following the logic of the arterial decomposition model in Chapter 5, the maximized bandwidth at each critical intersection obtained in Stage 1 will serve as an input for models in Stage 2, to select the optimal decomposition locations and adjust the offset as well as phase sequences so as to minimize the band discontinuity. Hence, to compute the progression offsets and decomposition locations for both modes, the model development for such needs shall consist of the following tasks:

- Decomposing the arterial into several segments and generating a maximized progression band for each segment concurrently for each mode, based on pre-specified critical intersections;
- Estimating traffic queues on both the left-turn bays and through lanes at those intersections having vehicles coming from the major road and the crossing street;
- Identifying those left-turn bays likely to incur queue spillback, or be blocked by the through vehicles under the existing signal settings;
- Formulating the impacts of the unique operational features of transit vehicles on the design of progression bands;
- Modeling the mutual interruptions between these two modes of flows on the arterial links;
- Analyzing the temporal relationship between two neighboring progression bands to identify their state of connection; and

- Computing the temporal and spatial distributions of queue patterns at each intersection under the optimized decomposition and signal plans.

For convenience of presenting the formulations for such a model, only those equations for the outbound direction will be presented in the remaining section. One can follow the similar logic to show the formulations for the inbound direction.

7.3.1 Formulating the progression segments for each mode

One can first employ a set of integer variables, $x_i^b\left(\overline{x}_i^b\right)$ and $x_i^c\left(\overline{x}_i^c\right)$, to indicate the progression segment that intersection *i* belongs to, for bus progression and passenger car flows, respectively, at the outbound (inbound) direction. Figure 7.2 shows an example of a decomposition plan for both modes on a long arterial with 11 intersections, where the results (e.g., $x_1^c = x_2^c = x_3^c = 1$) indicates that intersections 1-3 are included in Segment 1 for the outbound passenger car progression band. For those segments where a progression band does not exist for a specific mode and direction, such variables will be equal to 0. For example, in Figure 7.2, where the results of $x_1^b = x_2^b = x_3^b = x_4^b = 0$ indicates that the outbound bus bands are not designed within intersections 1 to 4.

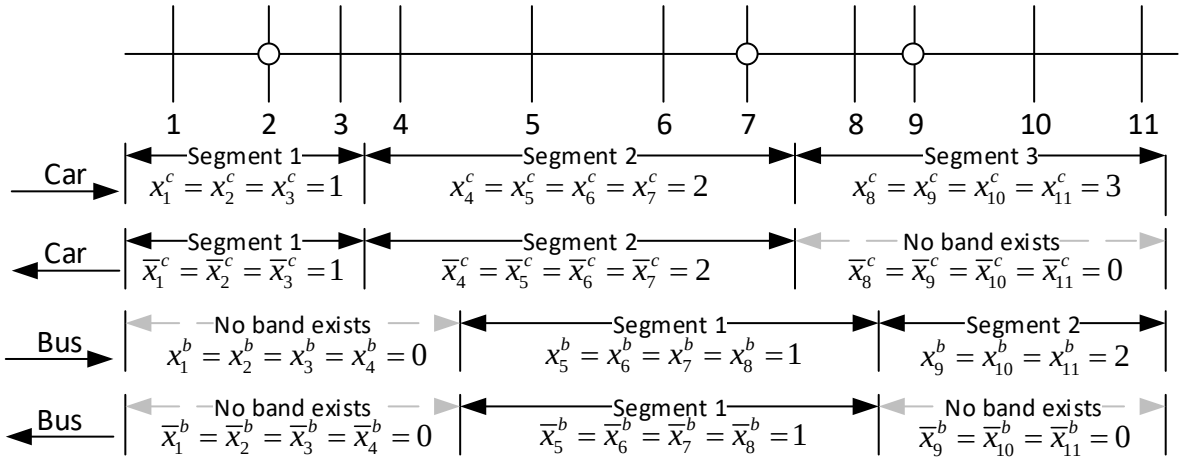

Figure 7.2 A multi-modal progression decomposition plan for a long arterial

In addition, this study introduces another set of binary variables, $y_i^b\left(\overline{y}_i^b\right)$ and $y_i^c\left(\overline{y}_i^c\right)$, which equals 1 when intersection *i* is included in a bus and/or passenger car bands in the outbound (inbound) direction. For the example shown in Figure 7.2, where the relation of $x_9^b = x_{10}^b = x_{11}^b = 1$ indicates that the outbound bus band is designed for intersections 9 to 11. With these two sets of newly introduced variables, the progression segments and decomposition locations for passengers and buses can be defined with constraints (7.1)-(7.9). The first set of constraints, expressing the relation between $y_i\left(\overline{y}_i\right)$ and $x_i\left(\overline{x}_i\right)$, are shown below:

$$y_i^b \le x_i^b \le N_{seg} \times y_i^b, y_i^c \le x_i^c \le N_{seg} \times y_i^c \tag{7.1}$$

$$\beta^c \times y_i^c \le b_i^c \le y_i^c, \beta^b \times y_i^b \le b_i^b \le y_i^b \tag{7.2}$$

Where, N_{seg} is a parameter denoting the maximum possible number of segments for the arterial; β^c and β^b is the minimum meaningful bandwidth for both modes. Eq. (7.1) functions to

ensure that a positive integer will be assigned to $x_i^c\left(\overline{x}_i^c\right)$ or $x_i^b\left(\overline{x}_i^b\right)$ if and only if intersection *i* is designed with a passenger car band or a bus band, and its minimum bandwidth is constrained by Eq. (7.2).

Then, Eq. (7.3) is developed to ensure that both directions have the same decomposition locations for the bands for one mode, as shown below,

$$\begin{aligned} x_i^c - \overline{x}_i^c &= x_{i+1}^c - \overline{x}_{i+1}^c \quad if \quad y_i^c = \overline{y}_i^c = y_{i+1}^c = \overline{y}_{i+1}^c = 1 \\ x_i^b - \overline{x}_i^b &= x_{i+1}^b - \overline{x}_{i+1}^b \quad if \quad y_i^b = \overline{y}_i^b = y_{i+1}^b = \overline{y}_{i+1}^b = 1 \end{aligned} \tag{7.3}$$

Eq. (7.4), derived to ensure the same bandwidth within a progression segment for one mode in one direction, can be expressed as:

$$b_i^c = b_{i+1}^c \;\; if \;\; x_i^c = x_{i+1}^c > 0;\; b_i^b = b_{i+1}^b \;\; if \;\; x_i^b = x_{i+1}^b > 0 \tag{7.4}$$

Where, $b_i^c\left(\overline{b}_i^c\right)$ and $b_i^b\left(\overline{b}_i^b\right)$ represent the bandwidth for passenger cars and for transit vehicles at intersection *i* in the outbound (inbound) direction.

Eq. (7.5) and (7.7) are developed to constrain the relation of numbering between adjacent intersections and among critical intersections.

$$N_{seg} \times \left(y_{i+1}^c - 1\right) \le x_{i+1}^c - x_i^c \le 1, N_{seg} \times \left(y_{i+1}^b - 1\right) \le x_{i+1}^b - x_i^b \le 1 \tag{7.5}$$

$$N_{seg} \times \left(y_{cr_{k+1}}^c - 1\right) \le x_{cr_{k+1}}^c - x_{cr_k}^c \le 1, N_{seg} \times \left(y_{cr_{k+1}}^b - 1\right) \le x_{cr_{k+1}}^b - x_{cr_k}^b \le 1 \tag{7.6}$$

$$x_{i-1}^{c} = x_{i}^{c} > 0 \ or \ x_{i+1}^{c} = x_{i+2}^{c} > 0 \ \ if \ \ x_{i}^{c} = x_{i+1}^{c} > 0; \\ x_{i-1}^{b} = x_{i}^{b} > 0 \ or \ x_{i+1}^{b} = x_{i+2}^{b} > 0 \ \ if \ \ x_{i}^{b} = x_{i+1}^{b} > 0 \tag{7.7}$$

Where, cr_k denotes the kth critical intersection. Eq. (7.5) is to ensure that the segment notation attached to each intersection can only be the same or one unit more than that of its upstream one. Eq. (7.6) is developed to limit the difference of the segment numbers between two adjacent critical intersections, so that only one decomposition point may exist between two neighboring critical intersections. Eq. (7.7) is derived to set the minimum segment length in terms of the number of intersections (i.e., 3 intersections in this study). Note that Eqs. (7.5)-(7.7) are designed to execute the similar functions as with Eqs. (5.2)-(5.4), they need to be revised to accommodate the objectives of concurrently optimizing progression length, modes, and directions in each segment.

The last set of constraints (7.8)-(7.9) are derived to ensure the continuity of those progression segments for a specific mode and direction so that the vehicles would not experience frequent stops at intermediate intersections between two progression segments, as expressed below:

$$\sum_{i} \left| y_{i+1}^{c} - y_{i}^{c} \right| \le 2; \sum_{i} \left| y_{i+1}^{b} - y_{i}^{b} \right| \le 2 \tag{7.8}$$

$$y_{1}^{c} \le 2 - \sum_{i} \left| y_{i+1}^{c} - y_{i}^{c} \right|; y_{1}^{b} \le 2 - \sum_{i} \left| y_{i+1}^{b} - y_{i}^{b} \right| \tag{7.9}$$

7.3.2 Enhanced interference constraints and progression constraints

Note that the progression constraints should be applied only between two adjacent intersections within the same progression segment, but not at the decomposition location or on a link not covered by a progression band for either mode. Therefore, the progression constraints expressed in Eq. (5.9)-(5.12) should be enhanced to accommodate the function of selecting the proper mode(s) and direction(s) for progression and optimizing the decomposition locations.

$$\theta_i + (1-\xi_i)\bar{g}_i^l + w_i^c + t_i^c + n_i^c = \theta_{i+1} + (1-\xi_{i+1})\bar{g}_{i+1}^l + w_i^c \quad if \quad x_i^c = x_{i+1}^c > 0 \tag{7.10}$$

$$\theta_i + (1-\xi_i)\bar{g}_i^l + w_i^b + t_i^b + t_{d,i} + n_i^b = \theta_{i+1} + (1-\xi_{i+1})\bar{g}_{i+1}^l + w_i^b \quad if \quad x_i^b = x_{i+1}^b > 0 \tag{7.11}$$

Where, $w_i^c\ (\bar{w}_i^c)$ and $w_i^b\ (\bar{w}_i^b)$ denote the time difference between the start of the through phase and the start of the outbound (inbound) bands for passenger car and bus flows, respectively.

The interference constraints, as introduced in Eqs. (4.1)-(4.2), should be enhanced to ensure that the queue clearance time should be taken into account only at the downstream intersection of a link covered in a progression band. Therefore, the interference constraints in Model V can be reformulated as follows,

$$w_i^c \geq 0, w_i^c + b_i^c \leq g_i^t, w_i^c \geq \tau_i^t \quad if \quad x_{i-1}^c = x_i^c > 0 \tag{7.12}$$

$$w_i^b \geq 0, w_i^b + b_i^b \leq g_i^t, w_i^b \geq \tau_i^t \quad if \quad x_{i-1}^b = x_i^b > 0 \tag{7.13}$$

7.3.3 Enhanced constraints to reflect the connection state between two progression segments

As introduced in Section 5.3.3, a penalty index derived from the band shift, *BS*, is used to represent the deviation of connection between two neighboring progression bands at the decomposition location. Optimization of such a connection state should also be considered for transit vehicles. Hence, the formulations in Eqs.(5.7)-(5.8) shall be restructured as follows,

$$BS_i^c = t_{t,i}^a + w_i^c + b_i^c - \left(t_{t,i-1}^a + t_{i-1}^c\right) \tag{7.14}$$

$$P_i^c = \begin{cases} \dfrac{\max\left(b_{d,i}^c - BS_i^c, 0\right)}{b_{d,i}^c} + \dfrac{\max\left(BS_i^c - b_{d,i}^c, 0\right)}{1 - b_{d,i}^c} & \text{if } b_{u,i}^c < b_{d,i}^c \\ \dfrac{\max\left(b_{u,i}^c - BS_i^c, 0\right)}{b_{u,i}^c} + \dfrac{\max\left(BS_i^c - b_{u,i}^c, 0\right)}{1 - b_{u,i}^c} & \text{if } b_{u,i}^c > b_{d,i}^c \end{cases} \tag{7.15}$$

$$BS_i^b = t_{t,i}^a + w_i^b + b_i^b - \left(t_{t,i-1}^a + t_{i-1}^b + t_{d,i-1}\right) \tag{7.16}$$

$$P_i^b = \begin{cases} \dfrac{\max\left(b_{d,i}^b - BS_i^b, 0\right)}{b_{d,i}^b} + \dfrac{\max\left(BS_i^b - b_{d,i}^b, 0\right)}{1 - b_{d,i}^b} & \text{if } b_{u,i}^b < b_{d,i}^b \\ \dfrac{\max\left(b_{u,i}^b - BS_i^b, 0\right)}{b_{u,i}^b} + \dfrac{\max\left(BS_i^b - b_{u,i}^b, 0\right)}{1 - b_{u,i}^b} & \text{if } b_{u,i}^b > b_{d,i}^b \end{cases} \tag{7.17}$$

where BS_i^c and BS_i^b denote the band shift at intersection *i* for passenger car bands and bus bands; P_i^c and P_i^b indicate the penalty index due to the band discontinuity at the intersection serving as the decomposition point for these two modes; and $b_{d,i}\left(b_{u,i}\right)$ represents the downstream(upstream) bandwidth. The penalty index for both modes will be minimized in Stage 2, based on their respective volume and loading factors.

7.3.4 Objective function and formulation in Stage 1

The objective function for the model in Stage 1, as expressed in Eq. (7.18), aims to first maximize the sum of the effective bandwidth weighted by the volumes of each mode, and then to minimize the expected number of intersections that may experience queue blockage or spillover:

Maximize

$$\sum_i \left(V_{c,i}^t k_c b''_{c,i} + \bar{V}_{c,i}^t k_c \bar{b}''_{c,i} + m_{b,i} u_b V_{b,i} k_b / C + \bar{m}_{b,i} u_b \xi \bar{V}_{b,i} \bar{k}_b / C \right) - k_1 \left(V_i^t \gamma_i^s + \bar{V}_i^t \bar{\gamma}_i^s + V_i^l \gamma_i^b + \bar{V}_i^l \bar{\gamma}_i^b \right) \tag{7.18}$$

Where, $V_{c,i}^t \left(\bar{V}_{c,i}^t \right)$ denotes the outbound (inbound) through volume for passenger cars; $V_{b,i}^t \left(\bar{V}_{b,i}^t \right)$ is for buses; and k_c and k_b are loading factors, respectively, for passenger cars and buses.

The constraints in Stage 1 include those in Chapter 5 for queue length estimation, and those in Chapter 6 to reflect the operational features of buses and the mutual interruptions between both modes. In brief, the entire model in Stage 1 can be summarized as follows:

Maximize

$$\sum_i \left(V_{c,i}^t k_c b''_{c,i} + \bar{V}_{c,i}^t k_c \bar{b}''_{c,i} + m_{b,i} u_b V_{b,i} k_b / C + \bar{m}_{b,i} u_b \bar{V}_{b,i} \bar{k}_b / C \right) - k_1 \left(V_i^t \gamma_i^s + \bar{V}_i^t \bar{\gamma}_i^s + V_i^l \gamma_i^b + \bar{V}_i^l \bar{\gamma}_i^b \right)$$

s.t.

Progression of passenger cars and buses on the arterial

$$w_i^c \geq 0, w_i^c + b_i^c \leq g_i^t, w_i^c \geq \tau_i^t \quad if \quad x_{i-1}^c = x_i^c > 0$$

$$w_i^b \geq 0, w_i^b + b_i^b \leq g_i^t, w_i^b \geq \tau_i^t \quad if \quad x_{i-1}^c = x_i^c > 0$$

$$\theta_i + (1-\xi_i)\bar{g}_i^l + w_i^c + t_i^c + n_i^c = \theta_{i+1} + (1-\xi_{i+1})\bar{g}_{i+1}^l + w_i^c \quad if \quad x_i^c = x_{i+1}^c > 0$$

$$\theta_i + (1-\xi_i)\bar{g}_i^l + w_i^b + t_i^b + t_{d,i} + n_i^b = \theta_{i+1} + (1-\xi_{i+1})\bar{g}_{i+1}^l + w_i^b \quad if \quad x_i^b = x_{i+1}^b > 0$$

Local progression and queue length calculation:

$$b'_{m,i} = \min\left(t_{d(m),i}^b, t_{u(m),i-1}^b + t_{i-1}\right) - \max\left(t_{d(m),i}^a + \tau_{d(m),i}, t_{u(m),i-1}^a + t_{i-1}\right) \qquad \forall m \in \{m_1, m_2, m_3, m_4\}$$

$$QL_{i+1}^l = \frac{C}{3600 n_{i+1}^l} V_i^t r_{i+1}^l \times \left(g_i^t - b_{m4,i+1}\right)$$

$$\tau_{i+1}^l = QL_{i+1}^l \frac{3600/C}{s - V_i^l / n_{i+1}^l} \times \alpha$$

$$QL_{i+1}^t = \frac{C}{3600 n_{i+1}^t}\left(V_i^t r_{i+1}^t \times \left(g_i^t - b_{m1,i+1}\right) + V_i^{'l} r_{i+1}^t \times \left(g_i^{'l} - b_{m2,i+1}\right) + V_i^{'r} r_{i+1}^t \times \left(g_i^{'r} - b_{m3,i+1}\right)\right)$$

$$\tau_{i+1}^t = QL_{i+1}^t \frac{3600/C}{s - V_{i+1}^t / n_{i+1}^t} \times \alpha$$

$$QL_i^l h \frac{s}{s - V_{l,i}} \leq L_i + M \times \gamma_i^s$$

$$QL_i^t h \frac{s}{s - V_{t,i}} \leq L_i + M \times \gamma_i^b$$

$$\bar{b}'_{m,i} = \min\left(\bar{t}_{d(m),i}^b, \bar{t}_{u(m),i+1}^b + \bar{t}_i\right) - \max\left(\bar{t}_{d(m),i}^a + \bar{\tau}_{d(m),i}, \bar{t}_{u(m),i+1}^a + \bar{t}_i\right) \qquad \forall m \in \{\bar{m}_1, \bar{m}_2, \bar{m}_3, \bar{m}_4\}$$

$$\bar{Q}\bar{L}_i^l = \frac{C}{3600\bar{n}_i^l}\bar{V}_{i+1}^t \bar{r}_i^l \times \left(\bar{g}_{i+1}^t - b_{m4,i}\right)$$

$$\bar{\tau}_i^l = \bar{Q}\bar{L}_i^l \frac{3600/C}{s - \bar{V}_i^l / \bar{n}_i^l} \times \alpha$$

$$\bar{Q}\bar{L}_i^t = \frac{C}{3600 n_i^t}\left(\bar{V}_{i+1}^t \bar{r}_i^t \times \left(\bar{g}_{i+1}^t - \bar{b}_{m1,i}\right) + \bar{V}'^l_{i+1}\, \bar{r}_i^t \times \left(g'^l_{i+1} - b_{m2,i}\right) + \bar{V}'^r_i\, \bar{r}_{i+1}^t \times \left(g'^r_{i+1} - b_{m3,i}\right)\right)$$

$$\bar{\tau}_i^t = \bar{Q}\bar{L}_i^t \frac{3600/C}{s - \bar{V}_i^t / \bar{n}_i^t} \times \alpha$$

$$\bar{Q}\bar{L}_i^l h \frac{s}{s - \bar{V}_{l,i}} \le \bar{L}_i + M \times \bar{\gamma}_i^s$$

$$\bar{Q}\bar{L}_i^t h \frac{s}{s - \bar{V}_{t,i}} \le \bar{L}_i + M \times \bar{\gamma}_i^b$$

Decomposition of the arterial and selection of proper modes and directions to provide proression:

$$y_i^b \le x_i^b \le N_{seg} \times y_i^b, y_i^c \le x_i^c \le N_{seg} \times y_i^c$$

$$\beta^c \times y_i^c \le b_i^c \le y_i^c, \beta^b \times y_i^b \le b_i^b \le y_i^b$$

$$x_i^c - \bar{x}_i^c = x_{i+1}^c - \bar{x}_{i+1}^c \quad if \quad y_i^c = \bar{y}_i^c = y_{i+1}^c = \bar{y}_{i+1}^c = 1$$
$$x_i^b - \bar{x}_i^b = x_{i+1}^b - \bar{x}_{i+1}^b \quad if \quad y_i^b = \bar{y}_i^b = y_{i+1}^b = \bar{y}_{i+1}^b = 1$$

$$b_i^c = b_{i+1}^c \;\; if \;\; x_i^c = x_{i+1}^c > 0;\; b_i^b = b_{i+1}^b \;\; if \;\; x_i^b = x_{i+1}^b > 0$$

$$N_{seg} \times \left(y_{i+1}^{c} - 1 \right) \le x_{i+1}^{c} - x_{i}^{c} \le 1, N_{seg} \times \left(y_{i+1}^{b} - 1 \right) \le x_{i+1}^{b} - x_{i}^{b} \le 1$$

$$N_{seg} \times \left(y_{cr_{k+1}}^{c} - 1 \right) \le x_{cr_{k+1}}^{c} - x_{cr_{k}}^{c} \le 1, N_{seg} \times \left(y_{cr_{k+1}}^{b} - 1 \right) \le x_{cr_{k+1}}^{b} - x_{cr_{k}}^{b} \le 1$$

$$x_{i-1}^{c} = x_{i}^{c} > 0 \; or \; x_{i+1}^{c} = x_{i+2}^{c} > 0 \;\; if \;\; x_{i}^{c} = x_{i+1}^{c} > 0;$$
$$x_{i-1}^{b} = x_{i}^{b} > 0 \; or \; x_{i+1}^{b} = x_{i+2}^{b} > 0 \;\; if \;\; x_{i}^{b} = x_{i+1}^{b} > 0$$

$$\sum_{i} \left| y_{i+1}^{c} - y_{i}^{c} \right| \le 2; \sum_{i} \left| y_{i+1}^{b} - y_{i}^{b} \right| \le 2$$

$$y_{1}^{c} \le 2 - \sum_{i} \left| y_{i+1}^{c} - y_{i}^{c} \right|; y_{1}^{b} \le 2 - \sum_{i} \left| y_{i+1}^{b} - y_{i}^{b} \right|$$

Bus operational features:

$$m_b u_b / C \le b_b$$

$$\bar{m}_b u_b / C \le \bar{b}_b$$

$$m_b \le \frac{V_b}{3600 / C}$$

$$\bar{m}_b \le \frac{\bar{V}_b}{3600 / C}$$

$$m_b \le q_i$$

$$\bar{m}_b \le \bar{q}_i$$

Mutual interruptions between passenger cars and buses:

$$w_{b,i+1} - t_i \frac{l_{i+1} s / \left(s - f_{i+1}\right)}{d_i} - t_{d,i} \ge \frac{l_{i+1}}{s - f_{i+1}} \xi - \left(1 - y_i\right) \times M$$

$$b_i^b = \min\left(t_{t,i}^b, t_{t,i-1}^b + t_{i-1} + t_{d,i-1}\right) - \max\left(t_{t,i}^a + \tau_{t,i}, t_{t,i-1}^a + t_{i-1} + + t_{d,i-1}\right)$$

$$QL_{i+1}^b = \frac{C}{3600} V_{b,i} \times \left(g_i^t - b_i^b\right)$$

$$b'_{c,i} = b_c - \max\left(\frac{QL_{i+1}^b u_b}{C} - w_i, 0\right) / z_i$$

$$t_{a,i} = \max\left(0, \min\left(1, w_{c,i} + b_c - w_{b,i}\right)\right)$$

$$t_{b,i} = \max\left(0, \min\left(1, w_{b,i} + b_b - w_{c,i}\right)\right)$$

$$b''_{c,i} = b'_{c,i} - \left(t_{a,i} + t_{b,i} - b_c \times p_i\right)$$

7.3.5 Objective function and formulation in Stage 2

The objective function in Stage 2 is first to minimize the penalty index for band discontinuity and the queue distribution index, and then to maximize the bandwidth at non-critical intersections, given the effective bandwidths at critical intersections from Stage 1, as expressed in Eq. (7.19):

Minimize

$$\sum_i \left(V_{c,i}^t P_{c,i} + \bar{V}_{c,i}^t \bar{P}_{c,i} + V_{b,i} P_{b,i} + \bar{V}_{b,i} \bar{P}_{b,i} \right) + e + \bar{e} - k_2 \sum_i \left(V_{c,i}^t b''_{c,i} + \bar{V}_{c,i}^t \bar{b}''_{c,i} + m_{b,i} u_b V_{b,i} k_b / C + \bar{m}_{b,i} u_b \bar{V}_{b,i} \bar{k}_b / C \right)$$

(7.19)

where, k_2 is weighting factor significantly smaller than 1

As stated in Section 5.3.6, the obtained maximized bandwidths at critical intersections from Stage 1 will serve as the input of Stage 2 to ensure the same maximized bandwidth at each critical intersection. The optimization of Stage 2 should also ensure that the number of intersections, suffering from left-turn bay spillbacks and blockages, will not exceed the results from Stage 1. One can express such relations with the following constraints:

$$b_i^c \geq B_i^c, \bar{b}_i^c \geq \bar{B}_i^c, b_i^b \geq B_i^b, \bar{b}_i^b \geq \bar{B}_i^b \qquad \forall i = \text{critical intersection} \tag{7.20}$$

$$\sum_i \gamma_i^s \leq \sum_i \Gamma_i^s, \sum_i \bar{\gamma}_i^s \leq \sum_i \bar{\Gamma}_i^s \tag{7.21}$$

$$\sum_i \gamma_i^b \leq \sum_i \Gamma_i^b, \sum_i \bar{\gamma}_i^b \leq \sum_i \bar{\Gamma}_i^b \tag{7.22}$$

Where, $B_i^c \left(\bar{B}_i^c \right)$ and $B_i^b \left(\bar{B}_i^b \right)$ denote the outbound (inbound) bandwidth at intersection *i* for passenger car and bus bands obtained from Stage 1.

In brief, the entire model in Stage 2 can be summarized as follows:

Maximize

$$\sum_i \left(V_{c,i}^t P_{c,i} + \bar{V}_{c,i}^t \bar{P}_{c,i} + V_{b,i} P_{b,i} + \bar{V}_{b,i} \bar{P}_{b,i} \right) + e + \bar{e} - k_2 \sum_i \left(V_{c,i}^t b''_{c,i} + \bar{V}_{c,i}^t \bar{b}''_{c,i} + m_{b,i} u_b V_{b,i} k_b / C + \bar{m}_{b,i} u_b \bar{V}_{b,i} \bar{k}_b / C \right)$$

s.t.

Progression of passenger cars and buses on the arterial

$$w_i^c \geq 0, w_i^c + b_i^c \leq g_i^t, w_i^c \geq \tau_i^t \quad if \quad x_{i-1}^c = x_i^c > 0$$

$$w_i^b \geq 0, w_i^b + b_i^b \leq g_i^t, w_i^b \geq \tau_i^t \quad if \quad x_{i-1}^c = x_i^c > 0$$

$$\theta_i + (1-\xi_i)\bar{g}_i^l + w_i^c + t_i^c + n_i^c = \theta_{i+1} + (1-\xi_{i+1})\bar{g}_{i+1}^l + w_i^c \quad if \quad x_i^c = x_{i+1}^c > 0$$

$$\theta_i + (1-\xi_i)\bar{g}_i^l + w_i^b + t_i^b + t_{d,i} + n_i^b = \theta_{i+1} + (1-\xi_{i+1})\bar{g}_{i+1}^l + w_i^b \quad if \quad x_i^b = x_{i+1}^b > 0$$

Local progression and queue length calculation:

$$b'_{m,i} = \min\left(t_{d(m),i}^b, t_{u(m),i-1}^b + t_{i-1} \right) - \max\left(t_{d(m),i}^a + \tau_{d(m),i}, t_{u(m),i-1}^a + t_{i-1} \right) \qquad \forall m \in \{m_1, m_2, m_3, m_4\}$$

$$QL_{i+1}^l = \frac{C}{3600 n_{i+1}^l} V_i^t r_{i+1}^l \times \left(g_i^t - b_{m4,i+1} \right)$$

$$\tau_{i+1}^l = QL_{i+1}^l \frac{3600/C}{s - V_i^l / n_{i+1}^l} \times \alpha$$

$$QL_{i+1}^t = \frac{C}{3600 n_{i+1}^t} \left(V_i^t r_{i+1}^t \times \left(g_i^t - b_{m1,i+1} \right) + V_i^{'l} r_{i+1}^t \times \left(g_i^{'l} - b_{m2,i+1} \right) + V_i^{'r} r_{i+1}^t \times \left(g_i^{'r} - b_{m3,i+1} \right) \right)$$

$$\tau_{i+1}^{t} = QL_{i+1}^{t} \frac{3600/C}{s - V_{i+1}^{t}/n_{i+1}^{t}} \times \alpha$$

$$QL_i^l h \frac{s}{s - V_{l,i}} \le L_i + M \times \gamma_i^s$$

$$QL_i^t h \frac{s}{s - V_{t,i}} \le L_i + M \times \gamma_i^b$$

$$\bar{b}'_{m,i} = \min\left(\bar{t}_{d(m),i}^{b}, \bar{t}_{u(m),i+1}^{b} + \bar{t}_i\right) - \max\left(\bar{t}_{d(m),i}^{a} + \bar{\tau}_{d(m),i}, \bar{t}_{u(m),i+1}^{a} + \bar{t}_i\right) \qquad \forall m \in \left\{\bar{m}_1, \bar{m}_2, \bar{m}_3, \bar{m}_4\right\}$$

$$\bar{Q}\bar{L}_i^l = \frac{C}{3600\bar{n}_i^l} \bar{V}_{i+1}^{t} \bar{r}_i^{l} \times \left(\bar{g}_{i+1}^{t} - b_{m4,i}\right)$$

$$\bar{\tau}_i^{l} = \bar{Q}\bar{L}_i^l \frac{3600/C}{s - \bar{V}_i^l/\bar{n}_i^l} \times \alpha$$

$$\bar{Q}\bar{L}_i^t = \frac{C}{3600 n_i^t}\left(\bar{V}_{i+1}^{t} \bar{r}_i^{t} \times \left(\bar{g}_{i+1}^{t} - \bar{b}_{m1,i}\right) + \bar{V}'^{l}_{i+1} \bar{r}_i^{t} \times \left(g'^{l}_{i+1} - b_{m2,i}\right) + \bar{V}'^{r}_{i} \bar{r}_{i+1}^{t} \times \left(g'^{r}_{i+1} - b_{m3,i}\right)\right)$$

$$\bar{\tau}_i^{t} = \bar{Q}\bar{L}_i^t \frac{3600/C}{s - \bar{V}_i^t/\bar{n}_i^t} \times \alpha$$

$$\bar{Q}\bar{L}_i^l h \frac{s}{s - \bar{V}_{l,i}} \le \bar{L}_i + M \times \bar{\gamma}_i^s$$

$$\bar{Q}\bar{L}_i^t h \frac{s}{s - \bar{V}_{t,i}} \le \bar{L}_i + M \times \bar{\gamma}_i^b$$

Decomposition of the arterial and selection of proper modes and directions to provide proression:

$$y_i^b \le x_i^b \le N_{seg} \times y_i^b, y_i^c \le x_i^c \le N_{seg} \times y_i^c$$

$$\beta^c \times y_i^c \le b_i^c \le y_i^c, \beta^b \times y_i^b \le b_i^b \le y_i^b$$

$$x_i^c - \overline{x}_i^c = x_{i+1}^c - \overline{x}_{i+1}^c \quad if \quad y_i^c = \overline{y}_i^c = y_{i+1}^c = \overline{y}_{i+1}^c = 1$$
$$x_i^b - \overline{x}_i^b = x_{i+1}^b - \overline{x}_{i+1}^b \quad if \quad y_i^b = \overline{y}_i^b = y_{i+1}^b = \overline{y}_{i+1}^b = 1$$

$$b_i^c = b_{i+1}^c \;\; if \;\; x_i^c = x_{i+1}^c > 0; \; b_i^b = b_{i+1}^b \;\; if \;\; x_i^b = x_{i+1}^b > 0$$

$$N_{seg} \times \left(y_{i+1}^c - 1 \right) \le x_{i+1}^c - x_i^c \le 1, N_{seg} \times \left(y_{i+1}^b - 1 \right) \le x_{i+1}^b - x_i^b \le 1$$

$$N_{seg} \times \left(y_{cr_{k+1}}^c - 1 \right) \le x_{cr_{k+1}}^c - x_{cr_k}^c \le 1, N_{seg} \times \left(y_{cr_{k+1}}^b - 1 \right) \le x_{cr_{k+1}}^b - x_{cr_k}^b \le 1$$

$$x_{i-1}^c = x_i^c > 0 \; or \; x_{i+1}^c = x_{i+2}^c > 0 \;\; if \;\; x_i^c = x_{i+1}^c > 0;$$
$$x_{i-1}^b = x_i^b > 0 \; or \; x_{i+1}^b = x_{i+2}^b > 0 \;\; if \;\; x_i^b = x_{i+1}^b > 0$$

$$\sum_i \left| y_{i+1}^c - y_i^c \right| \le 2; \sum_i \left| y_{i+1}^b - y_i^b \right| \le 2$$

$$y_1^c \le 2 - \sum_i \left| y_{i+1}^c - y_i^c \right|; y_1^b \le 2 - \sum_i \left| y_{i+1}^b - y_i^b \right|$$

Bus operational features:

$$m_b u_b / C \le b_b$$

$$\overline{m}_b u_b / C \le \overline{b}_b$$

$$m_b \le \frac{V_b}{3600 / C}$$

$$\bar{m}_b \le \frac{\bar{V}_b}{3600 / C}$$

$$m_b \le q_i$$

$$\bar{m}_b \le \bar{q}_i$$

Mutual interruptions between passenger cars and buses:

$$w_{b,i+1} - t_i \frac{l_{i+1} s / \left(s - f_{i+1}\right)}{d_i} - t_{d,i} \ge \frac{l_{i+1}}{s - f_{i+1}} \xi - \left(1 - y_i\right) \times M$$

$$b_i^b = \min\left(t_{t,i}^b, t_{t,i-1}^b + t_{i-1} + t_{d,i-1}\right) - \max\left(t_{t,i}^a + \tau_{t,i}, t_{t,i-1}^a + t_{i-1} + + t_{d,i-1}\right)$$

$$QL_{i+1}^b = \frac{C}{3600} V_{b,i} \times \left(g_i^t - b_i^b\right)$$

$$b'_{c,i} = b_c - \max\left(\frac{QL_{i+1}^b u_b}{C} - w_i, 0\right) / z_i$$

$$t_{a,i} = \max\left(0, \min\left(1, w_{c,i} + b_c - w_{b,i}\right)\right)$$

$$t_{b,i} = \max\left(0, \min\left(1, w_{b,i} + b_b - w_{c,i}\right)\right)$$

$$b''_{c,i} = b'_{c,i} - \left(t_{a,i} + t_{b,i} - b_c \times p_i\right)$$

Band connection states:

$$BS_i^c = t_{t,i}^a + w_i^c + b_i^c - \left(t_{t,i-1}^a + t_{i-1}^c\right)$$

$$P_i^c = \begin{cases} \dfrac{\max\left(b_{d,i}^c - BS_i^c, 0\right)}{b_{d,i}^c} + \dfrac{\max\left(BS_i^c - b_{d,i}^c, 0\right)}{1 - b_{d,i}^c} & \text{if } b_{u,i}^c < b_{d,i}^c \\ \dfrac{\max\left(b_{u,i}^c - BS_i^c, 0\right)}{b_{u,i}^c} + \dfrac{\max\left(BS_i^c - b_{u,i}^c, 0\right)}{1 - b_{u,i}^c} & \text{if } b_{u,i}^c > b_{d,i}^c \end{cases}$$

$$BS_i^b = t_{t,i}^a + w_i^b + b_i^b - \left(t_{t,i-1}^a + t_{i-1}^b + t_{d,i-1}\right)$$

$$P_i^b = \begin{cases} \dfrac{\max\left(b_{d,i}^b - BS_i^b, 0\right)}{b_{d,i}^b} + \dfrac{\max\left(BS_i^b - b_{d,i}^b, 0\right)}{1 - b_{d,i}^b} & \text{if } b_{u,i}^b < b_{d,i}^b \\ \dfrac{\max\left(b_{u,i}^b - BS_i^b, 0\right)}{b_{u,i}^b} + \dfrac{\max\left(BS_i^b - b_{u,i}^b, 0\right)}{1 - b_{u,i}^b} & \text{if } b_{u,i}^b > b_{d,i}^b \end{cases}$$

Distributing queues to less congested locations:

$$e = \sum_i \frac{1}{\beta - V_i^{total} / s} \times \frac{\max\left(QL_{i+1}^t, QL_{i+1}^l\right)}{LL_i}$$

$$\bar{e} = \sum_i \frac{1}{\beta - \bar{V}_i^{total} / s} \times \frac{\max\left(\bar{Q}\bar{L}_i^t, \bar{Q}\bar{L}_i^l\right)}{\bar{L}\bar{L}_i}$$

Ensuring the bandwidths at critical intersections and upper bound of number of intersections suffering from left-turn bay spillback and blockage:

$$b_i^c \geq B_i^c, \bar{b}_i^c \geq \bar{B}_i^c, b_i^b \geq B_i^b, \bar{b}_i^b \geq \bar{B}_i^b \qquad \forall i = \text{critical intersection}$$

$$\sum_i \gamma_i^s \leq \sum_i \Gamma_i^s, \sum_i \bar{\gamma}_i^s \leq \sum_i \bar{\Gamma}_i^s$$

$$\sum_i \gamma_i^b \leq \sum_i \Gamma_i^b, \sum_i \bar{\gamma}_i^b \leq \sum_i \bar{\Gamma}_i^b$$

7.4 Enhanced Stage 1 for arterials with an excessive number of intersections

Due to the large number of binary and integer variables in the formulations for Model V, the computing time for Stage 1 may increase exponentially with the number of intersections within the target arterial. Therefore, a solution technique that can improve the computational efficiency without sacrificing the optimality is developed for Stage 1 in Model V, as shown in Figure 7.3.

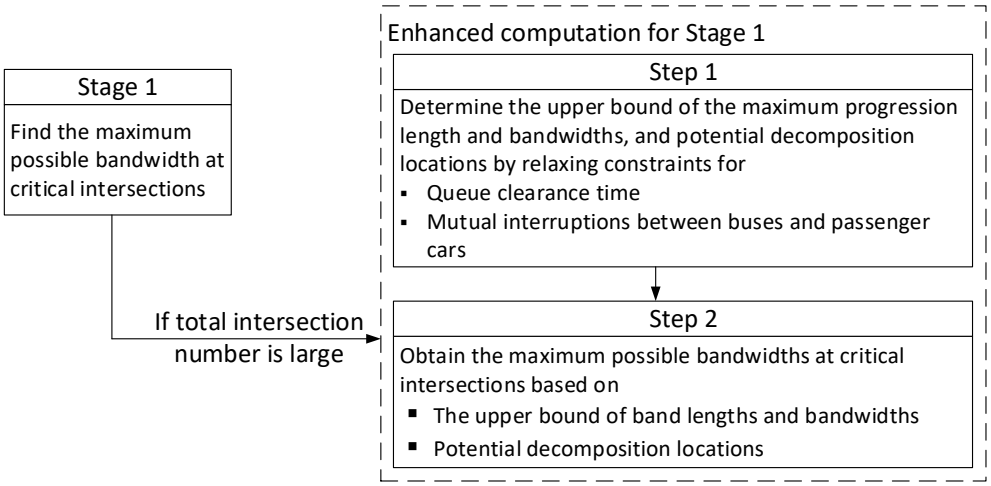

Figure 7.3 Solution technique for Model V for increasing the computing efficiency

The enhanced algorithm for Stage 1 consists of two steps, where the optimization in the first step does not include the constraints for queue formations and mutual interruptions between

two modes. Relaxing these sets of constraints will result in longer available green times that can be assigned to progression bands for both modes, and generate the upper bounds for both the effective bandwidths and the progression lengths (e.g., number of covered intersection) for both modes along the arterial. The second step will utilize the results from step 1 to search the actual maximum possible bandwidths at those critical locations, based on those constraints associated with queue clearance time and mutual interruptions between two modes. Note that Step 2 will also adopt the optimized decomposition locations from step 1, since decomposing at other non-optimal intersections would yield a smaller upper bound for the effective bandwidths.

With the enhanced algorithm for Stage 1, the computing time can be reduced significantly in each step due to the smaller number of integer variables and constraints. For an example of an arterial consisting of 11 intersections, the original formulations at Stage 1 contains 950 integer variables and 3161 constraints. With the enhanced algorithm, the model will, however, have only 419 integer variables and 1134 constraints in step 1. The optimization model at step 2 will contain 740 integer variables and 2466 constraints, but with a significantly smaller searching polyhedron due to the identified upper bounds for decision variables from Stage 1 results.

7.5 Case study

The case study consists of two numerical experiments for performance comparison. The first aims to show the properties of the proposed model with respect to wider and longer bands for the selected mode(s) and direction(s). The second is designed to verify the benefits of allowing different decomposition locations for each mode to optimize the progression plan along the arterial. The third part of the case study is a simulation experiment for performance comparison between

Model V and Models III and IV developed in Chapters 5 and 6. The platform is designed with VISSIM 9, and the MOEs are collected with simulation experiments of 2 hours.

7.5.1 Site description

Figure 7.1 shows the key geometric features and signal timings of the arterial of 11 intersections on North Ave. in Baltimore, MD, from Druid Hill Ave. to Charles St., for the case study. Three critical intersections on the arterial are denoted by the names of the crossing roads. Note that Mt. Royal Ave. serves as a connection to a freeway ramp. The bus stops on each direction, shown with white rectangles as well, have an average dwell time of 42 seconds.

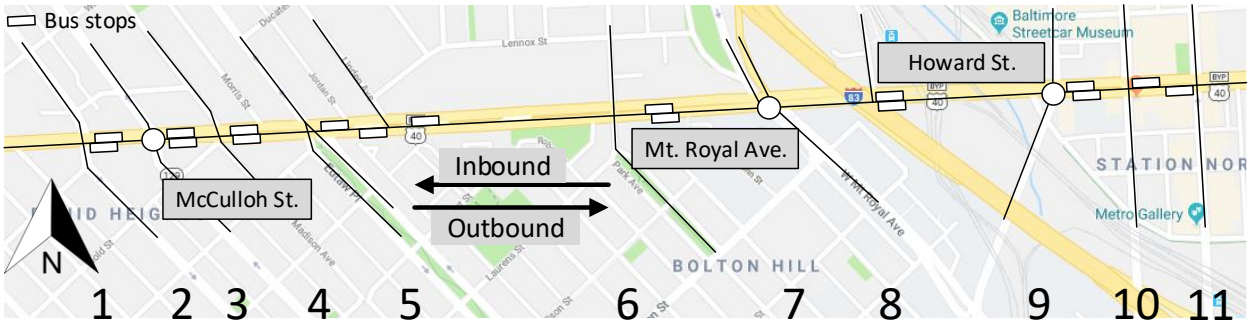

	1	2	3	4	5	6	7	8	9	10	11
OB Green Time (s)	93	84	72	75	120	72	63	99	66	69	96
IB Green Time (s)	93	84	99	75	90	72	63	69	66	93	75
OB LT bay length (ft)	-	-	-	159	134	208	180	70	-	-	100
IB LT bay length (ft)	-	-	160	112	-	226	188	-	130	110	-

Cycle length: 150s

Figure 7.4 Key information associated with the study site

To evaluate the model's performance under various demand patterns, this study has designed five scenarios of different volumes, bus ratios, and directional flow ratios, as shown in Table 7.1

Table 7.1 Volume scenarios adopted in the case study

Volume Scenarios	OB car volume (vph)	IB car volume (vph)	OB bus volume (vph)	IB bus volume (vph)	OB bus loading factors	IB bus loading factors	Feature
1	926	820	34	34	12	12	Light transit ridership & volume
2	826	670	33	44	22	22	Medium transit ridership & volume
3	826	670	50	50	45	40	Heavy transit ridership & volume
4	1019	656	30	50	30	28	Heavy outbound car volume
5	1019	656	80	25	40	20	Heavy outbound volume

Car loading factor: 1.2

7.5.2 Numerical examples

All volume scenarios in Table 7.1 are designed to test the proposed model's properties, and their generated bands are illustrated in Table 7.2, including the number of covered intersections and the average effective bandwidth for each mode and direction. Note that the bandwidths for cars in Table 7.2 are effective bandwidths, considering the interruptions due to buses at the stop bars and bus stops.

Table 7.2 Band coverage and average bandwidth for each mode and direction under various volume scenarios

Volume	OB car band		IB car band		OB bus band		IB bus band	
Scenarios	# inter	bandwidth	# inter	bandwidth	# inter	bandwidth	# inter	bandwidth
1	11	56s	11	53s	3	30s	3	10s
2	11	48s	11	50s	8	20s	3	20s

3	10	41s	10	50s	10	24s	3	20s
4	11	58s	11	44s	3	20s	6	20s
5	11	52s	11	53s	8	18s	0	0s

As shown in the table, comparison of the progression bands generated by the proposed model under various volume scenarios confirms its properties on prioritizing the maximization of the bandwidths for the mode(s) and direction(s) of higher volumes. For example, under Scenario 1 with light transit ridership, the bus bands produced by the proposed model can only cover three intersections, with the bandwidth of 30 seconds and 10 seconds, for outbound and inbound direction, respectively. In comparison, under Scenario 3 with a significantly higher bus ratio, the bus band produced by the proposed model will cover eight and three intersections, respectively for outbound and inbound directions and will have larger bandwidths of 24 and 20 seconds for buses. Note that compared to Scenarios 4, Scenarios 5 have the same car volumes but higher outbound bus volumes. Therefore, the resulting bus bands from the proposed model cover more intersections and have wider bandwidths under Scenarios 5 then under Scenario 4. In addition, since Scenario 5 has unbalanced bus volumes between two directions, the proposed model generates a zero bandwidth for the inbound bus band, allowing the green time to be allocated to other modes and directions of higher volumes.

The second numerical experiment is designed to verify the benefits to select different decomposition locations for two modes. Hence, this study will compare the total bandwidth under the models with and without such flexibility under the above five scenarios. Specifically, the models to be compared are:

- Model 1: the proposed Model V
- Model 2: the proposed model with the constraints of having the progression bands for both modes to decompose at the same intersections

Table 7.3 shows the sum of the bandwidths at all covered intersections for each mode and direction, generated with Model 1 and Model 2 under each volume scenario. The comparison between these two models shows that the proposed model with its flexibility to allow each mode to have its own decomposition locations can generate wider bands than Model 2. For example, under Scenario 5, Model 2 generates the lower total bandwidth for passenger cars than with Model 1, because, Model 2 forces the progression segments for both modes to be decomposed at the same locations and thus often results in non-optimal bandwidths. In other scenarios, Model 2 may produce a wider band for one mode and direction, but at a significant cost of bandwidth for the others. For example, Model 2 under Scenario 2 will produce a wider outbound car band than with Model 1, but generate narrower bands for both inbound passenger cars and outbound buses.

Table 7.3 Total bandwidth from Model 1 and Model 2 under various volume scenarios

Volume	OB car band total bandwidth (s)		IB car band total bandwidth (s)		OB bus band total bandwidth (s)		IB bus band total bandwidth (s)	
Scenarios	Model 1	Model 2	Model 1	Model 2	Model 1	Model 2	Model 1	Model 2
1	558	542	528	528	90	90	30	30
2	447	586	505	448	160	80	60	60
3	408	240	447	390	240	260	60	60
4	553	487	392	464	60	0	120	90
5	521	422	527	296	140	210	0	0

7.5.3 Simulation experiments

To show that the proposed model with the objective of maximizing weighted total bandwidths would not compromise other MOEs, the performance evaluation will be conducted with simulation experiments among the following three models under three volume scenarios:

- Model 1: The proposed Model V
- Model 3: The decomposition model for passenger cars (Model III Chapter 5)
- Model 4: Using decomposition points in model 2, apply dual modal progression model (Model IV in Chapter 6) in each segment. (Two modes share the same decomposition locations.)

Tables 7.4-7.6 show the average delay and number of stops for the arterial's through movements and the entire network with different models under volume scenarios 1-3 (see Table 7.1). Note that the last row in each table shows the average delay and number of stops per person, which are calculated based on the volumes and loading factors for buses and passenger cars.

Table 7.4 Average delay and number of stops from different models under Scenario 1

	Average delay (s/veh)			Number of stops		
	Model 1	Model 3	Model 4	Model 1	Model 3	Model 4
Arterial through movements						
OB car	112.3	111.0	145.2	3.58	3.70	4.23
IB car	142.4	132.9	210.4	4.61	3.85	6.49
Total car	126.4	121.3	175.8	4.06	3.77	5.29
OB bus	366.6	363.4	327.5	4.29	4.49	4.23
IB bus	353.0	374.1	397.3	4.85	4.79	6.49
Total bus	359.8	368.8	362.4	4.57	4.64	5.36
Network performance						
Car	111.9	115.9	130.5	2.80	2.79	3.09
Bus	274.6	280.1	271.9	4.12	4.13	4.20
Person	141.9	146.1	156.5	3.04	3.04	3.30

Table 7.5 Average delay and number of stops from different models under Scenario 2

	Average delay (s/veh)			Number of stops		
	Model 1	Model 3	Model 4	Model 1	Model 3	Model 4
Arterial through movements						
OB car	217.1	101.2	191.8	6.26	3.38	4.29
IB car	145.9	239.1	232.1	4.66	7.19	7.60
Total car	185.2	163.0	209.8	5.55	5.09	5.77
OB bus	349.9	359.5	386.9	4.33	4.37	4.51
IB bus	417.6	468.6	461.0	4.85	6.74	5.89
Total bus	388.5	421.7	429.1	4.63	5.72	5.30
Network performance						
Car	129.8	139.4	130.1	2.76	2.75	2.96
Bus	294.3	336.9	323.8	4.52	4.64	5.36
Person	179.3	199.0	188.4	3.32	3.36	3.73

Table 7.6 Average delay and number of stops from different models under Scenario 3

	Average delay (s/veh)			Number of stops		
	Model 1	Model 3	Model 4	Model 1	Model 3	Model 4
Arterial through movements						
OB car	154.5	110.2	153.7	4.23	3.44	5.38
IB car	212.5	235.8	395.6	5.51	7.15	11.93
Total car	180.4	166.4	262.0	4.80	5.10	8.31
OB bus	442.3	388.2	437.2	6.48	4.92	5.70
IB bus	417.7	483.7	507.9	5.26	7.64	9.20
Total bus	430.0	436.0	472.5	5.87	6.28	7.45
Network performance						
Car	132.6	143.4	170.8	3.02	3.37	4.10
Bus	412.4	419.0	454.9	5.66	6.02	7.18
Person	261.4	270.3	302.0	4.24	4.59	5.52

The results in Table 7.4 show that under a light transit ratio, Model 1 and Model 3 yield similar MOEs among all roadway users. For example, there exists no significant difference between these two models on per person delay (141.9s and 146.1s, respectively) and the number of stops (3.04 and 3.04, respectively) on the whole network. However, on an arterial with higher transit volumes, the proposed multi-modal decomposition model can yield lower average delays and a smaller number of stops for all roadway users, evidenced by the results in Tables 7.5 and

7.6. For example, under Scenarios 2 with medium bus volumes, the proposed Model V, considering both transit and car volumes, shows a 7.9% reduction in the average bus delay (from 421.7s to 388.5s) and 19.1% on the number of stops (from 5.72 to 4.63) along the arterial, compared to Model 3. Due to such improvements on bus operations, Model V can further generate lower average person delay than with Model 3 within the whole network. For example, as shown in Table 7.5, the average person delays under Scenario 2 are 179.3s and 199.0s for Model 1 and Model 3, respectively.

The resulting MOEs with Model 4 under the simulated volume scenarios further show that on a long arterial with heavy dual-modal flows, the non-optimal selection of decomposition location (by Model 3) cannot be remedied with the dual-modal progression model within each segment. For example, Model 4 under Scenario 3 yields a larger average delay and higher number of stops for both modes on the arterial and within the whole network. Compared to Model 1, Model 4 can increase the average person delay by 15.5% (from 261.4s to 302.0s) and the number of stops per person by 30.2% (from 4.24 to 5.52). The advantage of Model 1 over Model 4 can also be observed from the other two volume scenarios in the simulation experiments.

The higher traffic efficiency with Model 1, compared to both Models 3 and 4 under Scenarios 2 and 3, indicates the benefit of concurrently determining the decomposition locations for both modes, especially when the transit volume is considerably high. The non-optimal decomposition locations will result in less efficient traffic operations for all roadway users on the arterial. The comparison between MOEs generated with Models 1 and 4 also indicate that with a

set of predetermined decomposition locations for both modes, the dual-modal progression model (Model IV) cannot yield as lower traffic delay as with Model V.

In summary, the simulation results in this study show that:

- The proposed Model V can yield lower person delays and a smaller number of stops than with Model IV under the moderate to high bus volume scenarios;
- Traffic efficiency can be optimized by concurrently design of the decomposition locations for both modes, rather than for a sole mode;
- The total roadway user benefits can be maximized by optimizing the signal offsets and phase sequences concurrently with the decomposition locations;
- Under the scenarios of low bus volume, the performance of the multi-modal decomposed model is close to the decomposition model for passenger cars only.

7.6 Closure

Despite the advance in arterial progression algorithms during the last decades, their applications on long arterials with both heavy passenger car and bus flows often fall short of effectiveness. To ensure traffic efficiency over the entire arterial experiencing multi-modal flows, this chapter has introduced a signal optimization model to concurrently decompose a long arterial into the optimal number of control segments and to offer the maximized progression for buses and passenger cars within each of their respective segments.

To identify the optimized decomposition locations for both modes and design the offsets as well as phase sequence under the given geometric condition and pre-defined critical

intersections, Model V adopts the same logic as Model III with two-stage optimization to tackle various critical issues, including the competition of the progression band length and bandwidth between two modes, and their selection of different decomposition locations. The first stage intends to identify the maximum possible bandwidth for buses and passenger cars at all critical intersections and the preliminary set of decomposition locations. Using the results from Stage 1, the second stage will optimize the connection state between progression bands within adjacent segments for both modes so as to smooth the progression at the decomposition location. To improve the computing efficiency of Model V for an arterial comprising a high number of intersections, this study has further developed a solution technique to separate Stage 1 into two steps to reduce integer variables and constraints in each step.

The numerical examples have confirmed the properties of the proposed Model V with respect to the optimized decomposition locations and maximized bandwidths for each mode in each direction. The necessity to allow different decomposition locations for two modes to maximize the total bandwidths has also been verified with a performance comparison between the proposed model and the one without such flexibility. Further evaluation results with a real-world arterial system and extensive simulation experiments have also demonstrated that Model V can yield lower person delays and a smaller number of stops than with Model IV under the scenarios having the moderate to high bus volumes. The results from the simulation also show that the decomposition locations for these two modes should be concurrently designed to achieve the optimal traffic efficiency.

Chapter 8. Conclusions

8.1 Research Summary and Contributions

To design signal progression for both passenger cars and transit vehicles under various congestion levels and real-world constraints, this dissertation has developed a multi-modal signal optimization system for arterials of different lengths. The developed system with its embedded multiple functions allows the user to perform the arterial signal design from the most straightforward optimization of two-way one-mode progression to the most challenging task of concurrently producing the optimal control boundaries and the progression bands for the selected mode(s) and direction(s). Although much remains to be done on this subject, some contributions up to the stage of this study are summarized below:

--- *Completed a comprehensive analysis of existing studies on signal optimization, arterial progression, and TSP models*

All existing studies identified for review and analysis are classified into three categories: 1) signal optimization and progression design models, 2) arterial decomposition models for signal coordination; and 3) active and passive TSP control strategies. Key contributions and deficiencies of the existing studies on those three subjects have been identified. It has been noticed that despite the progress of the traffic community on the subject of arterial signal progression, some critical issues existing in real-world traffic systems remain to be tackled. For instance, the heavy turning flows, onto and from the arterial and their impacts on the progression quality, have not been adequately addressed in the literature. The interrelations between buses and passenger cars, sharing the same roadway segments and causing mutual impedance in their progression process, has

neither been taken into account in the arterial progression design. An effective method to identify the progression boundaries for a long arterial is also lacking in the existing studies.

--- *Developed a flexible multi-modal signal progression system for arterials of different geometric constraints and traffic flow patterns*

In response to the research needs identified in the literature review, the research focus of this dissertation has been devoted to proposing the structure of a multi-modal signal progression system that allows users to apply different modules on arterials with various traffic and geometric constraints. The proposed framework contains two key modules with five models to address those critical issues which are often encountered by users in design of signal plan for urban arterials with different features.

--- *Enhanced the signal progression model's effectiveness in tackling an arterial constrained by the limited bay length and short links*

This task is focused on developing a set of models that can be applied to address the following issues: 1) heavy left-turn volumes from and onto the arterial under the constraint of limited turning bay length; and 2) excessive queue lengths at near-saturated intersections and on short links. To address the former issue, this study has been introduced to: 1) design concurrent progression for both the through and left-turn movements, 2) account for mutual blockage between through and left-turn movements due to the limited bay length, and 3) reflect the impacts of residual queues from vehicles turning onto the arterial. The enhanced version of this model, Model II, has also been developed to balance the queues among all critical locations on the arterial with the further optimized signal control plans.

--- *Developed an arterial decomposition model to maximize the progression efficiency along the long arterial*

This task aims to decompose the arterial into the optimal number of control segments with a set of well-connected and maximized progression bands. To identify the optimized decomposition locations and the signal plans under the given geometric condition and critical intersections, this dissertation has proposed Model III, a two-stage process to tackle various issues that may prevent vehicles from progressing smoothly over the entire arterial. Such critical issues include 1) the relation between the decomposition locations and the maximized bandwidth in each segment, 2) progression discontinuity between segments, 3) queue formation on travel lanes and its impact on signal progression, 4) left-turn bay spillback and the blockage due to through queues, and 5) excessive queue lengths at critical locations.

--- *Developed a multi-modal progression model for an arterial experiencing both heavy passenger car and transit flows*

The primary efforts on this task have yielded a signal optimization model that can offer concurrent progression to the best selected mode(s) and direction(s), based on traffic volume, bus ratio, and geometric conditions. To ensure the quality of progression to both modes, the proposed Model IV has effectively taken into account all critical issues that may result in their mutual impedance, such as the potential blockage of passenger car queues to the roadside bus stops, the excessive start-up delays caused by transit vehicles queuing at the intersection, and the travel lanes reduced for progressing flows due to dwelling buses at roadside stations with limited storage capacity. In addition, by weighting the bandwidths with the passenger volumes by mode and by direction, the proposed model is capable of offering the progression only to the mode(s) and the

direction(s) that are justified to do so from the perspective of maximizing the benefits for all the arterial users.

--- *Integrated all developed models into a system for design of multi-modal progression on congested arterials*

This task has produced an integrated model for arterial signal design that can concurrently decompose a long arterial into the optimal number of control segments, offer the maximized progression for buses and passenger cars within each of their respective segments, circumvent all geometric constraints, and balance the progression length and bandwidth between those two modes, based on all related information. To improve the computing efficiency for arterials with a large number of congested intersections, this study has also designed a customized algorithm to overcome this issue.

8.2 Future Research

Despite the progress made by this study on arterial signal design, some critical issues remain to be addressed. Future studies along the line will be focused on the following directions.

--- *Development of a network-based progression system to account for congestion by crossing of major arterials*

The system proposed in this dissertation has focused on the progression efficiency at the arterial level, but not the relation among closely-spaced major arterials. In a congested urban network, the signal timings on neighboring major arterials should be further coordinated to ensure the improved efficiency on one arterial will not be at the expense of its crossing streets. Ideally,

those crossing major roads, with optimized signal designs, are expected to efficiently discharge the turning volumes from the arterial so as to avoid local bottleneck at the critical intersections. Design of the optimized progression plan at the network level shall also be capable of increasing its overall throughput.

The design for network-based progression shall address the following critical tasks: 1) providing multi-path progression on major arterials and their crossing major roads; 2) ensuring that the progression band for target modes and paths are consistent with their volumes or frequencies;3) designing the bus progression plan for various bus routes in the network, based on their volumes and passenger flows.

--- *Advancement of the key control models to real-time operations*

To ensure that the progression system designed in this study can serve as the solid basis for an online environment, one shall add the following functions: 1) detecting the non-recurrent congestions and adjusting priority for the progression band on each path in real time; 2) dynamically adjusting the key control parameters in the progression design in response to real-time flow fluctuations; and 3) accommodating preemption requests due to any emergency or incident.

--- *Enhancement of the current signal design system with advanced information/communication technologies*

As with most control systems, the effectiveness of the proposed models depends on the accuracy of the data from multiple sources. Information from recently developed vehicle-to-

vehicle (V2V) and vehicle-to-infrastructure (V2I) can certainly improve the reliability of the data sources to the control system. For example, the real-time estimation or prediction of volumes on each arterial can help the system better select the arterial segments and paths to offer progression. The real-time data related to the number of passengers, especially on buses, can also benefit the dual-modal progression design. The speed and delay data at intersections can enable the queue detection with better accuracy, and further allow the operator to take timely adjustment of the progression plan to effectively discharge any excessive queues.

Bibliography

Aboudolas, K., Papageorgiou, M., Kouvelas, A., and Kosmatopoulos, E. (2010). A rolling-horizon quadratic-programming approach to the signal control problem in large-scale congested urban road networks. Transportation Research Part C: Emerging Technologies, 18(5), 680-694.

Allsop, R.E. (1971). Delay-Minimizing Settings for Fixed-time Traffic Signals at a Single Road Junction. IMA Journal of Applied Mathematics, 8 (2): 164-185.

Allsop, R.E. (1972). Delay at a fixed time traffic signal-I: Theoretical analysis. Transportation Science, 6(3), 260-285.

Allsop, R.E. (1976). Sigcap: A Computer Program for Assessing the Traffic Capacity of Signal Controlled Road Junctions. Traffic Engineering and Control, 17, 338-341.

Allsop R. E. (1977) Priority for buses at signal-controlled junctions: some implications for signal timings. Proceedings of the 7th International Symposium on Transportation and Traffic Theory, Kyoto, August 1977. In Transportation and Traffic Theory (Edited by T. Sasaki and T. Yamaoka) pp. 247-270. Kyoto: The Institute of Systems Science Research.

Altun, S. Z., & Furth, P. G. (2009). Scheduling buses to take advantage of transit signal priority. Transportation Research Record, 2111(1), 50-59.

Balke, K. N., Dudek, C. L., & Urbanik, T. (2000). Development and evaluation of intelligent bus priority concept. Transportation Research Record, 1727(1), 12-19.

Bonneson, J. A., Sunkari, S. R., & Pratt, M. P. (2009). Traffic signal operations handbook (No. FHWA/TX-09/0-5629-P1). Texas Transportation Institute, Texas A & M University System.

Burrow, I. J. (1987). OSCADY: a computer program to model capacities, queues and delays at isolated traffic signal junctions (No. RR 105).

Chang, E. C., Cohen, S. L., Liu, C., Chaudhary, N. A., and Messer, C. (1988). MAXBAND-86: Program for optimizing left-turn phase sequence in multiarterial closed networks , Transportation Research Record, 1181, 61-67.

Chang, T. H., and Lin, J. T. (2000). Optimal signal timing for an oversaturated intersection. Transportation Research Part B: Methodological, 34(6), 471-491.

Chaudhary, N.A., V.G. Kovvali, C.-L. Chu, J. Kim, and S.M. Alam (2002). Software for Timing Signalized Arterials. Report FHWA/TX-03/4020-1, Texas Transportation Institute, the Texas A&M University System, College Station, Texas, September.

Chen, Y. H., Cheng, Y., & Chang, G. L. (2019). Concurrent Progression of Through and Turning Movements for Arterials Experiencing Heavy Turning Flows and Bay-Length Constraints. Transportation Research Record, 0361198119843480.

Cheng, Y., Kim, H., & Chang, G. L. (2019). Design of a Dual-Modal Signal Progression Model for Urban Arterials Accommodating Heavy Transit and Passenger Car Flows. Transportation Research Record, 0361198119846091.

Cheng, Y., Chang, G. L., & Rahwanji, S. (2018). Concurrent Optimization of Signal Progression and Crossover Spacing for Diverging Diamond Interchanges. Journal of Transportation Engineering, Part A: Systems, 144(3), 04018001.

Cheng, Y., & Yang, X. (2018). Signal coordination model for local arterial with heavy bus flows. Journal of Intelligent Transportation Systems, 22(5), 422-432.

Cooper, B. R., Vincent, R. A., & Wood, K. (1980). Bus-actuated traffic signals-initial assessment of part of the Swansea bus priority scheme (No. TRRL LR925 Monograph).

Cottinet M., Breteque A., Henry J. J. and Gabard F. (1980) Assessment by observation and by simulation studies of the interest of different methods of bus preemption at traffic lights. Proceeding of the international Symposium on Traffic Systems, Berkeley, California, Vol.2, pp. 92-105.

Daganzo, C. F. (1994). The cell transmission model: A dynamic representation of highway traffic consistent with the hydrodynamic theory. Transportation Research Part B: Methodological, 28(4), 269-287.

Dai, G., Wang, H., & Wang, W. (2015). A bandwidth approach to arterial signal optimisation with bus priority. Transportmetrica A: Transport Science, 11(7), 579-602.

Dai, G., Wang, H., & Wang, W. (2016). Signal optimization and coordination for bus progression based on MAXBAND. KSCE Journal of Civil Engineering, 20(2), 890-898.

Dion F. and Hesham R. (2005) Integration Transit Signal Priority with Adaptive Traffic Signal Control Systems, presented at 84th Annual Meeting of the Transportation Research Board, Washington, D.C.

El-Reedy, T. Y., & Ashworth, R. (1978). The effect of bus detection on the performance of a traffic signal controlled intersection. Transportation Research, 12(5), 337-342.

Evans H. and Skiles G. (1970) Improving public transit through bus preemption of traffic signals. In Traffic Quarterly, Vol.24, No.4, pp. 531-543

Feng, Y., Pei, Y. L., & Cao, C. H. (2007). Study of single bus priority signal planning under the mixed traffic flow. Journal of Harbin Institute of Technology, 2, 031.

Gallivan, S., Young, C. P., & Peirce, J. R. (1980). Bus priority in a network of traffic signals. In the ATEC Conference, Paris, Crowthorne: Transport and Road Research Laboratory.

Gartner, N. H., Assman, S. F., Lasaga, F., & Hou, D. L. (1991). A multi-band approach to arterial traffic signal optimization. Transportation Research Part B: Methodological, 25(1), 55-74.

Gartner, N. H., and Stamatiadis, C. (2002). Arterial-based control of traffic flow in urban grid networks. Mathematical and computer modelling, 35(5), 657-671.

Gartner, N. H., and Stamatiadis, C. (2004). Progression optimization featuring arterial-and route-based priority signal networks. Journal of Intelligent Transportation Systems, 8(2), 77-86

Garrow, M., & Machemehl, R. (1999). Development and evaluation of transit signal priority strategies. Journal of Public Transportation, 2(2), 4.

Gazis, D. C. (1964). Optimum control of a system of oversaturated intersections. Operations Research, 12(6), 815-831.

Hadi, M. A., and Wallace, C. E. (1993). Hybrid genetic algorithm to optimize signal phasing and timing. Transportation Research Record, 1421, 104-112.

He, Q., Head, K. L., & Ding, J. (2011). Heuristic algorithm for priority traffic signal control. Transportation Research Record, 2259(1), 1-7.

Hook, D., & Albers, A. (1999). Comparison of alternative methodologies to determine breakpoints in signal progression. In Transportation Frontiers for the Next Millennium: 69th Annual Meeting of the Institute of Transportation Engineers, Institute of Transportation Engineers (No. Publication No. CD-006).

Janos, M., & Furth, P. (2002). Bus priority with highly interruptible traffic signal control: simulation of San Juan's Avenida Ponce de Leon. Transportation Research Record: Journal of the Transportation Research Board, (1811), 157-165.

JI, Y. J., DENG, W., WANG, W., & ZHANG, W. H. (2004). Study on the Design of Signal Phase Based on Bus Priority Intersections [J]. Journal of Highway and Transportation Research and Development, 12, 031.

Kashani, H.R., and Saridis, G.N. (1983). Intelligent control for urban traffic systems. Automatica 19, 191–197.

Kim, H., Cheng, Y., & Chang, G. L. (2018). Variable Signal Progression Bands for Transit Vehicles Under Dwell Time Uncertainty and Traffic Queues. IEEE Transactions on Intelligent Transportation Systems.

Lan C.J., (2004). New optimal cycle length formulation for pre-timed signals at isolated intersections. Journal of Transportation Engineering, 130(5), 637–647.

Li, J.Q., (2014), Bandwidth Synchronization under Progression Time Uncertainty. IEEE Transactions on ITS, 15(2), 1-11.

Li, Z. (2012). Modeling Arterial Signal Optimization with Enhanced Cell Transmission Formulations. Journal of Transportation Engineering, 137(7), 445–454.

Lin, Y. J., Yang, X. F., Zou, N., Jia, L., & Pan, S. (2013a). New passive transit signal priority control strategy for the bus vehicles at urban arteries. Journal of Northeastern University (Natural Science), 39(4), 723-729.

Lin, Y., Yang, X., Chang, G. L., & Zou, N. (2013b). Transit priority strategies for multiple routes under headway-based operations. Transportation Research Record, 2366(1), 34-43.

Lin, Y., Yang, X., & Zou, N. (2017). Passive transit signal priority for high transit demand: model formulation and strategy selection. Transportation Letters, 1-11.

Lin, Y., Yang, X., Zou, N., & Jia, L. (2013c). Real-time bus arrival time prediction: Case study for Jinan, China. Journal of transportation engineering, 139(11), 1133-1140.

Ling, K., & Shalaby, A. (2004). Automated transit headway control via adaptive signal priority. Journal of advanced transportation, 38(1), 45-67.

Little J.D.C. (1966). The synchronization of traffic signals by mixed-integer linear programming. Operation Research, 14(4), pp. 568-594.

Little J.D.C., Kelson, M.D., and Gartner, N.H., (1981). MAXBAND: A program for setting signals on arteries and triangular networks. Transportation Research Record, 795, pp. 40-46.

Liu, Y., and Chang, G. L. (2011). An arterial signal optimization model for intersections experiencing queue spillback and lane blockage. Transportation research part C: emerging technologies, 19(1), 130-144.

Lo, H., (1999). A novel traffic signal control formulation. Transportation Research, Part A, 44, 436–448.

Lo, H., (2001). A cell-based traffic control formulation: strategies and benefits of dynamic timing plan. Transportation Science, 35, 148–164.

Lo, H., Chang, E., Chan. Y. C., (2001). Dynamic network traffic control. Transportation Research, Part A, 35, 721–744.

Ludwick, S. and John Jr. (1974) Simulation of an unconditional preemption bus priority system. Report MTP-400, Yhe Mitre CorporationMatson, T. M. (1955). Traffic engineering. McGraw-Hill.

Ma, W., & Yang, X. (2007). A passive transit signal priority approach for bus rapid transit system. In Intelligent Transportation Systems Conference, 2007. ITSC 2007. IEEE (pp. 413-418). IEEE.

Ma, W., Yang, X., & Liu, Y. (2010). Development and evaluation of a coordinated and conditional bus priority approach. Transportation Research Record: Journal of the Transportation Research Board, (2145), 49-58.

Ma W. and Yu B. (2007) Serve Sequence Optimization Approach for Multiple Bus Priority Requests Based on Decision Tree. Proceedings of the Seventh International Conference of Chinese Transportation Professionals Congress.

MacGowan J. and Fullerton I. J. (1979) Development and testing of advanced control strategies in the urban traffic control system. Public Roads, 43 (3), pp.97-105.

Machemehl, R. (1996). Class Notes: CE 391L, Advanced Traffic Engineering. The University of Texas at Austin, Spring.

Michalopoulos, P. G., and Stephanopoulos, G. (1977a). Oversaturated signal systems with queue length constraints—I: Single intersection. Transportation Research, 11(6), 413-421.

Michalopoulos, P. G., and Stephanopoulos, G. (1977b). Oversaturated signal systems with queue length constraints—II: Systems of intersections. Transportation Research, 11(6), 423-428.

Miller A.J. (1963). Settings for Fixed Cycle Traffic Signals. Operations Research Quarterly, Vol. 14, No. 4, pp. 373-386.

Mirchandani, P., Knyazyan, A., Head, L., & Wu, W. (2001). An approach towards the integration of bus priority, traffic adaptive signal control, and bus information/scheduling systems. In Computer-Aided Scheduling of Public Transport (pp. 319-334). Springer, Berlin, Heidelberg.

Morgan, J.T. and Little J.D.C. (1964). Synchronizing traffic signals for maximal bandwidth. Operation Research, 12(6), pp. 896-912.

Papageorgiou, M. (1995). An integrated control approach for traffic corridors. Transportation Research Part C 3, 19–30.

Park, B., Messer, C.J., and Urbanik, T. (1999). Traffic signal optimization program for oversaturated conditions: genetic algorithm approach. Transportation Research Record, 1683, 133–142.

Robertson, D. I. (1969). TRANSYT: a traffic network study tool. Report Number: TRRL-LR-253, Transport and Road Research Laboratory.

Satiennam, T., Fukuda, A., Muroi, T., Jansuwan, S., & Bangkok10110, N. K. W. (2005). An enhanced public transportation priority system for two-lane arterials with nearside bus stops. In Proceedings of the Eastern Asia Society for Transportation Studies (Vol. 5, pp. 1309-1321).

Smith, H. R., Hemily, B., & Ivanovic, M. (2005). Transit signal priority (TSP): A planning and implementation handbook.

Silcock, J. P. (1997). Designing signal-controlled junctions for group-based operation. Transportation Research Part A: Policy and Practice, 31(2), 157-173.

Stamatiadis, C., and Gartner, N. H. (1996). MULTIBAND-96: a program for variable-bandwidth progression optimization of multiarterial traffic networks. Transportation Research Record, 1554(1), 9-17.

Stevanovic, A., Martin, P.T., and Stevanovic, J., (2007). VisSim-based genetic algorithm optimization of signal timings. Transportation Research Record, 2035, 59–68.

Tamoff P. J. (1975) The results of FHWA urban traffic control research: an interim report. Traffic Engineering, 45 (4), 27-35.

Tian, Z., & Urbanik, T. (2007). System partition technique to improve signal coordination and traffic progression. Journal of Transportation Engineering, 133(2), 119-128.

Urbanik T, Holder RW and Fitzgerald AV. (1977). Evaluation of alternative concepts for priority use of urban freeways in Texas, Texas Transportation Institute Report, Texas, 205–1.

Webster F.V. (1956). Traffic Signal Settings. Road Research Technical Paper, No. 39, HMSO. Morgan

Wong, C. K., and Wong, S. C. (2003). Lane-based optimization of signal timings for isolated junctions. Transportation Research Part B: Methodological, 37(1), 63-84.

Wu, X., Tian, Z., Hu, P., & Yuan, Z. (2012). Bandwidth optimization of coordinated arterials based on group partition method. Procedia-Social and Behavioral Sciences, 43, 232-244.

Jian, Y. A. N. F. L. I. K. S. (2009). Detector location for transit signal priority at intersection with countdown signals. Journal of Transport Information and Safety, 6, 021.

Yang, X., Chang, G., and Rahwanji, S. (2014). Development of a Signal Optimization Model for Diverging Diamond Interchange. Journal of Transportation Engineering, 140(5), 04014010.

Yang, X., Cheng, Y., & Chang, G. L. (2015). A multi-path progression model for synchronization of arterial traffic signals. Transportation research part C: emerging technologies, 53, 93-111.

Yang, X., Cheng, Y., & Chang, G. L. (2016). Operational Analysis and Signal Design for Asymmetric Two-Leg Continuous-Flow Intersection. Transportation Research Record: Journal of the Transportation Research Board, (2553), 72-81.

Yang, X., Lu, Y., & Lin, Y. (2013). Interval optimization for signal timings with time-dependent uncertain arrivals. Journal of Computing in Civil Engineering, 29(5), 04014057.

Yin, Y., (2008). Robust optimal traffic signal timing, Transportation research Part B, 42, 911-924.

Yun, I., and Park, B., (2006). Application of stochastic optimization method for an urban corridor. Proceedings of the Winter Simulation Conference 3–6, 1493–1499.

Zhang, C., Xie, Y., Gartner, N. H., Stamatiadis, C., & Arsava, T. (2015). AM-band: an asymmetrical multi-band model for arterial traffic signal coordination. Transportation Research Part C: Emerging Technologies, 58, 515-531.

Zhang, T., & Zhang, Y. (2014). System Partition Method to Improve Arterial Signal Coordination (No. 14-3166).

Zhang, W. H., Lu, H. P., Shi, Q., & Liu, Q. (2004). Optimal signal-planning method of intersections based on bus priority. Journal of Traffic and Transportation Engineering, 4(3), 49-53.